ADDIS ABABA SCIENCE AND TECHNOLOGY UNIVERSITY

EXPERMENTAL INVESTIGATION ON

MICROSTRACTURAL PROPERTY OF EXPANSIVE

SOIL STABILIZED WITH IRON ORE TAILING

AND LIME

By

BINYAM DESSU TIKI

A Thesis Submitted as a Partial Fulfillment to the Requirements for the

Award of the Degree of Masters of science in Civil Engineering

(Geotechnical Engineering)

to

DEPARTMENT OF CIVIL ENGINEERING
COLLEGE OF ARCHITECTURE & CIVIL ENGINEERING

JUNE, 2021

Declaration

I hereby declare that this dissertation entitled "**Experimental Investigation on Microstructural Property of Expansive Soil Stabilized with Iron Ore Tailing & Lime**" was prepared by me, with the guidance of my advisor. The work contained herein is my own except where explicitly stated otherwise in the text, and that this work has not been submitted, in whole or in part, for any other degree or professional qualification.

Author; -   Signature, Date:

_____

Witnessed by:

Dr. Eleyas Assefa: Signature, Date:

_____

Approval Page

This is to certify that the thesis prepared by **Mr. Binyam Dessu Tiki** entitled **"Experimental Investigation on Microstructural Property of Expansive Soil Stabilized with Iron Ore Tailing & Lime"** and submitted as a partial fulfilment for the award of the Degree of Master of Science in Civil engineering specialization in **Geotechnical Engineering** complies with the regulations of the university and meets the accepted standards with respect to originality, content and quality.

Principal Advisor:

Dr. Eleyas Assefa
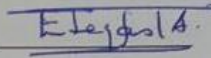
(Advisor)   Signature   Date

Members of the Examining Board:

Dr. Argaw Asha
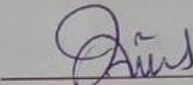
(External examiner)   Signature   Date

Dr. Endalu Tadele
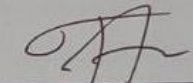
(Internal examiner)   Signature   Date

Dr. Melaku Sisay

(ERA PG coordinator Civil engineering)   Signature   Date
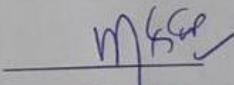
Alemayehu Feyisa

(Head, Civil engineering department)   Signature   Date
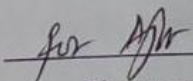
Dr. Sisay Demeku

Dean, college of Architecture and   Signature   Date
Civil engineering department
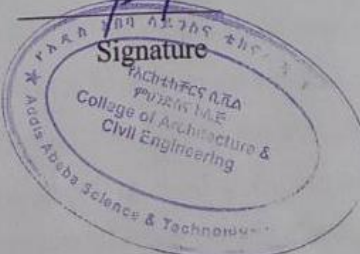
Abstract

Black cotton soils are poor materials to employ in highway or airfield construction because they contain a higher percentage of clay content. However, researchers have been intensified into new and innovative use of industrial waste material are continually being advanced, particularly concerning the usability, feasibility, environmental suitability, and performance of waste materials. In this study Iron ore tailing (IOT) which is an industrial by-product of the mining or extraction process iron ores used as stabilizer and lime to improve the strength and index properties of Black cotton soil (BCS). The study aimed to improve the geotechnical index property of BCS and its microstructural effect. Experimental analysis was done by three groups which are Problematic soil treated alone, BCS with 2, 4, 6, 8, 10, 12, 14, 16 IOT% and also BCS with 2% lime and 5, 10, 15, 20% IOT content by dry weight of soil. To meet the objective thesis experimental laboratory tests were done including according to ASHTO and ASTM standards. Test carried out include sieve analysis, hydrometer, Atterberg limits, specific gravity, free swell, compaction, California bearing ratio (CBR), unconfined compressive strength (UCS), and microstructural analysis done using Scanning Electron Microscopy (SEM) for BCS and treated samples by selecting based on strength and geotechnical index properties. SEM image analyses were done using Image J software. According to laboratory results, untreated soil is classified as A-7-5 (20) in AASHTO and MH in USCS systems. Experimental result shows that liquid limit of BCS decrease for both BCS-IOT and BCS-lime -IOT Content. Other hand plastic limit decrease with increasing IOT content while the Plasticity index decreases from 45 % for BCS to 24 % for 2 % lime with 20 % IOT. Maximum dry density (MDD) of BCS was increased while Optimum moisture content (OMC) decreased with higher IOT content. OMC value recorded for BCS were 29 % decreased to 20.60% & 19.31% for 16% IOT, 2 % lime and 20 % IOT respectively. The strength (i.e, UCS and CBR values) of treated soil significantly changed due to the addition of IOT, however addition 2% lime content to BCS changes enormously to peak value CBR recorded at 2 % lime and 15 % IOT. SEM results show changes in the morphology of clay particles and the concentration of calcium is higher on the border of the particles. Based on the experimental study, an optimal 2% lime and 15% IOT is recommended for the treatment of black cotton soil for use as subgrade material in road construction. The benefits of the application include a reduction in the environmental impact of the disposal of iron tailing.

Keywords: Iron ore Tailing (IOT) & Scanning electron microscope (SEM)

Acknowledgment

Table of Contents

List of Abbreviations and Acronyms

AASHTO	American Association of Highway and Transportation Officials
ANSS	Anyway Natural Soil Stabilizer
ASTM	American Society for Testing and Materials
CAH	Calcium Aluminate Hydrate
CBR	California Bearing Ratio
CEC	Cation Exchange Capacity
CSH	Calcium Silicate Hydrate
DDL	Double Diffusion Layer
ERA	Ethiopia Road Authority
EMA	Ethiopian Metrological Agency
FSI	Free Swell Index
FS	Free Swell
GS	Specific gravity
IOT	Iron Ore Tailing
LL	Liquid Limit
MDD	Maximum Dray Density
OMC	Optimum Moisture Content
PI	Plasticity Index
PL	Plastic Limit
SEM	Scanning Electron Microscope
TDS	Total Dissolved Solids
UCS	Unconfined Compressive Strength

Units

$^{\circ}$C	degree centigrade
cc	centimeter cube
Cm^3	centimeter cube
E	easting
kPa	kilo pascal
kN	kilo newton
kN/m^2	kilo newton per meter square
g	gram
g/cm^3	gram per centimeter cube
meq	mill equivalent
mm	millimeter
μm	micrometer
N	northing

List of Tables

List of Figures

CHAPTER ONE
INTRODUCTION

1.1 Background

Soil is one of the essential elements of this nature. Everyone's life is attached directly or indirectly to the soil. Basic facilities of life whether it concerned with food, cloth, and house have been fulfilled with soil. The word "soil" is derived from the Latin word Solium which according to Webster's dictionary means an upper layer of the earth. Soils are formed by the repetition of physical disintegration and the chemical decomposition of rocks. For formation soil, there are five key factors. These are climate, organisms, relief, parent material, and time. Expansive soil by its nature is Problematic soils. Construction over expansive soil generally poses a major problem due to the ability of the soils to swell and shrink considerably with changes in moisture content, which consequently lead to low bearing values when wet, and sever cracking when dry resulting in enormous financial loss.

Black cotton soil (BCS) is an expansive soil (Tomlinson, 1999; Osinubi et al., 2010). Engineering definition for black cotton soil as a dark grey to black soil with a high content of clay, usually over 50 % in which montmorillonite is the principal clay mineral and which is commonly expansive (Morin, 1971). BCS are problematic soils that need treatment before any engineerical application. Soil stabilization is a technique introduced many years ago with the main purpose of improving the soil capacity of meeting the requirement of engineering projects. The soil stabilization technique is used to obtain improve the geotechnical properties soil by mixing together with BCS such as lime, cement or industrial by-products such as fly ash. Different study have been done for decays and still going on waste materials. Previous studies by Phanikumar and Sharma 2004; Osinubi and Stephen, 2005; Samadou, 2015, Annafi.Q et al., 2020 etc) focused on the potinesal use of industrial waste and it improve geotechnical index property of the soil.

The utilization of industrial by-products helps in the reduction of cost and also reduces the carbon footprint due to cement utilization. The total world production of iron ore in 2019 was 2.85 billion tons and for each ton of beneficiated iron ore, it is estimated that about 40% of tailing are produced. Iron ore tailing (IOT) which is the waste product of mining industries, for this study used as an admixture for the stabilization. Studies have been carried out using IOTs alone and to improve its

index geotechnical properties 2% lime used as admixture. However, this paper will focus on the study improvement of BCS with using IOT and lime as an admixture and microstructural analysis.

1.2 Statement of the problem

Black cotton soil has proved itself as a source of damage to property and economical loss. Swelling and shrink of black cotton soil cause various problems to the civil engineers not only at the time of construction but also throughout the life of structures. Uneven shrink and swelling reduce the serviceability of the structures. It causes the emergence of hairline cracks, differential settlements, and sometimes even severe cracks, which may initiate the collapse of structures, railway lines, and roadways. A decrease in the availability of suitable soil for construction has forced researchers to search for an appropriate method to improve the performance of locally available problematic soil. During the last four decades, lots of researches have been conducted on black cotton soil to reduce its expansion and contraction, and to save a lot of resources. that Ethiopia encountered major engineering problems due to these soils many researchers have been conducted an important study using traditional, nontraditional, and byproduct stabilizers for decades. However, in Ethiopian black cotton soil there is no specific study on the microstructural behavior of the stabilized soils this creates a knowledge gap to understand the mechanism of the stabilization.

1.3 Objectives

1.3.1 General objective

The general objective of this study is to evaluate the effect of IOT and lime on geotechnical index property and microstructural analysis of black cotton soil.

1.3.2 Specific objectives

Specific objectives of this research are:

- To evaluate the effect of IOT and lime on index, mechanical properties of black cotton soil, and determination of optimum amount of IOT and black cotton soil with IOT and lime.
- To compare changes in properties of black cotton soil with respect to IOT and IOT with lime stabilized soil.

- To evaluate the microstructural behavioral changes of stabilized soils by using scanning electron microscope (SEM) analysis.
- Put recommendations for future researchers to reveal the unexpected behavior and characteristics effect of IOT on the geotechnical and microstructural properties of black cotton soil.

1.3 Significant of the study

Significances of this study will be to Proper treatment of expansive soil, increasing its overall strength of expansive soil, use of industrial waste material properly, decide of its practical value on an application in the field, and Creating further research opportunities regarding the microstructural study on expansive soil stabilization.

1.4 Scope and limitations of study

This study will be carried out on the effect of iron ore tailing (IOT) and lime on the treatment of Black cotton soil. Black cotton soil has a number of mineralogical groups, for this paper I will try one group but furthermore, studies and researches should be conducted on the mineralogical group of Black Cotton soil. The limitation of is an experimental study and from research publication in short terms test, the study will not analyses the effective time how long the composition of lime and iron ore tailing (IOT).

1.6 Organization of thesis

The thesis consists of five chapters. The first chapter is the introduction part and it discusses briefly the general background thesis, problem statement, objective, the significance of the study, and scopes with its limitation. The second chapter is a literature review on the expansive mineralogical formation of soil in detail and important findings from previous studies are also included. The third chapter deals with the material used and the methodology followed for the study. The fourth chapter covers laboratory data collection and analysis of the laboratory test results of the different blended soils with lime- IOT material at various percentages. The fifth chapter consists of the conclusion and recommendation of the thesis.

CHAPTER TWO
LITERATURE REVIEW

2.1 Introduction

Expansive soils are poor material to employ in highway or airfield construction because they contain high percentages of plastic clay. Expansive soil is a type of clayey soil that expands when it comes in contact with water and shrinks when the water evaporates. Several amounts of damages occurred on the structure found on this soil. The damages normally appear as cracks on buildings, canal beds, and linings, pavements, lifting of water supply pipelines and sewerage lines, etc. (Sabat, 2012). The expansive soils are also called swelling soils or black cotton soils. Black cotton soil owing to its black color which is a result of high iron, hummus, and magnesium minerals derived from trap and basalt.

2.2 Formation of expansive soil

The parent material of expansive soil may be classified into two groups. (Arya, S.C.O Neill, M. W.Pincus, G, 1981) The first group comprises the basic igneous rocks like basalt, dolerite sills and dykes, gabbro's, etc., where feldspar and pyroxene minerals of the parent rocks decompose to form montmorillonite, which is a predominant mineral of expansive soil and secondary minerals. The second group comprises sedimentary rocks that contain montmorillonite, and break down physical to expansive soils. There are indications that confirm that the expansive soils of Ethiopia are derived from both groups. According to Dudal (1965), the estimated coverage of dark clay soils in Ethiopia in the Rift valley and Ethiopian plateau is 24.7%. The formation of montmorillonite was probably the weathering and erosion in the highlands and carried by streams to the coastal plains. And volcanic eruptions sending up clouds of ash felt on the plains and the seas with the ashes to be altered to montmorillonite (Chen, 1998).

2.3 Mineralogy of expansive soils

The soil classification system defines clay particles having a diameter size of two microns (0.002mm) or less. The most important grain property for fine-grained soils is the mineralogical composition (Chen, 1998). Clay minerals are classified according to their chemical composition and structure. Mineral sheets are the lowest mineral level to make layers. Layers of two to four

sheets make up the smallest unit cell of clay minerals. According to their structural composition they are grouped into two basic structural units (a) silica tetrahedral sheet and (b) alumina octahedral sheet.

(a) Silica tetrahedral sheet: they consist of four oxygen atoms (O^{2-}) surrounding silicon atoms (Si^{4+}) and they form a tetrahedral atom. A combination of tetrahedral silica units gives a silica sheet.

   ◯ & ◌ Oxygen   ● & ⌐ Silicon

     (a)   (b)
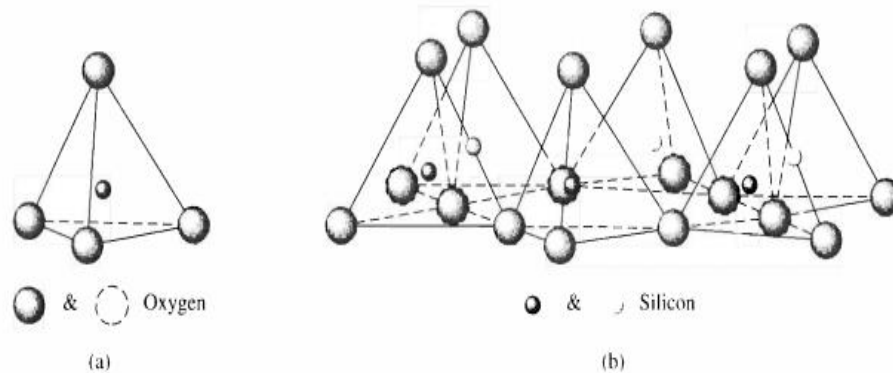
Figure 2. 1 a, Silica Tetrahedral and b, Silica tetrahedral sheet (after Grim, 1959)

(b) Alumina octahedral sheet: consists of six hydroxyls (OH^-) surrounding an aluminum atom (Al^{+3}). The combination of octahedral aluminum hydroxyl units will give an octahedral sheet. A combination of several octahedral units will give Gibbsite Sheet. Sometimes magnesium replaces the aluminum atoms in an octahedral unit this case the octahedral is called Brucite sheet.

   ◯ & ◌ Hydroxyl   ● Aluminum

     (c)   (d)
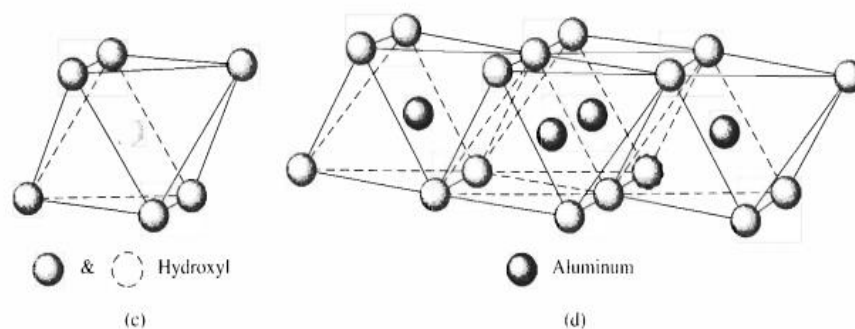
Figure 2. 2 c, Alumina octahedral sheet and d, Gibbsite Sheet (after grim, 1959)
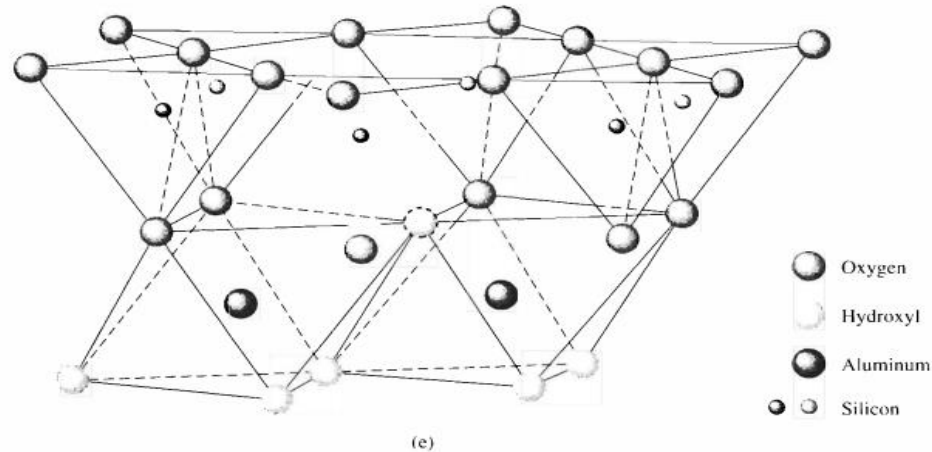
Figure 2. 3 elemental silica-gibbsite sheet (after Grim, 1959)

Clay have three important group minerals namely as follow kaolinite, illite and montmorillonite.
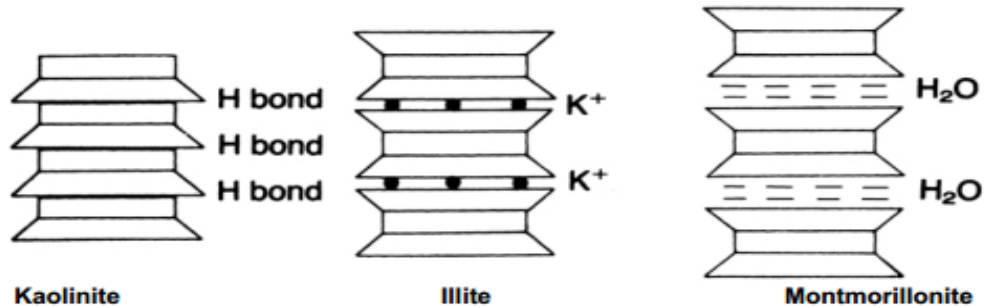
Figure 2. 4 Schematic Representations of Clay Minerals (Craig, 1997)

2.3.1 Kaolinite

Kaolin minerals are a group of clay minerals. Having basic structural unit consists of an alumina sheet combined with a silica sheet. Kaolinites are very stable due to the hydrogen bond, which develops between the oxygen of the silica sheet and hydroxyls of the alumina sheet. As the bond is fairly strong and stable water can't enter the structural unit and also due to this their shrinkage and swelling small compared to the other mineral group. The kaolin minerals are a group of clay minerals consisting of hydrous aluminum silicates. Kaolinite tends to be found in regions of heavier rainfall.
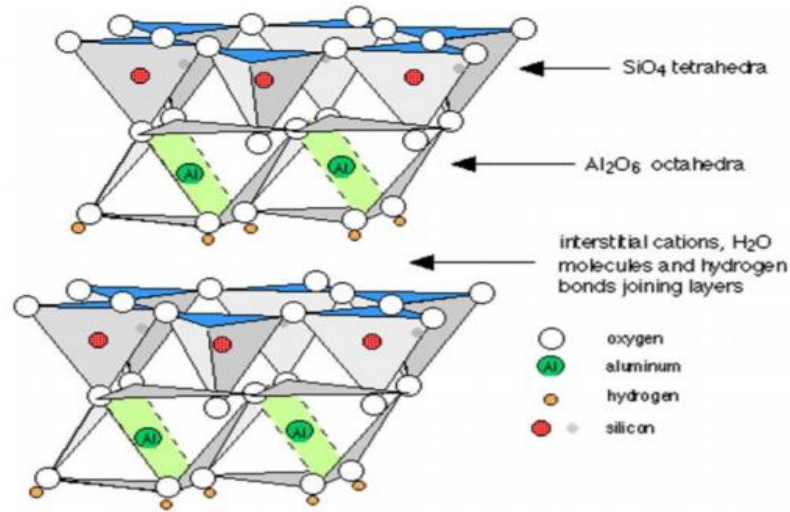
Figure 2. 5 Schematic diagrams of the structure of kaolinite (Aboudi Mana et al.2017)
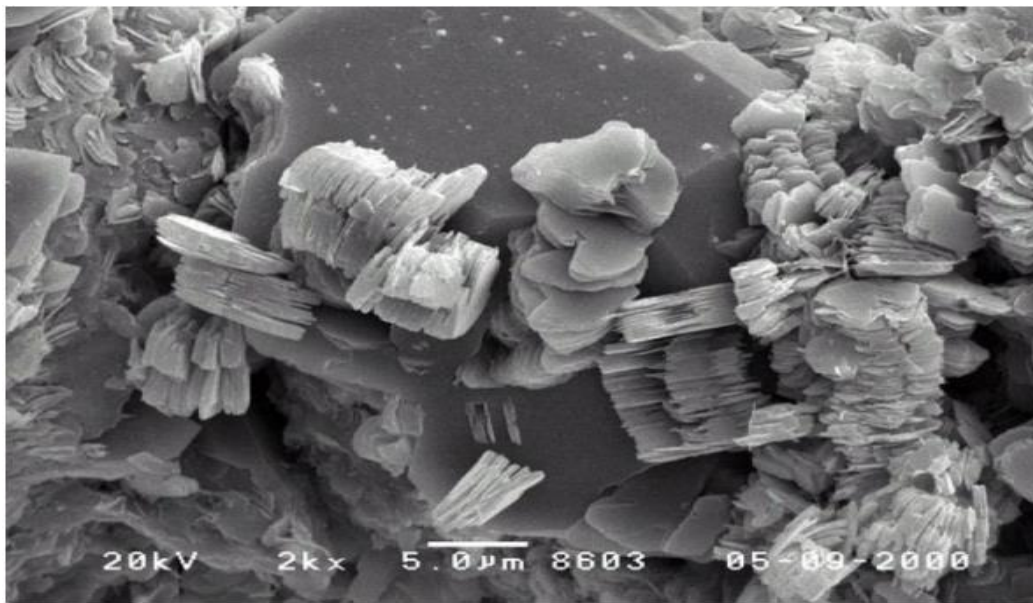
Figure 2. 6 SEM image of kaolinite (Source
http://webmineral.com/specimens/picshow.php?id=1283#.XHNZZuhKg2w)

2.3.2 Illite

Illite is the main mineral of illite group. The illite layer is bonded by potassium ion (k+). The negative charge to balance the potassium ion comes from the substitution of aluminum for some silicon in the tetrahedral sheets bond considerably weaker than hydrogen bond of kaolinite. The swelling of illite higher than that of kaolinite mineral group.
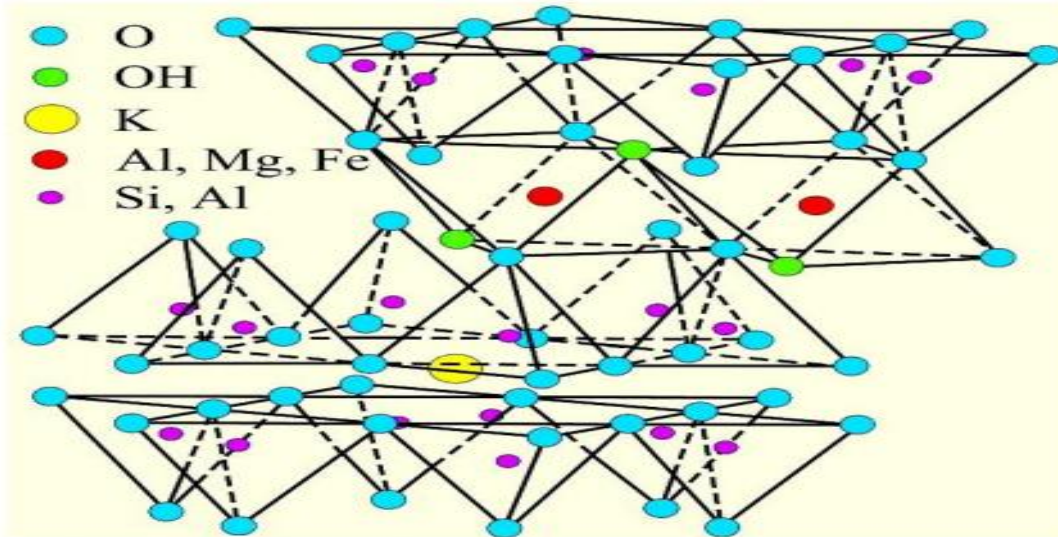
Figure 2. 7 Diagrammatic Sketch of the Illite (Onur Baser, 2009)

Figure 2. 8 SEM imagine of Illite (Source: http://
webmineral.com/specimens/picshow.php?id=1284#.XHNZEOhKg2w)
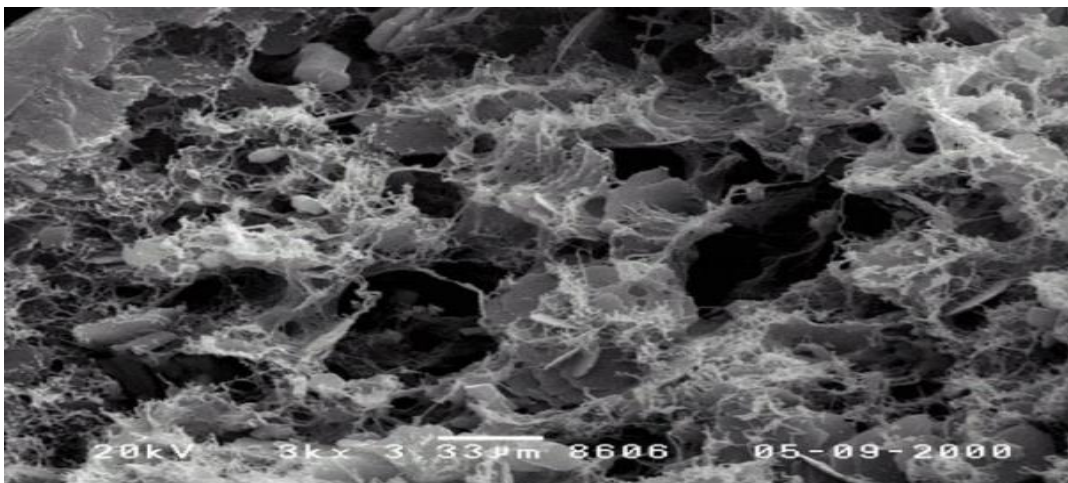
2.3.3 Montmorillonite

Montmorillonite structure is similar to illite which is one gibbsite sheet sandwiched between two silica sheets. Montmorillonite exhibits extremely high water absorption, swelling, and shrinkage characteristics. Due to its weak van der Waals bond between two successive structural units. The space between the combined sheets is occupied by water molecules and exchangeable cation. Montmorillonite is formed from weathering of volcanic ash under poor drainage conditions or in marine water.
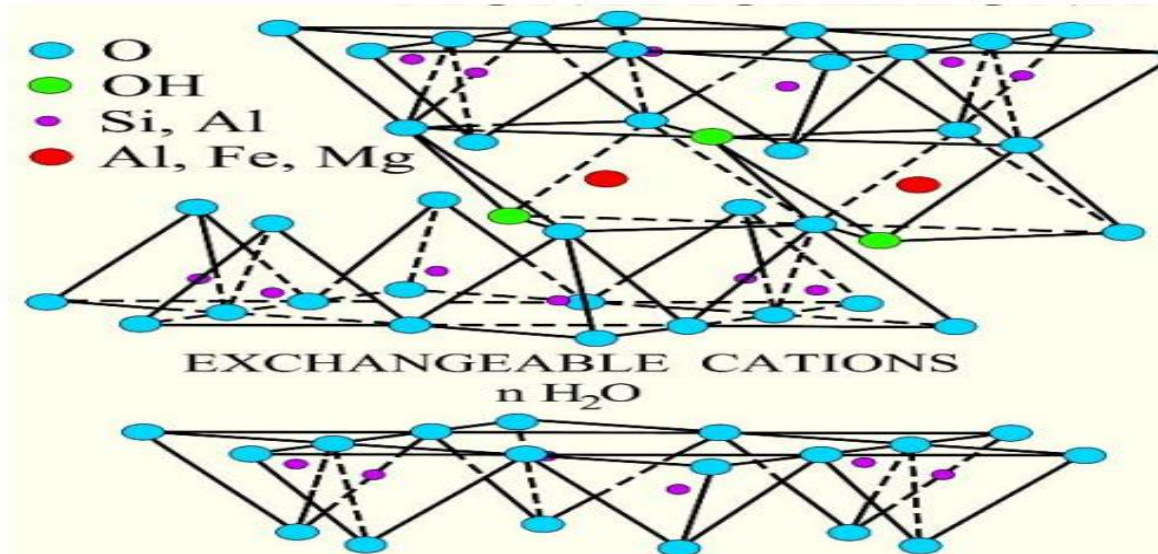
Figure 2. 9 Diagrammatic Sketch of the Montmorillonite (Onur Baser, 2009)
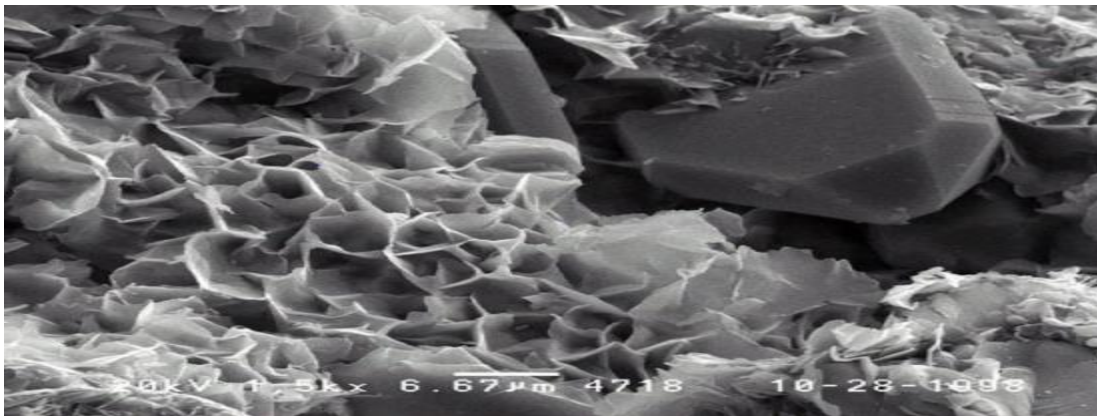
Figure 2. 10 SEM imagine of Montmorillonite (Source: http://
webmineral.com/specimens/picshow.php?id=1285&target=Montmoreillonite#.XHL9VOhKg2w)

2.4 Distribution of expansive soil

Expansive soil has been reported like USA, Australia, Canada, India, Spain, Israel, Turkey, Argentina, Venezuela, etc. (Teferra and Leikun, 1999). Even in the African continent expansive soil are widespread in Ethiopia, Kenya, South Africa, Mozambique, Morocco, Ghana, Nigeria, etc. The aerial coverage of expansive soils in Ethiopia is estimated to be 24.7 million acres (Lyon associates, 1971; as cited by Nebro, D., 2002). They are widely spread in the central part of Ethiopia. The distributions are shown in Figure 2.11 below
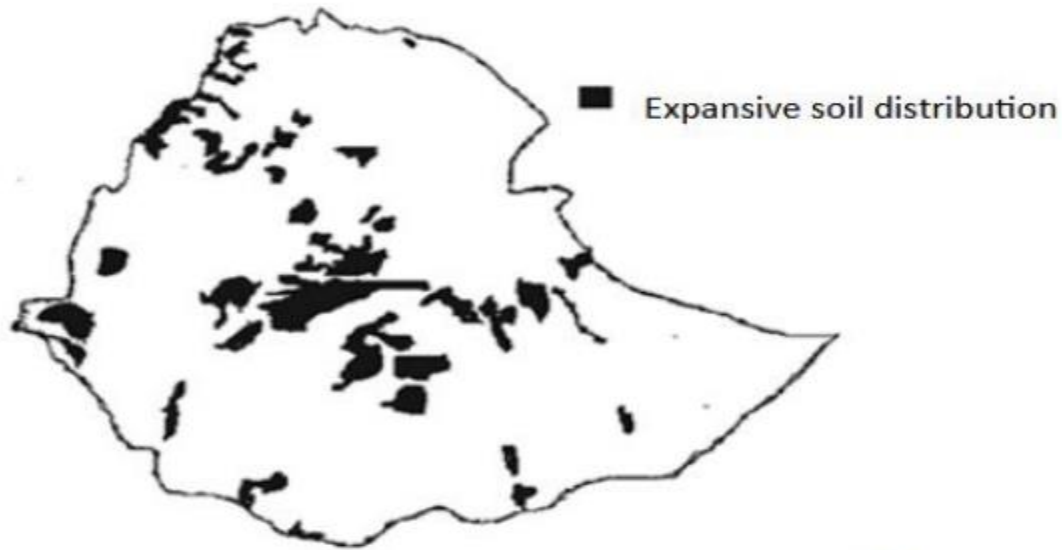
Figure 2. 11 Distribution of expansive soil in Ethiopia

2.5 Identification of expansive soil

Proper identification and characterization of soils become crucial in the perspective of geotechnical engineering. Identification of expansive soil consists of two important phases. The first is the visual identification and recognition as expansive soil and the second phase is sampling and conducting laboratory tests. The aim of this sub-topic is to discuss the commonly used identification method used for expansive soil.

2.5.1 Filed identification

Expansive soil deposits can be easily identified by visualization on the field. During reconnaissance and preliminary stage of the site. The method used for the identification of expansive soil is simple and easy to use. Some of the identification methods as follow usually have color black and gray

> ➢ On field deep or wide shrinkage cracks
> ➢ Have low strength wet condition and high strength during dry condition
> ➢ During excavation cut surfaces have a shiny appearance
> ➢ Occurred on regions where seasonal moisture variation
> ➢ Wet samples are sticky on hands

2.5.2 Laboratory identification

Laboratory identification of expansive soil can be divided in to two parts namely mineralogical identification & Inferential testing methods.

2.5.2.1 Mineralogical Identification

Mineralogical identification of expansive soil is crucial for exploring the basic properties of clays. The mineralogical composition of expansive soils has an important bearing on the swelling potentials. There are five techniques that help in identifying the mineralogy of expansive soils (Chen, 1998).

X-ray Diffraction

This method is used in determining the proportion of various minerals present in colloidal clay. It consists especially of comparing the ratios of the intensities of diffraction liens from the different minerals with the intensities of liens from standard substances (Chen, 1998).

Differential thermal analysis

This method is well established as a technique for control of the material that undergoes characteristics changes on heating. The test by itself is not accurate in identifying the expansive soils instead it is used in conjunction with x-ray diffraction (Chen, 1998).

Dye absorption

Minerals can be identified by characteristic colors formed by dyes that are absorbed by the minerals of the soil sample. When a clay sample is pretreated with acid, the color assumed by the absorbed dye depends on the Base Exchange capacity of the various stabilizations of expansive soils with lime clay mineral present. The presence of the montmorillonite can be identified if the selected sample contains a mineral that is greater than about 5-10% (Chen, 1998).

Chemical analysis

This method is a valuable addition to other methods such as X-ray Diffraction. In the montmorillonite group of clay minerals, the chemical analysis can be used to determine the nature of isomorphism and to show the origin and location of the charge on the lattice (Chen, 1998).

Electron microscope Revolution

Chen (1988) opined that these techniques should be used in combination for better and reliable results. However, these techniques have restricted usage and are confined to research laboratories only in view of their requirement of sophisticated and specialized

instrumentation, which is costly and also the expert interpretation of result data. Microscopic examination of clay minerals offers the direct observation of the material. Two clays may give the same x-ray pattern and the dame differential thermal curve but will show up distinct morphological characteristics under electron resolution (Chen, 1998).

2.5.2.2 Inferential Testing Methods

This method try to relate some of the index properties of fine grained soils with the soil clay mineralogy composition and hence, to estimate their swell potential. They can be grouped into indirect method and direct method.

Indirect Method

On this method simple soil index property test can be used for the evaluation and identifying expansive soil. Tests can be used for evaluation of swelling potential of expansive soil and test can be performed easily in soil mechanics laboratory. Such test includes.

i)   **Atterberg Limits test**

Here measurement of the liquid limit and plasticity index are useful makes for identification of the swelling of expansive soils. Liquid limit is regarded as the water holding capacity of soil swell potential. Many classification schemes are available in the geotechnical engineering literature to recognize the degree of soil swell based on the liquid limit of fine-grained soil given in ***Table 2.1*** Expansive soil classification Based on Liquid Limit.

Table 2. 1 Expansive soil classification Based on Liquid Limit.

Swell potential	Liquid limit (%)		
	Chen (1965)	Snethan et al (1977)	IS: 1498 (1970)
Low	<30	<50	20 - 35
Medium	30 - 40	50 - 60	35 - 50
High	40 - 60	>60	50 - 70
Very high	>60	-	70 - 90

Plasticity index is the difference between the liquid limit and plastic limit of fine grained soils. Higher the plasticity index, more plastic soil and swelling potential will be higher. Swelling potential based on plasticity index is given in *Table 2. 2 Expansive soil classification based on plasticity index*.

Table 2. 2 Expansive soil classification based on plasticity index

Swell potential	Plasticity index (%)

	Chen (1965)	Snethan et al (1977)	IS: 1498 (1970)
Low	<18	0 - 15	<12
Medium	15 - 28	10 - 35	12 - 23
High	25 - 41	20 - 55	23 - 32
Very high	>35	>35	>32

ii)   Free swell test

This test was first proposed by Holtz and Gibbs (1956). Free swell test is a measurement of volume change in clay upon saturated and is one of the most commonly used simple test to estimate the swelling potential of expansive soil clay. Free swell is given by

$$FS = \frac{(V - V_o)}{V_o} * 100\% \qquad (2.1)$$

FS= Free Swell %

V = Soil volume after swelling

V_o =Volume of dry soil, $10m^3$

iii)   Free Swell Index

Free swell index is the increase in volume of soil without any external constraint when subjected to submergence in water. The procedure involves in taking two oven dried soil samples passing through 425µm sieve, 10cc each were placed separately in two 100ml graduated soil sample. Distilled water was filled in one cylinder and kerosene in the other cylinder up to 100ml mark. The final volume of soil is computed after 24hours to calculate free swell index. Free Swell index is given by

$$Free\ Swell\ Index\ (FSI) = \frac{(V_d - V_k)}{V_k} * 100\% \qquad (2.2)$$

FSI= Free Swell Index

V_d = Final Volume in Water

V_k= Final volume in kerosene

The swell potential of the soil based on FSI is classified as per the guidelines given in *Table 2. 3 Expansive soil classification based on FSI (IS 1498 1970)*

Table 2. 3 Expansive soil classification based on FSI (IS 1498 1970)

13

Swell potential	FSI (%)
Low	<50
Medium	50 -100
High	100 – 200
Very high	>200

Direct Method

The most accurate and dependable method of determining the swelling potential and the swelling pressure of expansive clay is by direct measurement. The method quantitatively evaluates the volume change characteristics of expansive soil. The test can be done using a consolidometer but care should be taken on the test procedure. A standardized procedure that considers the factors that affect the shrink-swell potential as well as simulate the expected loading condition should be adopted.

2.6 Expansive soil classification

Classification expansive soil have number of use for geotechnical engineers. Some of them are to group similar properties, to short list and for easy communication. On classification expansive soil different system are used to classify the soil. Classification bases on general classification system based on correlation with actual performances and using direct and indirect method of swelling potential as well as combination to arrive at a rating. Some of classification systems are as follow

I. Unified Soil classification system

It is most widely used system among geotechnical engineers. The system uses a two - letter symbol scheme to represent various soils.

Table 2. 4 First latter symbols used in USC system (Arora, 2004)

Symbol	Soil Type
S	Sand
G	Gravel
C	Clay
M	Silt
O	Organic
Note: The first latter indicates the principal soil type	

Table 2. 5 Second Latter Symbols used in USC system (Arora, 2004)

Soil Type

Symbol	Coarse		Fine
P	Poorly Graded	L	Lean (i.e Low plastic)
G	Well Graded	H	Fat (i.e High Plastic)
C	Clayey		
M	Silty		
Note: The second latter indicates the behavior of that soil.			

II. AASHTO classification

AASHTO Soil classification system was developed by the American Association of state Highway and Transportation Official and used for classification of soil. The classification system was first developed by Hogentogler and Tarzaghi in 1929 but has been revised several times. Classification system have seven groups A -1 through A − 7 and system uses both grain size distribution and Atterberg limits data to group.

Table 2. 6 AASHTO Soil Classification System (from AASHTO M 145 or ASTM D3282)

General Classification	Granular Materials (35% or less passing the 0.075mm (No.200) sieve)							Silt -Clay Materials (>35% passing the 0.075mm(No.200)) sieve)			
	A-1		A-3	A-2				A-4	A-5	A-6	A-7
Group Classification	A-1-a	A-1-b		A-2-4	A-2-5	A-2-6	A-2-7				A-7-5 A-7-6
Sieve Analysis, % passing											
2.00 mm (No.10)	50 max										
0.4255 mm (No.40)	30 max	50 max	51 min								
0.0755 mm (No.200)	15 max	25 max	10 max	35 max	35 max	35 max	35 max	36 min	36 min	36 min	36 min
Characteristics of fraction passing 0.425 mm (No. 40)											
Liquid Limit	…		…	40 max	41 min	40 max	41 min	40 max	41 min	40 max	41 min
Plasticity Index	6 max		N.P.	10 max	10 max	11 min	11 min	10 max	10 max	11min	11 min[1]
Usual type of significant constituent materials	stone fragments, gravel and sand		fine sand	sility or clayey gravel and sand				sility soils		clayey soils	
General rating as subgrade	excellent to good							fair to poor			

2.6.1 Classification specific to expansive soil

Above classification system uses general classification system it may indicates expansive character but does not provide valuable information. Direct use of such classification system as basis for design may lead to overly conservative construction in some places and inadequate construction in some area (Nelson, 1992). Hence, it is very important to emphasize that design decision has to base on predicting testing and analysis which provide reliable information. Some of classification system are as follow

i. Method of Daksanamurthy and Raman (1973)

This system of classification based on a modification of Casagrande's plastic chart, which includes Plasticity index and shrinkage index with the addition of the shrinkage index.
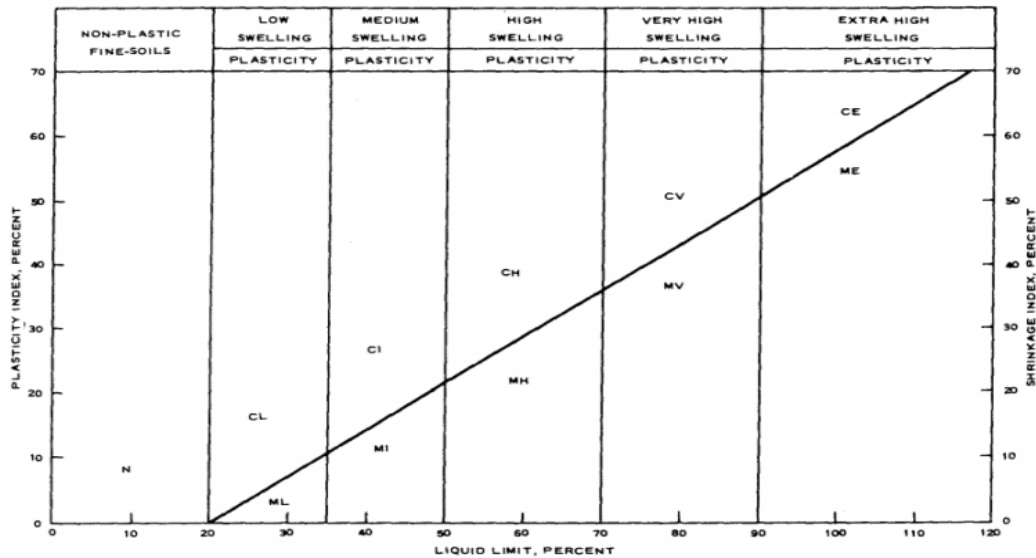
Figure 2. 12 Chart of potential expansiveness of soil

ii. **Skempton (Mckeen, 1976)**

This method is developed, by combining Atterberg limits and clay content into a single parameter called Activity. kempton suggested three classes of clays according to their activity shown below

Table 2. 7 Relation between clay activity and potential of expansion (Chen, 1988)

Activity	Potential of expansion
Ac < 0.75	Low (inactive)
0.75 < Ac < 1.25	Medium (normal)
Ac > 1.25	High (active)

iii. **Chen Method (1988)**

Chen, (1988) presented a single index method for identifying expansive soils using only plasticity index. According to plasticity indices shown below

Table 2. 8 Relation between the swelling potential of clays and the plasticity index, (Chen, 1988)

Swelling Potential	Plasticity Index

17

Low	0 - 15
Medium	10 - 35
High	20 - 35
Very High	935 and above

iv.   USBR Method

This method developed by Holtz and Gibbs; it is based on direct correlation of observed volume change with colloid content, plastic index and shrinkage limit. The classification given below

Table 2. 9 Classification based on bureau of reclamation method

Colloid Content (%)	Plasticity Index (%)	Shrinkage Limit (%)	Probable Expansion (%)	Degree of Expansion
< 18	> 15	> 15	< 10	Low
15 – 28	15 – 28	10 - 20	10 - 20	Medium
25 – 41	25 – 41	20 - 30	20 - 30	High
> 35	> 35	> 30	> 30	Very High

2.7 Soil stabilization

Chen, F.H (1981) and Perloff W.H (1976) soil stabilization may be defined as the alteration or preservation of one or more soil properties to improve the engineering characteristics and performance of soil. Expansive soil can create significant problems for pavements Black cotton soil exhibits low bearing capacity when it is subjected to moisture, has the ability to absorb and dissipate water with subsequent change in volume. Construction of pavement on this type of soil requires either replacement of soil by importing a better material or stabilizing existing soil to the desired property. On-Road construction subgrade soil is a foundation for the Road pavement it should support traffic loading and pavement itself. The stabilization process may include blending of soils to achieve a desired gradation or mixing of commercially available additives that may alter the gradation, texture, or plasticity or act as a binder for cementation of soil (Guyer et al, 2011). There are two types of stabilization of soils namely mechanical stabilization and chemical stabilization.

2.7.1 Mechanical Stabilization

Mechanical stabilization is the process of improving the mechanical properties of the soil by blending or mixing soil adhesives with the soil to obtain a material that meets the required specification. In this process stability and shear strength characteristics of sol without altering the chemical properties of the soil.

2.7.2 Chemical Stabilization

Soil stabilization using chemical admixtures to stabilized subgrade soil. Chemical stabilization involves mixing if one or more admixture together with problematic soil to improve or control its stability, strength, swelling, permeability and durability. Common chemical stabilizing agents are port land cement, lime, asphalt, calcium chloride, sodium chloride and paper mill wastes. The selection of particular additive depends on its costs, benefits, availability and practicality of is application (US army, 1994). Chemical stabilization proceed through a combination of four basic mechanisms: (i) Cation exchange or ion exchange; (ii) flocculation and agglomeration; (iii) pozzolanic reaction; and (iv) carbonation (Bell FG, 1996) However carbonation reaction is not desired in lime treatment because it would subtract the lime to other modification/stabilization reactions and hence has minor influence or sometimes detrimental effect on the strength behaviour (Diamond et al, 1965).

(i)   Cation exchange

Ion exchange is reversible property of soil. Cations or anions that are absorbed on the soil surface are exchanged with another cation or anion in soil. Cation and anion exchange in soils occurs on the surfaces of clay minerals and organic matters. These ions can be replaced by a group of different ions having the same total charge, by altering the chemical composition of the equilibrium electrolyte solution. Negatively charged clay particles adsorb cations of specific type and amount. The ease of replacement or exchange of cations depends on several factors, primarily the valence of the cation. Higher valence cations easily replace cations of lower valence. For ions of the same valence, the size of the hydrated ion becomes important; the larger the ion, the greater the replacement power. If other conditions are equal, trivalent cations are held more tightly than divalent and divalent cations are held more tightly than monovalent cations. The most common exchangeable cations are Ca^{++}, Mg^{++}, H^+, K^+, $NH4^+$, Na^+, often in about that order of general relative abundance. Chemicals in balance with the negatively charged clay surface and the positive cations in the solution adjacent to the clay are referred to as the double diffusion layer (DDL).

When these DDLs ''s occur there is a repulsion force generated between the clay particles due to the concentration of negative and positive charge. This contributes to the swell pressure. The replacement of univalent ions by divalent ions provides a strong attraction between particles as these reactions take place thickness of the diffused double layer decreases. Hence, swelling potential decreases (Bililgn, 2019).

(ii)   Flocculation and agglomeration

Flocculation and agglomeration is the rearrangement of clay particles from face to orientation to the more compact edge–face orientation. Fine-grained soil changes to more cores grained with much more improved strength or stiffness as well as workability (Brook, 2009). Due to changes in texture, there will be a significate reduction in swelling of soil to occur.
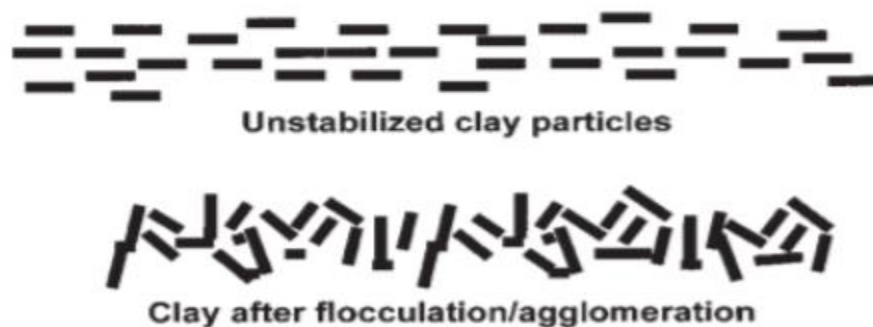
Figure 2. 13 Flocculation and Agglomeration of clay Particles (Prusinski and Bhattacharja 1999)

(iii)   Pozzolanic reaction

Soil stabilization occurs mainly due to the pozzolanic reactions. Pozzolanic reaction are facilitated by the dissolution silica (Sio_3^{2-}) and alumina ($Al_2O_3^{2-}$) from clay particles at highly alkaline environment in pore chemistry. Pozzolanic constituents produce calcium silicate (CSH) and Calcium aluminate hydrate (CAH) These compounds bind the flocculated soil particles and fill the soil matrix, leading to increase in shear strength and improve volume change behavior. Pozzolanic reaction in order to occurred PH of is necessary (Eades, 1960).

2.8 Previous works

Rajasekaran et al., (1995) investigated the influence of sodium hydroxide on the fabric of lime treated marine clays using scanning electron microscopy (SEM) technique. And found that lime stabilization is very effective for marine clays. Adding sodium hydroxide additive resulted in the better formation of pozzolanic compounds. The study conducted by using SEM indicated that there is an overall improvement in the structure of the soil system resulting in a porous system and aggregate formation. However, this study was limited to only lime-stabilization.

Bethlehem (2015) Investigated the effect of sugarcane bagasse ash on the geotechnical properties of A-7-6 class lateritic soil collected from Mekenajo, 456 km west of Addis Ababa. The lateritic soil stabilized with 2 %, 4 %, 6 %, 8 %, and 16 % of Sugarcane bagasse ash by weight of dry soil. Test specimens subjected to the Atterberg limit, free swell, linear shrinkage, and compaction and CBR tests. The analysis of results showed a little decrease within the utmost dry density and soaked CBR values. The free swell also showed a little decrement up to 4 % of ash, then showed an increase. A small increase in plasticity index, shrinkage limit, and optimum moisture content and unsoaked CBR values also observed. The rise of the curing period showed an insignificant effect on the CBR values of the stabilized soils. From the results concluded that sugarcane bagasse ash wasn't an efficient stabilizer for the development of a number of the geotechnical properties of the soil on its own.

Anoop et al., (2017) studied the properties of soil stabilized by lime and eggshell powder, and Tests conducted to assess the potential of eggshell powder in replacing lime, which may make the general stabilization process economical and eco-friendly. Results obtained show that each one of the treated mixes gave far better strength than untreated soil. The Eggshell powder introduced in quantities of 0.5 %, 1 %, 1.5 % and 2 % of the weight of soil. In his study, 50% lime used for stabilization. It observed that 25 % replacement of lime by eggshell powder gave better strength properties and can be adopted for practical purposes.

Cheng-lon (2018) studied the consequences of initial water content on the compressibility, strength, microstructure, and composition of a lean clay soil stabilized by

compound calcium-based stabilizer investigated by static compaction test, unconfined compression test, optical microscope observations, environment scanning electron microscopy, energy-dispersive X-ray spectroscopy, and X-ray diffraction spectroscopy. The results show that as the initial water content increases in the range studied, both the compaction energy and the maximum compaction force decrease linearly and there are fewer soil aggregates or agglomerations, and a smaller proportion of large pores in the compacted mixture structure. In addition, for specimens cured with or without external water supply and under different compaction degrees, the variation law of the unconfined compressive strength with initial water content is different and therefore the highest strength value is obtained at various initial water contents. With the rise of initial water content, the share of oxygen element extends within the reaction products of the calciumbased stabilizer, whereas the crystalline mineral of the soil did not change obviously.

Sudhakaran and sharma (2018) Study with the bottom ash and areca fiber wastes for the stabilization of clay soil. The varies volumes are substitution of bottom ash in percentages is 0 %, 10 %, 20 %, 30 % and 40 %, the areca fiber percentages is 0 %, 0.5 %, 1 %, 1.5 % with an addition of 3 % cement used. From the test results, its usage of bottom ash on the MDD is increased gradually 1.44 g/cm3 to 1.65 g/cm3. The max occurs at 30 % of bottom ash if adding more than 30% MDD decreased. It decreases OMC from 28.7 % to 18.5% for the addition of 30 % of bottom ash. CBR for soil in case of unsoaked condition its increases from 2.25 % to 39.45 %, soaked condition its increases from 1.2 % AASTU 28 to 29.98 % a mix of (30 % bottom ash + 1.5 areca fiber + 3 % cement). It concludes the improve the properties of clayey subgrade soil by use of 30 % bottom ash along with 1.5 % areca fiber and 3% cement in soil content.

Reshid Musema 2014 studied stabilization of expansive soils with lime. Acase study on A Case Study on the Adura-Burbey DS6 Road Segment 150km away from the Gambela town, Ethiopia. He pointed out the addition of lime reduces the plasticity index and reduction of free swell of the soil. Also he mentioned lime up to 12% dose not bring a significant improvement in California bearing ration which falls in the range of 7 -12 %5 percent But the achievement improving the sub grade quality is cost effective because this will reduce the use of borrow materials on the project.

Habtamu Solomon has evaluated the performance of locally manufactured hydrated lime and an imported industrial product Anyway Natural Soil Stabilizer (ANSS) in laboratory test. Expansive subgrade soil were collected from Gerji, North eastern Addis Ababa. Two soil layer were observed dark gray clay and light gray clay soils, their chemical property and necessary laboratory test were done. Finally he concluded that increase amount of lime has significant effect than that of increasing the curing period. The performance of hydrated lime is better than that of ANSS (Habtamu.S , 2011).

K.J.Osinubi studied effect of iron ore tailing (IOT) on cement modified black cotton soil. For his study black cotton soil sampled from a borrow pit Gombe State, Nigeria. Ordinary port land cement and iron ore tailing were used through his study. From his study maximum dray density (MDD) values of the soil increase while optimum moisture content (OMC) decreases with high cement and iron ore tailings content. Microanalysis carried out shows an improvement of the geotechnical properties of the modified soil. The experiment shows that 4% cement and 6% IOT improved workability of the soil (K.J.Osinubi, 2015).

R.K.Etim evaluated the stabilization of black cotton soil with lime and iron ore tailing used as admixture. Black cotton soil sampled from a deposit along Gombe – Biu road, Nigeria. Compaction characteristics of black cotton soil generally followed the trend of increasing MDD and corresponding decrease in OMC with higher lime and IOT contents. Scanning electron microscope (SEM) analysis shown that crystalline hydration products were present in the lime-IOT treated soil and these hydration products were assumed to be major factor contributing to strength improvement (R.K.Etim. et al, 2017).

CHAPTER THREE
MATERIAL AND METHODS

3.1 Introduction

Soil formation is highly dominated by the surrounding environmental factors, such as climate conditions and the geological and physiographical setup of a specific area. The stability and durability of pavement and building are largely dependent on characteristics of subgrade soil. For a proper treatment of expansive soils, it is important to adequately identify and understand the characteristics of expansive soils and materials used for soil treatment. Proper treatment procedures should also be adopted for the successful characteristic improvement of expansive soil. The material used and method adopted for the research work, are described briefly in this chapter.

3.2 Description of the study area

3.2.1 Location and topography

The study area is located southeast of the city Addis Ababa, Akakki Kality sub-city Addis Ababa Ethiopia. This is 25 Km from the capital city of Addis Ababa. The sample was taken from 483275.499 E 982151.613 N and 2226.91m elevations from sea level. In general, the area is accessible by foot and four-wheel drive vehicles, mainly during dry seasons. During rainy seasons, most parts of the study area are waterlogged and the soil becomes sticky and slippery making accessibility difficult. The location of the study area is shown in **Figure 3.1.**

Figure 3. 1 Study area, (Google Earth Map)

3.2.2 Climate condition

Ethiopia is classified into five climatic zones (EMA, 1981). These include "Kur"(Alpine), above 3000 m mean sea level; "Dega" (Temperate), 2300 m to about 3000 m; "Weina Dega" (Subtropical), 1500 m to about 2300 m; "Kolla" (Tropical), 800 m to about 1500 m and "Bereha" (Desert), less than 800 m. Most parts of Addis Ababa fall under the Weina Dega (Subtropical) category. The maximum temperature of Addis Ababa ranges between 17 0c (in the wet season) to 27 ^{0}c (in the dry season) for the last 10 years.
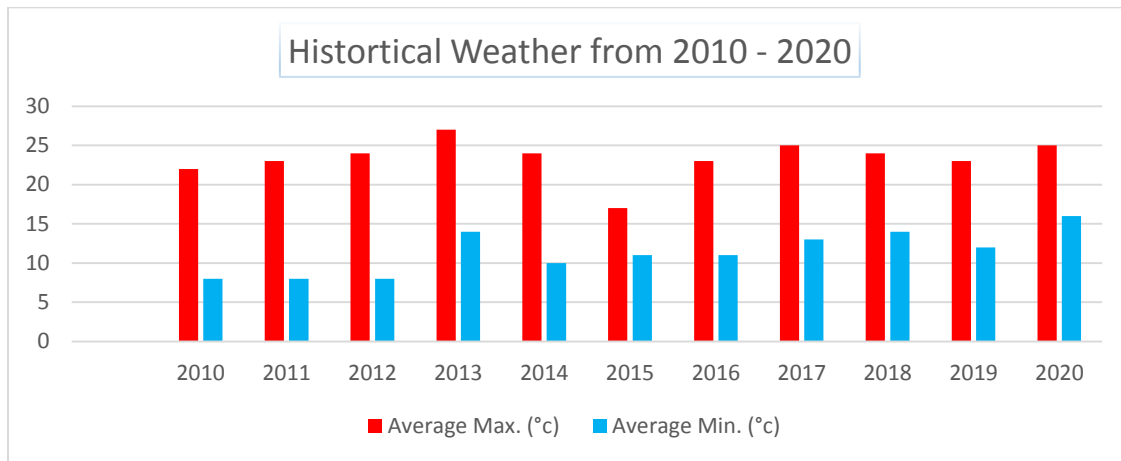
Figure 3. 2 Average temperature in Addis Ababa City from 2010 – 2020 (World Weather)

3.2.3 Geology

Addis Ababa is found in the rift valley of Ethiopia and consists of different volcanic rocks that range from basic to acidic composition, belong to the trap series (Tamiru et al., 2006). The physiographic map of Addis Ababa shows that the city is founded on an area with a well-developed morphology as shown in Figure 3.3. It is surrounded by high rising mountain systems in all directions and the center of the city lies on an undulating topography with some flat land areas. The urban area of the city is deeply dissected by numerous valleys formed by the river systems crossing the city from north to east.

The North and North Eastern area (the Entoto Mountain, the northern and northeastern Addis Ababa) is covered with trachytes, rhyolites, basalts and several episodes of pyroclastic materials of older volcanism occur in the upper part and foothill sides of Entoto ridge. Overlying these, younger basaltic rocks (Addis Ababa Basalt) are found covering the central and southern parts of the city. Outcrops of ignimbrites north of the Bole area (Eastern Addis) and Lideta area (Central Addis) have been observed underlying the Addis Ababa basalt. Younger volcanic of trachy-basalt,

trachytes, ignimbrites, and tuff belonging to the Wochecha, Furi and Yerer volcanoes are recognized overlying un-conformably on the Addis Ababa basalt in the western, South-Western, and eastern part. The lacustrine formations covers Bole, Lideta, Mekanisa, Akaki-Aba Samuel area. Some alluvial deposits also occur along the Akaki river in the southern and south-western part of Addis and minor deposits also occur along the Kebena river in the area North-West of Bole (Solomon, and Yirga, 2006).
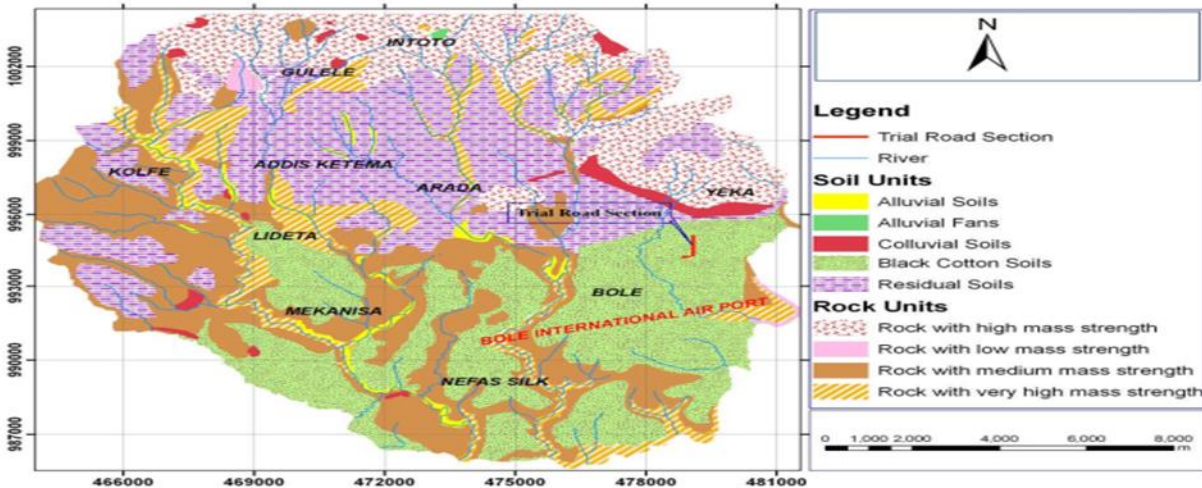
Figure 3. 3 Engineering Geological Map of Addis Ababa (Kebede and Tadesse, 1990)

3.3 Materials

3.3.1 Expansive Soil

The expansive soil sample used for this research work was collected from an active site in Addis Ababa Akaki Kality sub-city, Housing development project 18 Road project. The location was a sample taken from Road 27 station 0+530 RHS & 0+630 center of the road according to the project site location. The soil is grayish-black in color and a disturbed sample was collected at depth of 1.2 m from natural ground level in order to avoid the inclusion of organic matter.

Figure 3.4 Soil Sampling

3.3.2 Lime

There are different types of lime used for stabilization, the most commonly used products are hydrated high-calcium lime, monohydrated dolomitic lime, quicklime, and dolomitic quick lime. For this study lime was used from commercial hydrated lime from authorized dealers in Addis Ababa.

Figure 3. 5 Lime Powder

3.3.3 Iron ore tailing

Iron ore tailing for this study was sampled from Ethiopian Metal Melting Factory, which located in Akaki Sub-city Addis Ababa 8° 51′ 07″ N, 38° 47′ 19″ E elevation. For research purposes, 30 Kg waste iron tailing was taken from wastage accumulated and tried to change well graded by hand hammer to decreases its size. Then properly packed in sacks and transported to the laboratory.

Figure 3. 6 Iron Ore tailing collection process from Ethiopian Metal Melting Factory

3.4 Experimental program

3.4.1 Sample preparation

Sample preparation made on natural soil, lime, and Iron ore tailing to make them suitable for successive laboratory tests. The sample was prepared by the method described in AASHTO T87-86. The moist soil sample which is taken from the site were Air dried and clumped soil was crushed using a rubber-covered hammer and quartered to get representative samples. Depending on the laboratory test require soil and IOT samples were prepared by 0.425 mm (No 40 sieve), 4.75 mm (No 4 sieve), and 2.00 mm (No 10 sieve).

3.4.1.1 Mixing soil and stabilizers

i. Percentage Rates

Percentage rates can be specified in many different ways. Traditionally used powder stabilizers are proportioned by weight, commercially available liquid stabilizers are proportioned by weight, commercially available liquid stabilizers are proportioned by volume and some are specified by the manufacturer. The most common way to define the percentage rate is based on the dry weight of soil to be treated. For this study, stabilizers used in this research are by a percentage of the dry weight of the untreated soil. The experimental study was conducted into three groups including untreated soil, untreated soil with stabilizer iron ore tailing, and untreated soil with iron ore tailing and lime. Lime was used in this study as an admixture in order to improve its geotechnical index properties from the border of standard specification requirements. Accordingly, Table 3.1 shows the mix design. The mix design for the study was done after conducting a laboratory test to find

the optimum amount of IOT together with black cotton soil and after optimum amount of IOT obtain by adding lime by different proportion by basing the optimum amount of IOT was done.

Table 3. 1 Mixing proportion of material

Mix	BCS (%)	Lime (%)	IOT (%)
BCS	100	-	-
BCS +IOT	98	-	2
BCS +IOT	96	-	4
BCS +IOT	94	-	6
BCS +IOT	92	-	8
BCS +IOT	90	-	10
BCS +IOT	88	-	12
BCS +IOT	86	-	14
BCS +IOT	84	-	16
BCS + Lime + IOT	93	2	5
BCS + Lime + IOT	88	2	10
BCS + Lime + IOT	83	2	15
BCS + Lime + IOT	78	2	20

ii. Mixing Procedures

After the soil Air dried and pass through the 4.75 mm sieve size which is required laboratory test. The same techniques were done based on their experimental groups.

(i)   (ii)

Figure 3. 7 (i) sample mix & (ii) Thorough hand mix for the soil

3.4.2 Laboratory test

I. Grain size analysis (AASHTO T-27)

Grain size analysis of soil is generally carried out by two methods dry sieving and wet sieving. The analysis is done by wet sieving for analysis by measuring 200 g of oven-dried soil, passing 4.75 mm (No.4 sieve). Soil soaked in a tray containing water for 5 hrs. Then soaked soil washed using 0.075 mm (No.200 sieve). Sieve placed on a bucket. Poured the clear water on the sieve continue to pour the water till water passing the sieve is substantially clear washed or retained 0.075 mm (No. 200 sieve) placed in an oven at 110 °c for 24 hr. Dry soil (in the oven) performed sieve analysis was done and test results were attached on the Appendix. Both AASHTO and USCS define grain size ranges (Bowles, 1992) as:

AASHTO	USCS
Gravel > 2 mm	Gravel > 4.75 mm
Sand 0.075-2 mm	Sand 0.075-2 mm
Silt 0.002-0.075 mm	Silt 0.002-0.075 mm USCS
Clay < 0.002 mm	Clay < 0.002 mm USCS

(a)   (b)

Figure 3. 8 Grain Size Analysis (a & b)

II. Moisture content of the soil (AASHTOT-265)

The test is conducted by AASHTO T265   the oven-drying method was used to determine the moisture content of the disturbed soil samples. Representative natural soil specimens were

obtained from a medium-grained 250 g soil sample taken by a clean dry metal container. Soil specimen placed loosely in the metal container and its weight measured. The container is placed in the oven at 110 °c for 24 hrs. After this, the container is taken out of the oven, keep for cooling. Final dry weight is determent and the difference in weight was assumed to be the weight of the water driven off during drying. The difference in weight was divided by the weight of the dry soil, recorded as the initial moisture content.

III.   Specific gravity (AASHTO T-100)

The density bottle method followed to experiment. On the first step clean bottle, its name and weight were recorded. Oven-dried soil which passes 2mm sieve about 15g measured and inserted into the bottle. Together soil and bottle masse recorded and after this bottle filled by soil with distilled water about its half. Bottle put on the stove until there are no more air bubbles are observed in the soil-water mixture. And then filled it with water and its weight recorded. After this bottle makes empty and filled with free distilled water wipe and weigh. After making this process and recording necessary data specific gravity calculated for natural soil and all soil lime – IOT mixture.

IV.   Atterberg Limit

In Swedish Agricultural engineer, Atterberg mentioned that a fine-grained soil can exist in four states namely liquid, semi-plastic or solid-state. The water contents at which soil changes from one to another are known as consistency limits of Atterberg's limits (ARORA, 2004). The test is a consistency Limit identification test based on moisture content. It includes the determination of; the liquid limits, plastic limits, and the plasticity index for the natural soil and the soil-lime-IOT mixtures. The tests are conducted by AASHTO T89-90 and T90-96 testing procedures.

a) Liquid Limit

The soil sample for the liquid limit was air-dried and 200 g of the material passing through 0.425 mm (No.40 sieve) was obtained and thoroughly mixed on a flat glass plate with water to form a homogeneous paste. A portion of the soil water mixture was then placed in the cup of the Casagrande apparatus leveled off parallel to the base, The liquid limit (LL) is arbitrarily defined as the water content in percent at which pat of soil in Cassagrande's cup cut by a groove of standard dimensions will flow together at the base of the groove for a distance of 13 mm. when subjected to 25 blows from the cup being dropped 10 mm in a standard liquid limit apparatus operated at a rate of two blows per second. The test is performed for well–spaced out moisture content from the drier to the wetter states. The values of the moisture content determined and the corresponding number of blows are then plotted on a semi-logarithmic graph. The liquid limit is determined as

the moisture content corresponding to 25 blows from the graph. The same procedure is also carried out for the soil treated with varied contents of lime and IOT.

b) Plastic Limit

About 15 g of oven-dried soil specimen passing through 0.425 mm (No.40 sieve) is taken and mixed thoroughly with distilled water until the soil specimen becomes plastic enough to easily mold into a ball with fingers. A portion of the ball and rolled on a glass plate with a palm to form the soil mass into a thread of uniform diameter of 3 mm is reached. The soil is remolded again into a ball. Repeated the test with 2 more samples. The tread of uniform diameter of 3 mm soil and soil-IOT, soil –lime - IOT mixture is then put in the moisture container and the moisture content determined. The plastic limit is taken as the average of the three water content values.

c) Plasticity Index

The plasticity index of the natural soil and soil–lime-IOT mixture is the numerical difference between the liquid limits and their corresponding plastic limit. The plasticity indexes of the samples are calculated by

$$PI = LL - PL \qquad\qquad (3.1)$$

Figure 3. 9 Atterberg Limit Testing

This test includes the determination of the free swell index of the natural soil, soil -IOT, and soil–lime-IOT mixture treated samples in accordance AASHTO T-256 testing procedure. The test is performed by taking 10 g soil specimen of oven-dry soil passing a sieve size of sieve 0.425 mm (No. 40 sieve). Soil specimen poured into a graduated cylinder of 50 ml capacity. And then graduated cylinder filled with distilled water up to 50 ml mark. Samples are left undisturbed to attain an equilibrium state of volume without any further change in the volume of the soil for 24 hrs. Then the swelled Volume of the soil after the material settles is measured. Free swell index is computed using Equation (3.2) shown below. The same procedure was followed for the treated soil.

$$Free\ Swell\ (Fs) = \frac{(Vf - Vo)}{Vo} * 100\% \hspace{3cm} (3.2)$$

V_f = Soil Volume after swelling, cm^3
V_o = Volume of dry soil, 10 cm^3

Figure 3. 10 Free swell index test

VI. Shrinkage Limit

Shrinkage limit is the maximum water content at which a reduction of water content will not cause a decrease in volume of soil mass. The sample is first air-dried and placed in an oven for complete drying. On further drying, the water begins to withdraw from the interior of the soil, whose color then changes from dark to light. The surface of the desiccating soil shows a characteristics pattern of shrinkage crack. The finer the particle of the soil.

a) Linear Shrinkage

Linear shrinkage is a measure of how a sample will reduce in length upon complete drying expressed as a percentage of the original length. A linear shrinkage test was carried out to determine the linear shrinkage characteristics of the natural as well as the treated soil. Linear shrinkage (LS) was calculated as a percentage of the original specimen from the equation,

$$Linear\ Shrinkage\ (Ls) = \frac{(Lo - Ld)}{Ld} * 100\% \qquad (3.3)$$

Lo = Original Length of the Mold
Ld = Length of dry specimen

Figure 3. 11 Linear Shrinkage

VII Compaction

This test includes the determination of the maximum dry density and the optimum moisture content in accordance with AASHTO T99-94 testing procedures. The test is conducted for both the natural and soil-lime IOT mixtures. By varying the moisture content for each trial, air dried soil sample of about 2.0 kg are used. Every sample is then compacted into the 890 cubic centimeters of mass; in three layers of approximately equal mass with each layer receiving 25 blows. The blows tried to make uniformly distributed over the surface of each layer. The collar is then removed and the compacted sample leveled off at the top of the mould with a straight edge. The mould containing the leveled sample is then weighed to the nearest 1 g. One small representative sample is then taken from the middle of compacted soil for the determination of moisture content. The same procedure is repeated until minimum of five sets

of samples are taken for moisture content determination. The bulk and dry densities are then calculated for each compacted specimen. The values of the dry densities are plotted against their respective moisture contents; MDD is deduced as the maximum point on the resulting curves. The corresponding value of moisture contents at maximum dry densities, which is deduced from the graph of dry density against moisture content, gives the optimum moisture content OMC.

(a)   (b)

Figure 3. 12 Compaction Test

VIII. Unconfined Compression Test

The Unconfined Compression Test determines approximate undrained shear strengths due to the slightly relaxed in situ pressures of the sample. This test is a fast and economical means of approximating the shear strength at shallow depths. A cylindrical soil sample diameter of 38 mm and height of which is 76 mm without any confining pressure, is subjected to an axial compressive load until failure occurs. Tests are performed by AASHTO T 208 for the natural as well as lime-IOT treated soils. Remolded samples were prepared after the required quantity of soil is determent from previously calculated values of the bulk density and moisture content of the compaction Tests. The equation to determine the unconfined compressive strength is given by

$$\text{Compresive force (P)} = \frac{qu}{A} \tag{3.4}$$

P= Compressive force (KN)

q_u=Unconfined Compressive Strength (Kpa)

A= Cross sectional Area (m²)

The changed average cross sectional area at particular deformation during the test was calculated using the following equation

$$A = \frac{Ao}{1-\varepsilon} \qquad\qquad (3.5)$$

A= Corrected cross sectional Area (m²)

Ao= Original cross sectional area (m²)

Ɛ= Axial strain, $\varepsilon = \frac{\Delta L}{L}$

The shear Strength is defined as half the compressive strength.

$$C = \frac{qu}{L} \qquad\qquad (3.6)$$

The total quantity of each needed to prepare the required number of test specimens each prescribed stabilizers percentage of maximum dry unit weight and water content specified in the Appendices.

Figure 3. 13 Unconfined compressive test

IX. California Bearing Ratio

The CBR and CBR Swell test are conducted following AASHTO T193 – 93 for the natural soil, soil - IOT, and soil - lime – IOT mixture. Soil sample tests were conducted for soaked soil samples. 6000 g of natural soil and soil-lime-IOT mixture are mixed at their respective optimum moisture

content which is obtained from the compaction test in 2124 cubic centimeters mold. The sample was compacted in three layers with 56 blows by 2.5 Kg rammer. Compacted soil samples of the CBR mold were soaked for 96 hrs in a water bath to get the soaked CBR and CBR swell of the soil. CBR swell of the soil is measured by placing the tripod with the dial indicator on the top of the soaked CBR mold. The initial dial reading of the dial indicator on the soaked CBR mold is taken just after soaking the sample. At the end of 96 hrs, the final dial reading of the dial indicator is taken hence the swell percentage of the initial sample length is given by:

$$CBR\ Swell = \frac{Change\ in\ height\ in\ mm\ During\ soaking}{116.3mm} \qquad (3.7)$$

After checking CBR swell is less than two. CBR mold is taken out from the water bath and left for a moment to let water drain from the mold before it's taken to the CBR test apparatus. The CBR is obtained as the ratio of load required to protrude a certain depth of penetration of a standard penetration piston into a compacted specimen of the soil at some water content and density of the standard load required to obtain the same depth of penetration on a standard sample of crushed stone. i.e

$$CBR\% = \frac{Test\ Load\ on\ the\ sample}{Standard\ Load\ on\ Crushed\ Stone} \qquad (3.8)$$

Figure 3. 14 CBR Test

Standard method of test for determining pH of soil using AASHTO T289. Using pH meter, an electrode is immersed in a sample of distilled water mixed together with 10 g soil which passes through 2.00 mm (No 10 sieve) natural soil and lime-IOT treated soil.
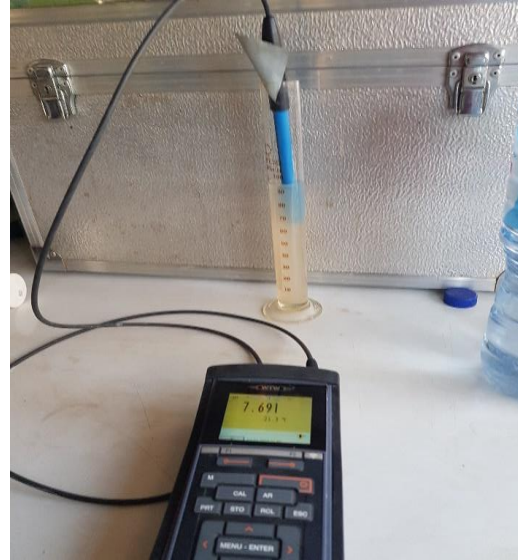
Figure 3. 15 pH Test

CHAPTER FOUR
TEST RESULT AND DISSCUSSION

4.1 Introduction

In this chapter, laboratory test results are briefly discussed and the effect of IOT on Black cotton soil and IOT- lime effect on Black cotton soil evaluated based on their laboratory test result. The

procedure followed for the analysis of the data primarily consists of performing mathematical and graphical illustration analysis coupled with subjective evaluation. Tabular and graphical analysis was adopted to determine whether lime stabilization has an effect on Atterberg limits, shrinkage limits, linear shrinkage, moisture density relations, California bearing ratios, and unconfined compressive strength of the sample.

4.2 Index of material used in the research

4.2.1 Natural Soil

A summary of the index properties of the natural black cotton soil before applying lime – IOT powder is presented in *Table 4.1*. According to the laboratory test result of the natural soil sample obtained during the present study almost 93.72% of the soil is passing through No. 200 sieves. It exhibits a liquid limit of 92%, a plastic limit of 47%, and plastic index of 45%. Liquid limit less than 35% indicates low plasticity between 35% and 50% intermediate plasticity between 50% and 70% high plasticity and between 70% and 90% very high plasticity (Nelson, 1992). The value obtained here is even beyond this range. Hence the value indicates that the soil highly plastic clay. The liquid limit and plastic index values are also very much greater than Ethiopian Road Authorities requirements (i.e liquid limit less than 60% and plastic limit index less than 30%).Based on the AASHTO classification system the soil falls under the A-7-5(20). According to the UCS soil classification system, the soil is MH (Elastic-Plastic clay). Hence, these test results indicate that the soil is highly plastic clay. Such soils are expansive soils that have high volume-changing properties with variation in moisture content (Chen, 1988). As far as the engineering performance of soils of these classes is concerned, such soils are potentially expansive soil that has high volume changing prosperity with a variation of moisture content (Chen, 1988; Mckeen, 1976). Swelling characteristics of soil show that the soil is highly expansive clay with a free swell of about 105% which is greater than 100%. The soil has a maximum dry density of 1.51 g/cm3, Optimum moisture content of 28.91%. The UCS value for remolded sample 147.09 Kpa and CBR value of 1.71%. This shows that the soil sample does not fulfill the requirements as a sub-grade material and unsuitable for sub-grade in road construction. Therefore, the soil requires initial modification and/or stabilization to improve its workability and engineering property.

Table 4. 1 Geotechnical Property of Natural Soil

Property	Station 0+530	Station 0+630

Colour	Grayish Black	Grayish Black
Percentage passing No. 200 Sieve (%)	93.39	95.2
Liquid Limit (%)	92	90
Plastic Limit (%)	47	48
Plasticity Index	45	52
Specific Gravity	2.72	2.74
AASHTO Classification	A-7-5(20)	A-7-5(20)
USCS	CH	CH
Natural Moisture content	11.98	10.5
Optimum moisture content (%)	28.91	30
Maximum Dry Density (g/cm^3)	1.51	1.32
Free swell index (%)	105	98
Linear shrinkage limit (%)	15.71	14
pH	7.69	7.57
Unconfined compressive strength (Kpa)	147.96	152
CBR	1.71	2
CBR Swell Value (%)	8.70	8

For stabilizing soil with lime-IOT, from the two station I used station 0+530. Because comping the station index values station 0+530 high expansive than the other station.
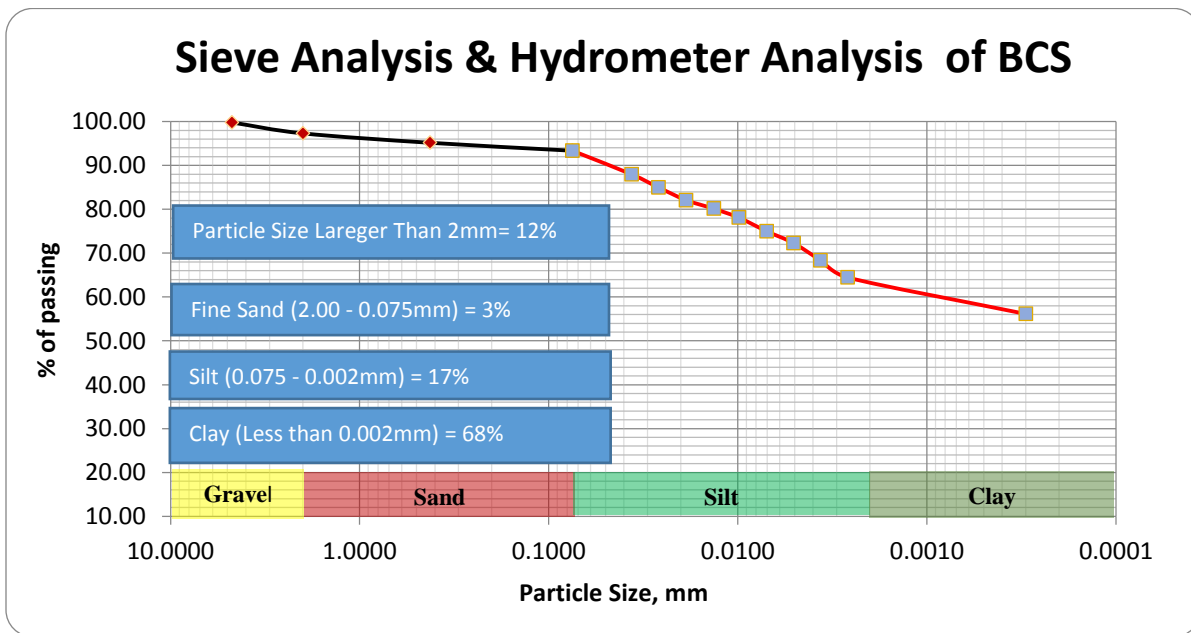
Figure 4. 1Particle size Distribution curve of the natural expansive soil

4.2.2 Iron ore tailing

Iron ore tailing which is used in this study gradation of the particles falls within the fine aggregates and having a bulk density of 1594 4kg/m^3. Size analysis of the tailings show that it ranges from fine (75µm) to coarse ($\leq$ 32mm). And having its specific gravity 3.33 which is heavier than untreated soil and its free swell also 0%.

4.3 Effects of admixture add on stabilized soil

4.3.1 Effect of Lime – IOT on Soil PH

Effect IOT alone and IOT with lime were observed by a varying proportion of the mix. The increase in the pH of the stabilized BCS indicates that the solubility of aluminate and silicate in soil increases, which can accelerate the pozzolanic reaction between the soil and stabilizers. Correspondingly Total Dissolved Solid (TDS) test shows increases.

4.3.2 Effect of Lime – IOT on Atterberg Limits

a) Effect of Lime – IOT on Liquid Limit

The variation of Liquid Limit of BCS – lime mixture with IOT content. Liquid limit decease with increase IOT content. This may be attributed to decrease in silt and clay fractions because of agglomeration and flocculation of the particles. This could be inked to cation exchange reactions were Ca^{2+} in IOT and lime reacted with lower valence ions present in clay structure (Ramesh et al, 2013 & Etim, R et al, 2017). The addition of lime and IOT introduced Ca^{2+} needed for strength which activated to decrease in the repulsive force of the soil mixture, requiring additional water for the soil to reach its dynamic shear strength (Osinubi.K, 1995). In another words, Calcium (Ca^{2+}) and hydroxides (OH-) produced by the addition of lime to the soil water system combined with silica (Si) and Alumina (Al) in the clay fraction to form calcium silicate hydrates and calcium aluminate hydrates(Bell,1988).

Table 4. 2 Summary of Atterberg Limits

Stabilization Description	Liquid Limit (LL) %	Plastic Limit (PL) %	Plastic Index (PI) %
BCS	92	47	45
Soil + 2% Lime + 5% IOT	74	34	40
Soil + 2% Lime + 10% IOT	65	33	32

Soil + 2% Lime + 15% IOT	55	28	27
Soil + 2% Lime + 20% IOT	49	25	24

Liquid Limit BCS reduced to 69% from 92% for BCS with IOT mixture. However, with IOT – lime mixture a minimum value of 49% was recorded at 2% lime and 20% IOT. A similar trend was reported by (Phani Kumar. et.al, 2004).
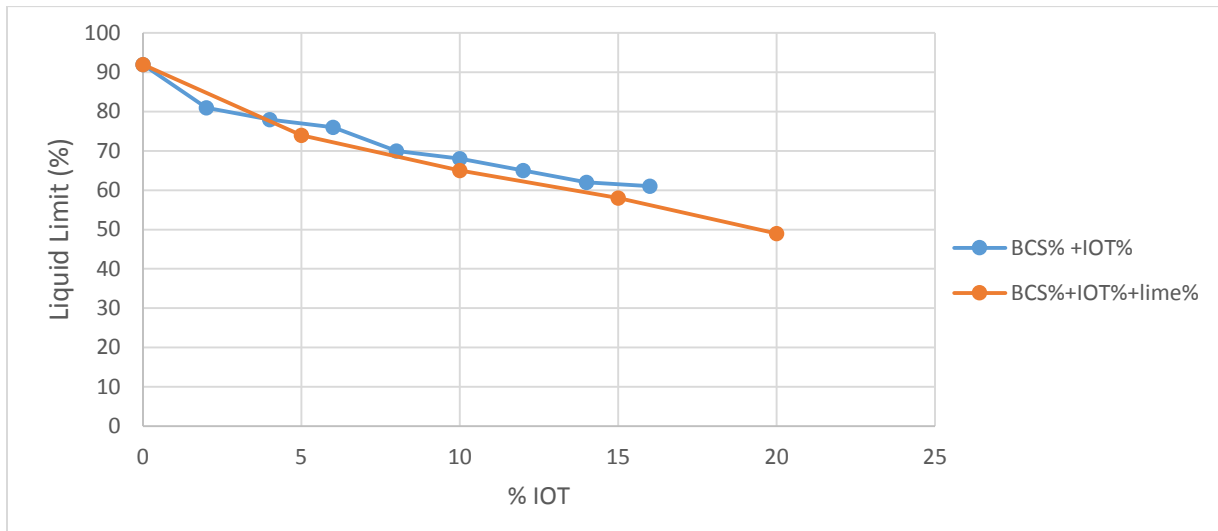
Figure 4. 2 Variation of Liquid Limit of BCS with IOT and IOT – lime mixture

b) Effect of Lime – IOT on Plastic Limit

The variation in the plastic limit (PL) of BCS-IOT mixture and BCS - IOT- lime mixtures is shown in Figure 4.3. PL decrease with increase IOT treatment alone and IOT - lime treatment from a value of 47% for the natural soil to a minimum value of 25% for 20% IOT with 2% IOT treatment. The observation decrease may be due to cation exchange reaction that liberated adsorbed water particles in the soil leading to the flocculation and aggregation of the soil (Osinubi, 1995).

42
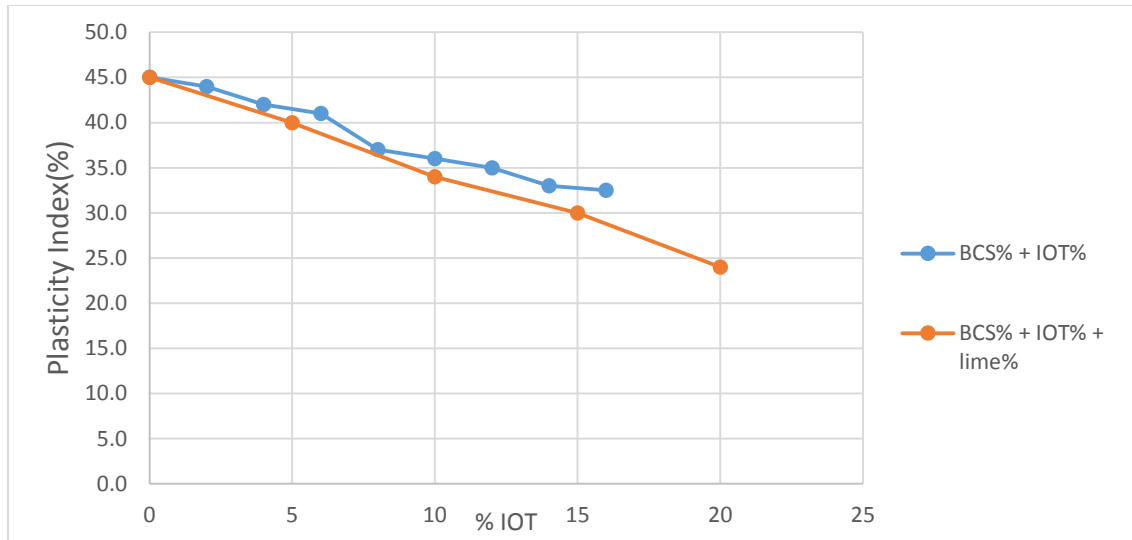
Figure 4. 3 Variation of Plasticity Index of BCS with Lime-IOT mixture

4.3.3 Effect of IOT and IOT with swell on free Swell

Free swell value decrease with increasing for both group of mix and shown figure 4.5. Soil treated with 2% lime & 20% IOT shows the highest reduction from 105% to 40%. The reduction in a free swell of black cotton soil could be attributed to a physicochemical reaction between the soil particles and lime-IOT blend that resulted in the formation of calcium silicate in the soil. This is responsible for the substitution of Ca2+ for absorbed H+ ions and neutralization of the net montmorillonite clay layer negative charge as reported by (Umar & Osinubi, 2003).
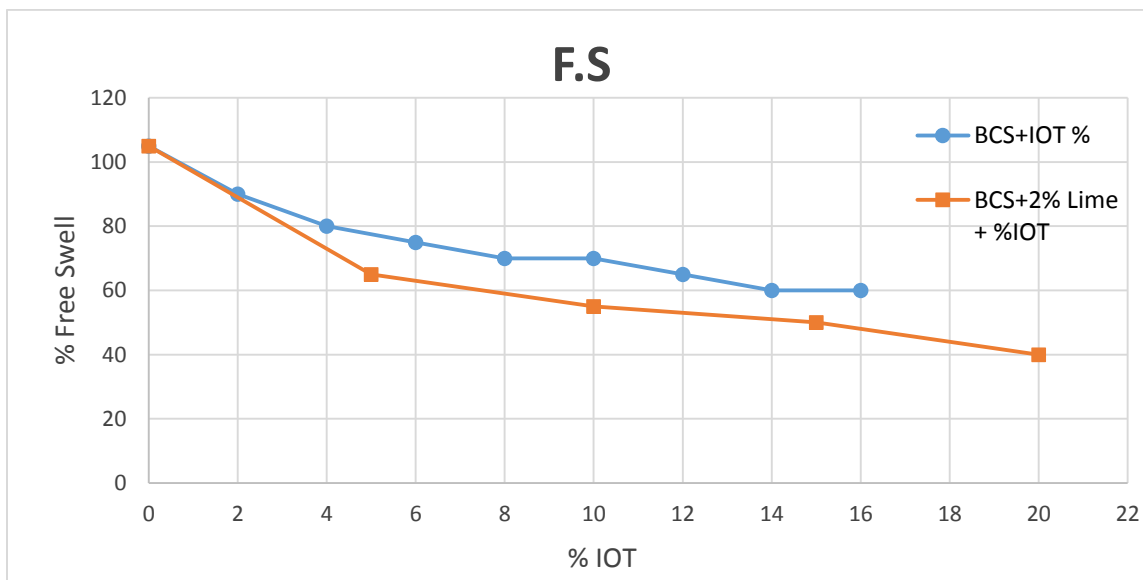
Figure 4. 4 Lime - IOT content Vs Free Swell

4.3.4 Effect of IOT and IOT with lime on specific gravity

The effect of lime – IOT powder on the specific gravity of expansive soil is shown in Figure 4.5 specific gravity increase from 2.72 to 2.88 with addition lime – IOT content from 5% to 20%. The observed increase in specific gravity could be attributed due to the higher specific gravity of Iron ore tailing (IOT) substituting the soil particles with lower specific gravity of 2.72.
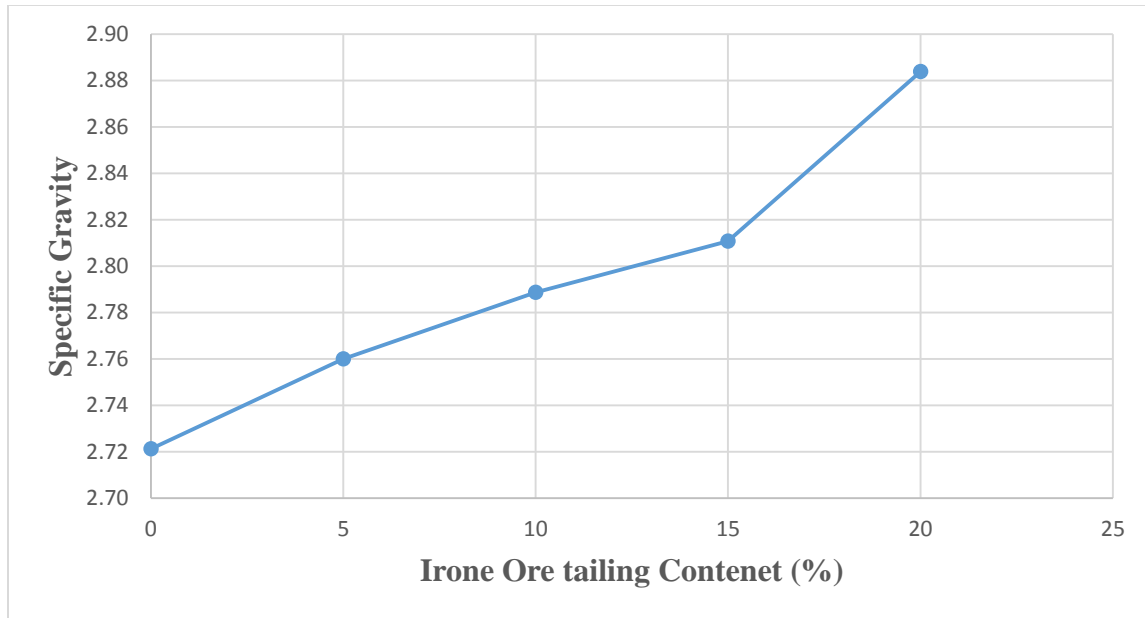
Figure 4. 5 Summary of specific gravity test

4.3.5 Effect of IOT and IOT with lime on compaction characteristics

The variation of maximum dry density (MDD) of black cotton soil mixture with IOT alone and IOT- lime is shown in Table 4.4. Generally, MDD values increased with lime-IOT content. The highest MDD value of 1.66 g/cm3 was recorded at 2% lime and 20% IOT treatment. The reason for to increase in MDD values was a result of the lime – IOT particles filling the voids with the soil matrix which resulted in better packing and denser material (Moses. G, 2008; Oriola. et.al, 2010 & Eti. R, 2017) and in the addition, the flocculation and agglomeration of the clay particles due to cation exchange (O' Flaherty,1988). Also, IOT with specific gravity (3.31) replacing the soil particles which have a lesser specific gravity of 2.72, contributed to the development of a mixture with higher specific gravity with higher MDD was formed as reported by (Ishola, 2014).

Table 4. 3 Summary of Compaction Test

Stabilization Description	MDD g/cm3	OMC%

BCS	1.51	29.00
Soil% + 2% IOT	1.52	26.14
Soil%+4% IOT	1.53	25.50
Soil%+6% IOT	1.54	23.68
Soil%+8% IOT	1.55	23.24
Soil%+10% IOT	1.58	21.55
Soil % +12% IOT	1.61	21.37
Soil % + 14% IOT	1.62	20.92
Soil % + 16% IOT	1.62	20.60
Soil + 2% Lime + 5% IOT	1.54	25.37
Soil + 2% Lime + 10% IOT	1.60	23.88
Soil + 2% Lime + 15% IOT	1.63	20.42
Soil + 2% Lime + 20% IOT	1.66	19.31

OMC of BCS mixture decrease with an increase in IOT-lime content. OMC value of natural soil decrease from 28.91% to 19.31% at 2% lime and 20% IOT treatment. The decreases in OMC may be linked to self-desiccation in which all the water was used, resulting in low hydration. When no water movement to or from soil- lime-IOT matrix is permitted, the water is used up in the hydration reaction, until too little is left to saturate the solid surfaces and hence the relative humidity within the paste decreases (Moses et al, 2012).
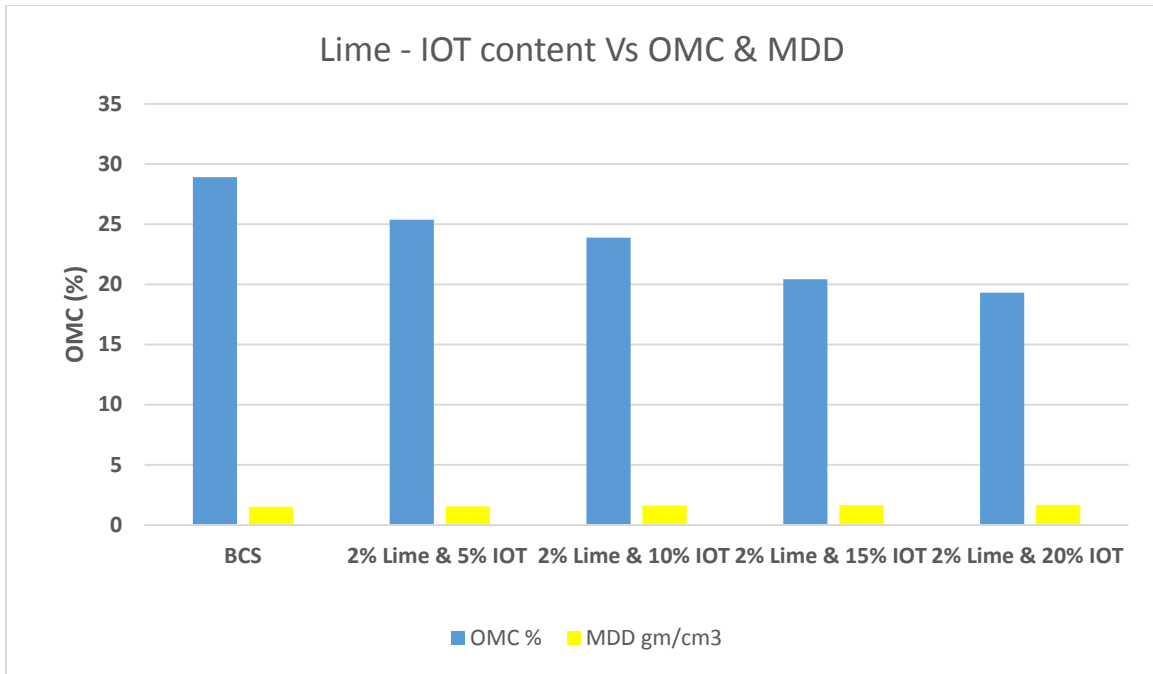
Figure 4. 6 Lime – IOT content Vs OMC & MDD

4.3.6 Effect of IOT and IOT with lime california bearing Swell & california bearing ratio (CBR)

4.3.6.1 California bearing ratio

The California bearing ratio (CBR) value improved with an increase in IOT and lime contents. The variation of CBR values of black cotton soil treatments with IOT - lime was recorded. CBR values increased from the natural soil value of 1.71% to 18.1% which the highest value was observed at 2% lime and 15% IOT treatment. This shows that the load-bearing capacity of the sample increased considerably with IOT - lime treatment can strongly improve the strength of expansive soils. However, 2% lime and 20% IOT show a reduction in CBR values. The decrease in strength with IOT content may be linked to excess IOT yielding lesser valence cations that could not be utilized with the available greater valence cations. This reaction increased the affinity of H+ caused the reduction.
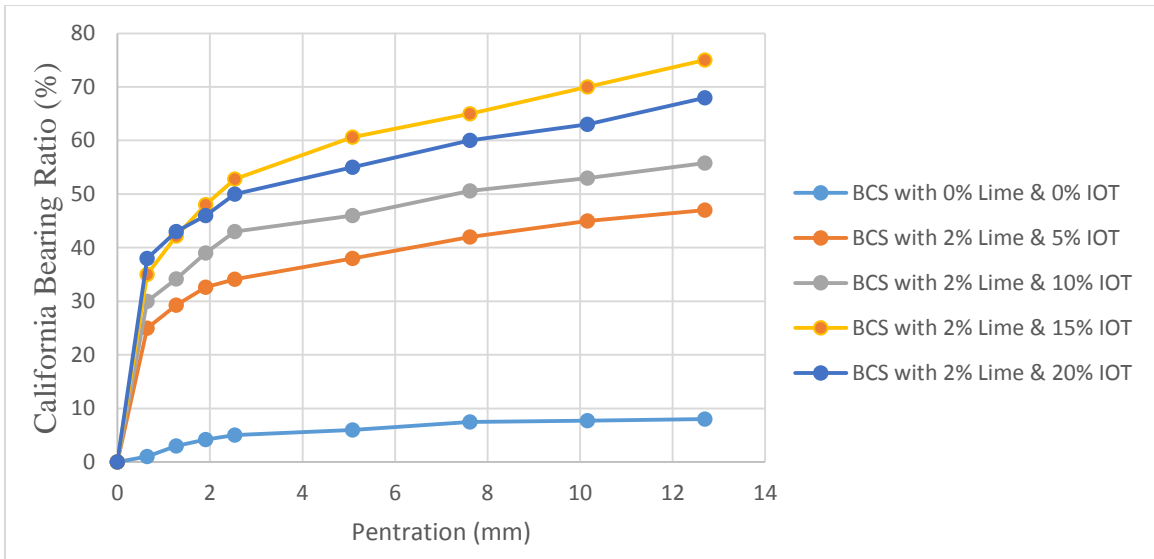
Figure 4. 8 CBR Penetration Curve Summary

4.3.6.1 California Bearing Ratio –Swell

CBR- Swell of all treated soil dramatically decreases with all lime - IOT & IOT treated soil results are shown in Figure 4.8. When expansive soil is treated with lime – IOT mixture decrease for all mixes from a natural soil value of 8.7% to 1.6% with the addition of 2% lime & 20% IOT powder. The main reason for to decrease is since material free swell is very low especially IOT compering to BCS.
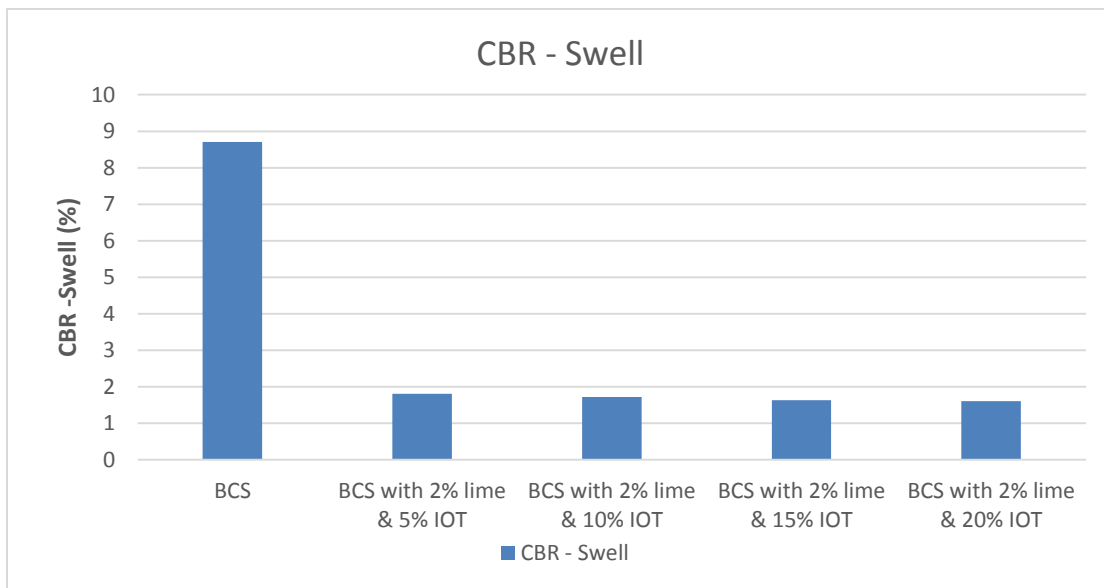
Figure 4. 9 CBR-Swell Summary

4.3.7 Effect of Lime – IOT on unified compressive strength (UCS)

The Variation of UCS of BCS – lime mixture with different proportion of IOT were shown in Table 4.5. UCS value increased with an increase in IOT content from 147.96 Kpa of BCS to 327.03 Kpa. And 7 days cured shows significant change 396.07 Kpa. The improvement in UCS was probably due to the development of substances like calcium silicate hydrates (CSH) Calcium aluminate hydrates (CAH) which leading to strength development (Ola S.A, 1983 & Negi S.S et al, 2013). The reaction continued in the presence of moisture and could have been a reason for the increase in UCS value.

Table 4. 4 Summary of UCS Value

Stabilization Description	UCS(qu), Kpa	Cohesion (Cu= qu/2), Kpa
BCS	147.96	73.54
BCS% + 2% IOT	182.11	91.05
BCS% + 4% IOT	189.86	94.93
BCS % + 6% IOT	205.36	102.68
BCS % + 8% IOT	236.29	118.14
BCS %+10% IOT	247.40	123.70
BCS % +12% IOT	252.13	126.06
BCS % + 14% IOT	274.93	137.46
BCS % + 16% IOT	286.52	143.26
BCS with 2% Lime with 5% IOT	180.67	90.33
BCS with 2% Lime with 10% IOT	249.63	124.82
BCS with 2% Lime with 15% IOT	306.10	153.05
BCS with 2% Lime with 20% IOT	327.03	163.51

4.3.8 Microstructural analysis by SEM

As shown the strength results obtained on stabilized soil expansive soil with IOT appeared appropriate for soil stabilization. The results obtained from unconfined compressive strength tests are compared with the results from SEM investigations. The Results of scanning electron microscopy obtained for untreated and selected treated sample are shown in figure. The

micrographs are taken from UCS test samples after 7curing days. The soil sample in the untreated condition, from individual clusters of various size are clearly obtained from SEM analysis. SEM results of (2% lime+5% IOT,2% lime +10% IOT,2% lime +15% IOT ,2% lime +20% IOT) sample pozzolanic product and of clusters in to denser structure in treated samples images, signifies the improvement in unconfined compressive strength of IOT- lime mixture with BCS.

From the raw soil and the selected sample, Powdered Specimens that are finer than 150mic sieve size were prepared since the samples are nonconductive material; they are coated with a thin layer of carbon. Figure 4-10 to 4-14 show the sample preparation for the SEM testing

Figure 4. 10 Preparation of Sample

Figure 4. 11 Inserting Powdered Sample to SEM imaging device

Observed features from the SEM imagining

In this study, the SEM image result were discussed based on two observation features, configuration of the sample and particle boundary relationship.
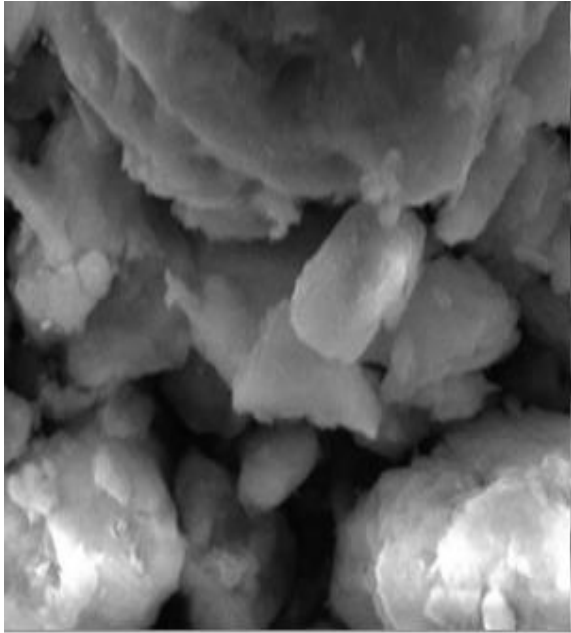
(a).4691x
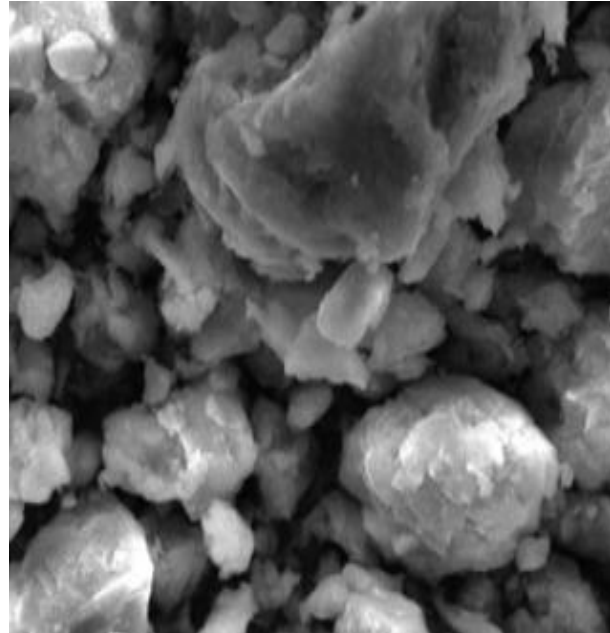
(b).11402x
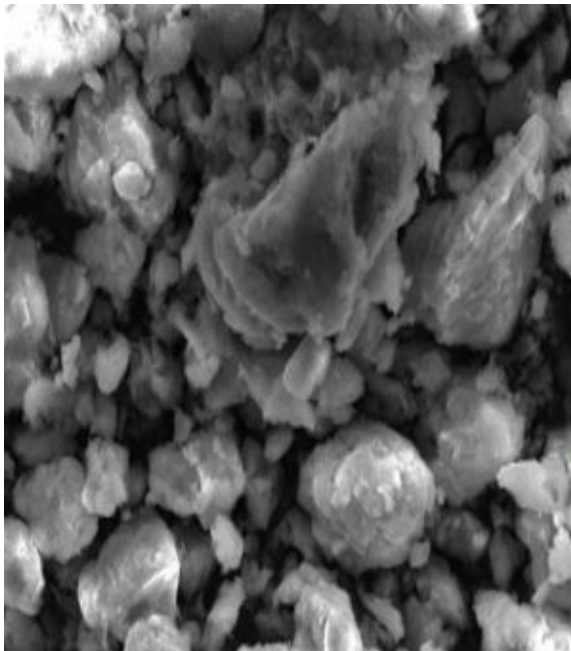
(c). 19173x
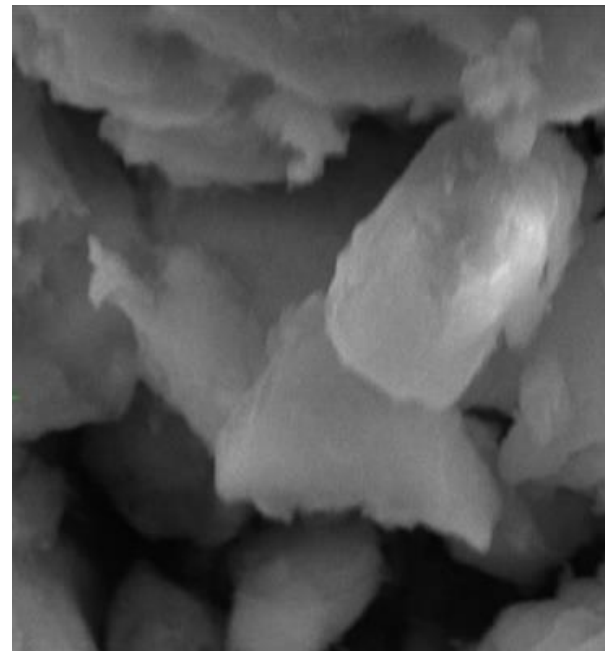
(d). 86249x

Figure 4. 12 SEM image of Black Cotton soil at different Magnification (a),(b),(c) and (d)
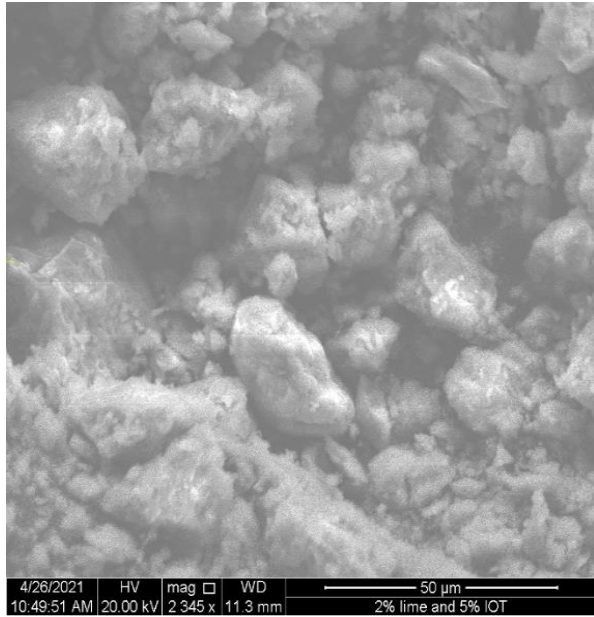
(a). 7234x
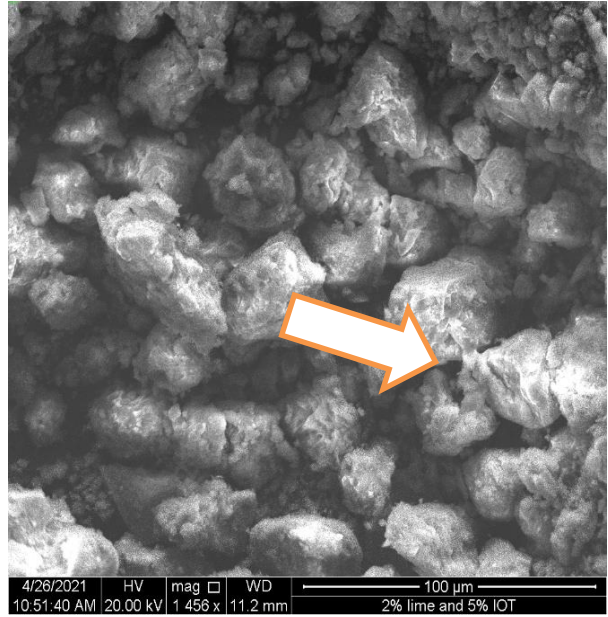
(b).14466x
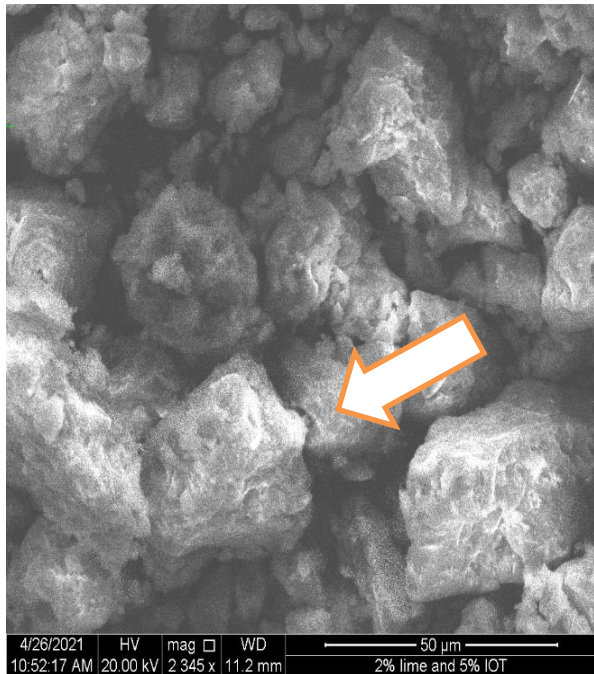
(c).23811x
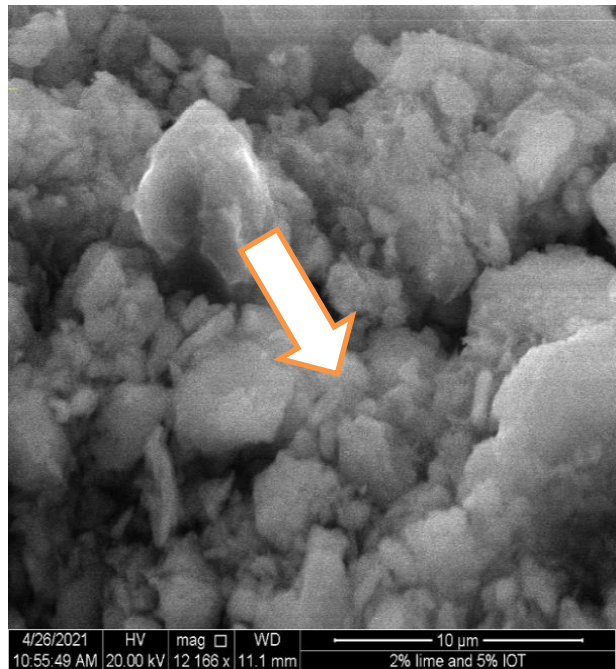
(d).97328x

Figure 4. 13 (a), (b),(c),and (d) SEM image of raw 2% lime +5 % IOT black cotton soil At different Magnification rate
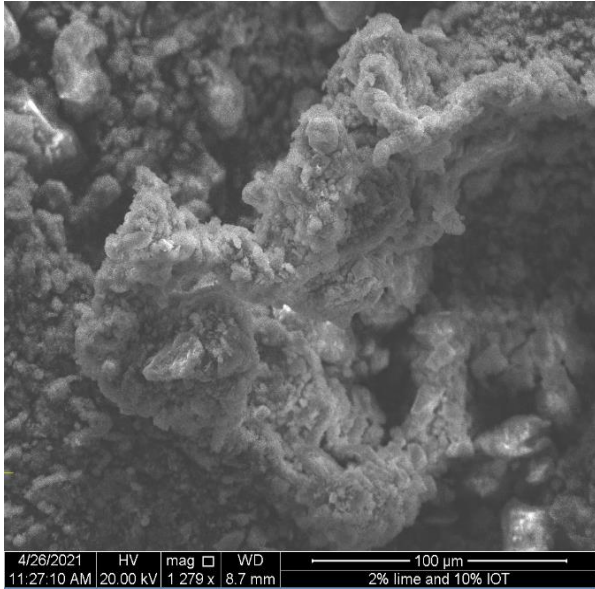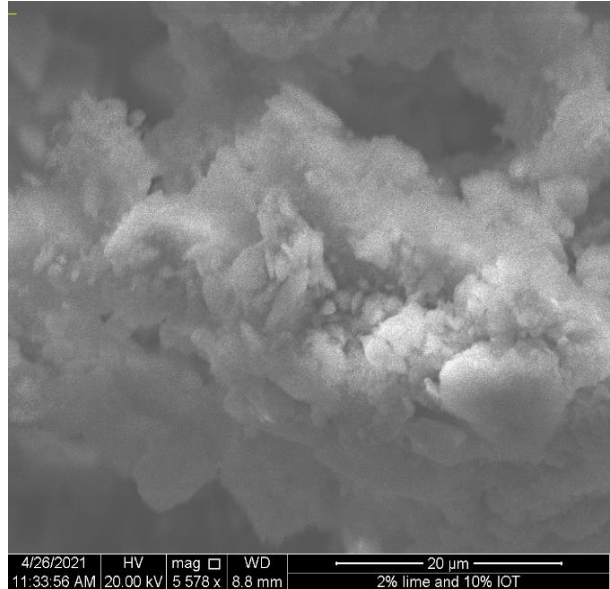
(a).3617x (b).12166x
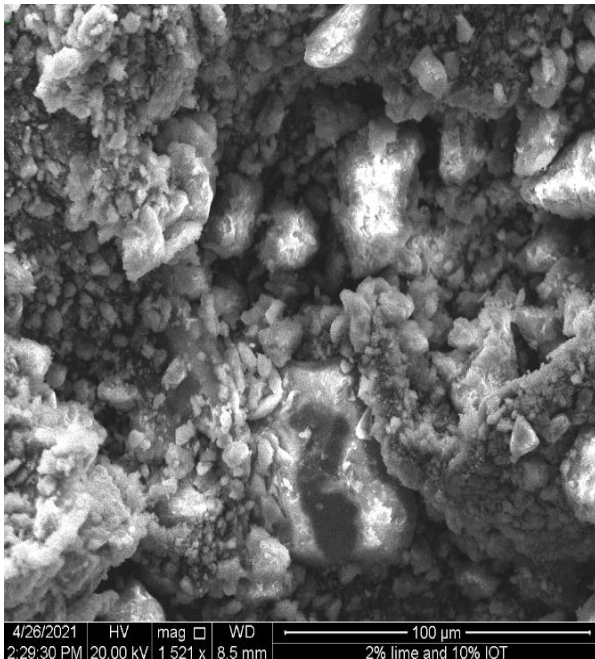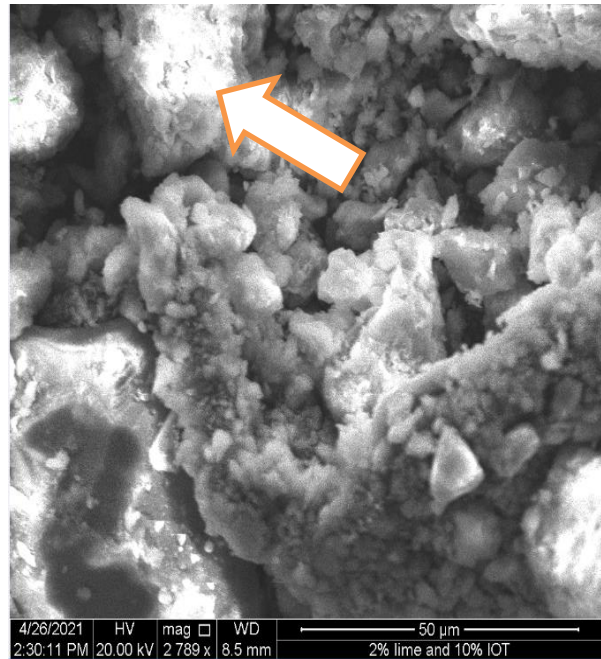
(c).23811x (d).97328x

Figure 4. 14 (a),(b),(c),and (d) SEM image of raw 2% lime + 10% IOT with black cotton soil At different Magnification rate
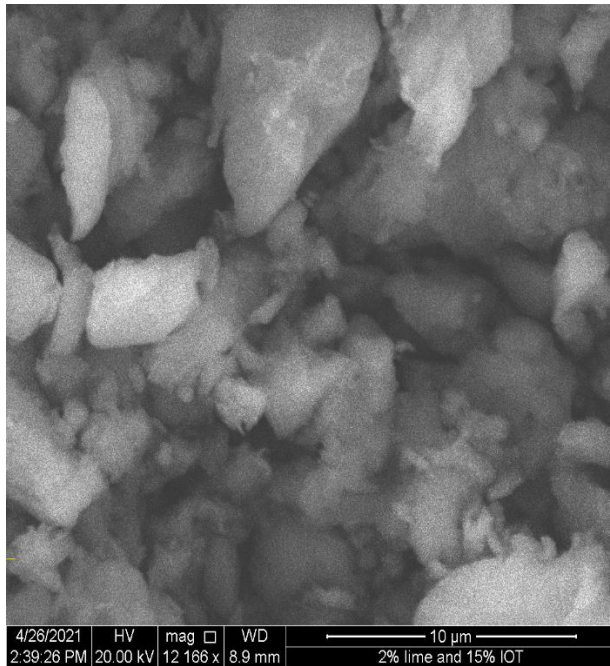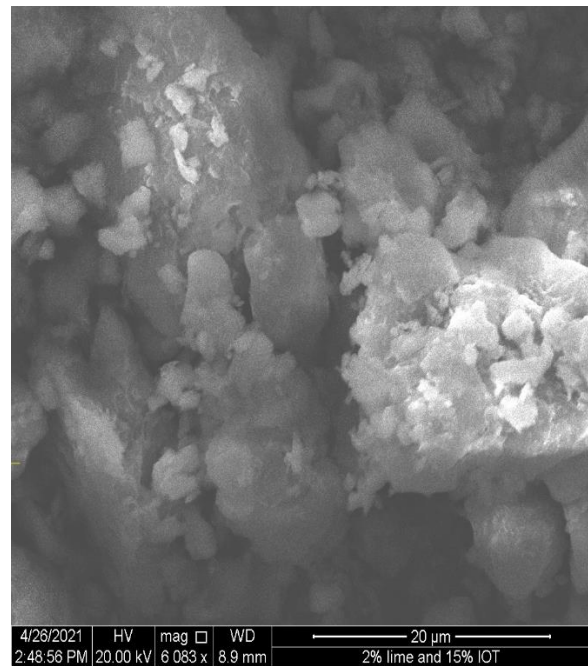
<div align="center">(a).11905x   (b) .23811x</div>

Figure 4. 15 (a) and (b)) SEM image of 2 % lime + 15% IOT with black cotton soil At different Magnification rate

Figure 4.12 The SEM image shows the configuration of the dry powder black cotton soil due to the dispensability of montmorillonite; the image shows the edges of the particles instead of the faces. The black circle in Figure 4.13 contains is dimensional film-like scales and scaly particles, indicating that the soil is a group of spectates. As shown in Figure 4.14, (b) the original soil shape is compact and agglomerated, but after mixed treatment by IOT and lime stabilizer, the shape becomes flocculants, as shown in Figure 4.15(a and b) the fine particles are slightly agglomerated relative to the raw black cotton soil.

When IOT and water Adding to the soil causes the soil pH to rise rapidly, thereby making the clay particles decompose. Silica and alumina are released and react with calcium lime forms calcium silicate hydrate (CSH) and luminescent calcium hydrate (CAH). CSA and CAH are similar to cement products formed in Portland cement. This Adding IOT to the soil forms a matrix that helps strengthen the soil IOT stabilized soil layer. And transform the scaly and flocculent structure of soil into Crystallized or massive structure to improve the compactness of soil samples, such as the percentage of IOT has increased.

The Quantitative description

53

The quantitative analysis of the SEM image test result showed relative differences in the pore space in Table 4.5 the pore space decrease from 43.2% for untreated soil to 16.21% of BCS with 2% Lime with 20% IOT treated soil. Particle analysis also shows a relative increase as the IOT increase these is due to After the addition of IOT and lime, the ion exchange and pozzolanic reaction of IOT and lime makes the flaky and flocculent structures of soil into crystal or blocky structures, thereby enhancing the compactness of soil samples and decrease the porosity.

Table 4. 5 Porosity and particle size of SEM image test result

Bleding Ratio	Porosity (%)	Particle size (µm)
BCS	43.2	1.89
BCS with 2% Lime with 5% IOT	28.6	2.60
BCS with 2% Lime with 10% IOT	21.4	3.12
BCS with 2% Lime with 15% IOT	18.66	3.52
BCS with 2% Lime with 20% IOT	16.21	4.22

CHAPTER FIVE
CONCLUSION AND RECOMONDATION

5.1 Conclusion

Investigation on the microstructural effect of lime and IOT on the stabilization of BCS was studied. Based on the experimental studied the followings are conclusion drawn:

1. The plasticity index was significantly reduced with the addition of Iron ore tailing combined with lime. However, the addition of Iron ore tailing powder alone has a minor effect on the plasticity index of expansive soil.

2. MDD increased value of the BCS with lime –IOT mixtures increased with the addition of IOT. MDD value of natural black cotton soil increased from 1.51 g/cm3 to a peak value of 1.66 at 2% lime and 20% IOT treatment. Corresponding OMC decreased from 29 to 19.31% with higher IOT content.

3. CBR values increased with the addition of IOT powder. However the addition of lime – IOT mixture to the soil considerably improved CBR value. This is due to IOT powder have a high concentration of silica, iron oxide, and alumina with a low amount of calcium content in the IOT powder. Addition lime balance concentration of IOT powder. After the addition of lime to BCS- IOT mixture CBR value significantly increased.

4. UCS test results showed significant increment during BCS treatment with lime-IOT

5. Black cotton soil treated with the addition of Iron ore tailing alone gave a reduction of the free swell, reduction in plasticity limit, improve CBR value, an increase of unconfined compressive strength.

6. However treating expansive soil, by addition of Iron ore tailing in combination with lime improved the CBR value, and plasticity index decreased significantly than Iron ore tailing alone. Hence the geotechnical property of the expansive soil improved.

5.2 Recommendation

Based on the findings of this research, the following recommendations are forwarded.The results obtained during this investigation as discussed in the previous sections showed.

- The Iron ore tailing in collaboration with higher education organizations in the Country should work together and establish a research team to further study the use of waste ceramic powder as a soil stabilizing material on different types of soils.

- Recycling of industrial waste materials in a more useful and economical way should be encouraged by government and any organization with viable programs and adequate funds to encourage interested researchers.

Reference

1) Annafi Quadri Babatunde, Eberemu Adrian Oshioname, Yohanna Paul and Osinubi Kolawole Junwolo "effect of elapsed time after mixing on the strength properties off lime and iron ore tailing treated black cotton soil as a road construction material" Department of Civil Engineering, Ahmadu Bello University, Kaduna State, Nigeria 2020.

2) Arvind Kumar,P.V.Sivapullaiah "Lime stabilization of soil: A physico-chemical and Micro mechanistic perspective,"Manipal University Jaipur, India 2019.

3) Basma AA, Tuncer ER (1991) Effect of lime on volume change and compressibility of expansive clays. Transp Res Rec 1295:52-61

4) Bililgn, F.," Stabilization of Expansive Subgrade soil using Waste Ceramic Powder,"Msc. Thesis Addis Ababa University, Addis Ababa 2019.

5) Bell FG (1996) Lime stabilization of clay mineral and soil. Eng Geo 42(4): 223 -237.

6) Brooks, R.M., "Soil Stabilization with Fly ash and Rice Husk Ash, "International Journal of Research and Reviews in Applied Sciences, Volume 1, Issue 3, 2009.

7) Chen, F.H., "Foundation on expansive soils," Elsevier, Amsterdam, 1988 & Chen, James A. & Idusuyi, Felix O.(2015),"Effect of waste ceramic dust on index properties of shrink swell soils." ISSN 2504-8848 Vol. 1 No.8 2015.

8) Dallas N. Little (1995). Hand book for stabilization of Pavement subgrades and Base courses with lime.

9) Diamond S, Hussain M (2011) Lime stabilization of soil –lime stabilization. Highw Res Rec 92:83 -102

10) Dr. K.R. ARORA "Soil mechanics and foundation engineering" KOTA, 2004.

11) Eades and Grim,1960 cited in Harty , 1970

12) Eades JL, Grim RE (1966) A quick test to determine lime requirements of lime stabilization. Highw Res Rec 139:61-72

13) Etim,R.; O Eberemu, A.; Osinubi, K.Stabilization of black cotton soil with lime and iron ore tailings admixture.Transp. Geotech. 2017, 10, 85-95.

14) Guyer, J. P.,"Introduction to Soil Stabilization in Pavements," New York, 2011

15) Habtamu S., Chemical Stabilization of Expansive Sub-grde Soil Performance Evaluation on selected Road Section in NorthEastern Addis Ababa. Msc Thesis Addis Ababa University 2011.

16) Ishola, K. Modification of Lateritic Soil with Iron Ore Tailing. Master's Thesis, Civil Engineering Department, Ahmadu Bello University, /Nigeria, 2014.

17) J. Paul Guyer (2011). Introduction to Soil Stabilization in Pavements. Continuing Education and Development, Inc. 9 Greyridge Farm Court Stony Point, NY 10980.

18) K.J.Osinubi, P. Yohanna and A.O.Eberemu "Cement modified of tropical black clay using iron ore tailings as admixture" Ahmadu Bello University, Kaduna State, Nigeria 2015.

19) Lees, G., et al., "Sodium Chloride as an Additive in Lime-Soil Stabilization," Highway Engineer, Vol. 29, No. 12, pp. 2-8, 1982

20) Moses, G. Stabilization of black cotton soil with ordinary Portland Cement Using Bagasse ash as admixture. IRJI. Res. Eng.2008, 5,107-115.

21) Nebro, D., Stabilization of Potentially Expansive Subgrade Soil Using Lime and Con-Aid. MSc. Thesis, Addis Ababa University, Addis Ababa, 2002.

22) Nwadiogbu, C.P. The effect of Elapsed Time on Lateritic Soil Modified with Lime and Locust Bean Ash. Master's Thesis, Department of Civil Engineering, Ahmadu Bello University, Zaria, Nigeria 2012.

23) Onur Baser (2009).Stabilization of expansive soils with waste marble dust. A Thesis submitted to School of Graduate Studies of Middle east technical University in Partial Fulfillment of the Requirements for the degree of Master of Science in civil.eng.

24) Oriola, F; Moses, G.Groundnut Shell Ash Stabilization of Black cotton Soil.Electron.J.Geotech.Eng. 2010, 15, 415-428.

25) Osinubi, K.J. (1995). "Lime modification of fblack cotton soils." Spectrum Journal,Vol. 2, Nos 1and 2, pp.112 – 122.

26) Ramesh, H.N.: krishnaiah, A.j.; Shilpa, S.S Effect of lime on the index properties of Black cotton soil and mine tailing mixtures. IQSR j. Eng. 2013 3 01-07. (Cross Ref).

27) Reshid M., "Stabilization of expansive soils with lime (A Case Study on the Adura-Burbey DS6 Road Segment)," Msc. Thesis Addis Ababa University, Addis Ababa 2014.

28) R.K. Etim, A.O.Eberemu and K.J.Osinubi "Stabilization of black cotton soil with lime and iron ore tailing used as admixture" Akwa Ibom State University,Ikot Akpaden, Nigeria 2017.

29) Phani, K.B.R.: Sharama, R.s Effect oc flay ash on engineering properties of expansive soils. J.Geotech. Geoenviron. Eng 2004, 130 764-767.

30) Prusinski, J., and Bhattacharja, S. 1999. Effectiveness of Portland cement and lime in stabilizing clay soils. Transportation Research Record: Journal of the Transportation Research Board, (1652): 215–227. Transportation Research Board of the National Academies.

31) Sabat, A. K. (2012), "A study on some geotechnical properties of lime stabilized expansive soil-quarry dust mixes", *Int. Journal of emerging trends in Engineering and Development*, ISSn 2249-6149 issue2, vol. 1, pp. 42-49

32) Tesfaye, A., "Chemical Treatment of "Black Cotton" Soil to make it Usable as a Foundation Material," MSc. Thesis, Addis Ababa University, Addis Ababa, October 2001.

33) Yisa, G.L. Stabilization of Lateritic Soil with Iron-Ore Tailing. Master's Thesis, Department of Civil Engineering, Ahmadu Bello University Zaria, Nigeria 2014.

34) Zelalem, A. (2005) Basic Engineering Properties of Latritic soil found in Nejo-mendi Road construction Area, welega. Thesis presented to school of Graduate studies, Addis Ababa University, Addis Ababa.

35) Image j bundled with Java 1.8.0_172 SEM image analysis

36) https://www.business-standard.com/article/markets/global-iron-ore-production-set-for-modest-growth-on-china-s-falling-demand-119111100820_1.html

37) https://satellites.pro/Koye_map.Adis_Abeba.Ethiopia#8.886577,38.848171,16

38) http://webmineral.com/specimens/picshow.php?id=1285&target=Montmorillonite #.XHL9VOhKg2w

39) http://webmineral.com/specimens/picshow.php?id=1284#.XHNZEOhKg2w

40) http://webmineral.com/specimens/picshow.php?id=1283#.XHNZZuhKg2w

41) https://www.worldweatheronline.com/addis-ababa-weather-history/et.aspx

APPENIX

APPENIX A: Natural soil test result
APPENIX B: Natural soil with IOT test result
APPENIX C: Natural soil with IOT and lime test result

Table A1 Particle size distribution data

Sieve No	Sieve Size, mm	Mass of Empty Sieve	Mass of sieve + soil Retained (g)	Soil Retained	Accumulative Retained (g)	% Percent Retained	% Passing,
#4	4.75	954.9	959.1	0		0.000	100.00
#10	2	778.6	778.9	0.3	0.3	0.060	99.94
#20	0.85	673.5	674.6	1.1	1.4	0.280	99.72
#40	0.43	625.7	627.2	1.5	2.9	0.580	99.42
#60	0.25	782.7	784	1.3	4.2	0.840	99.16
#200	0.075	789	790	1	5.2	1.040	98.96
pan=		857.5	862.3	494.8	500	100.000	
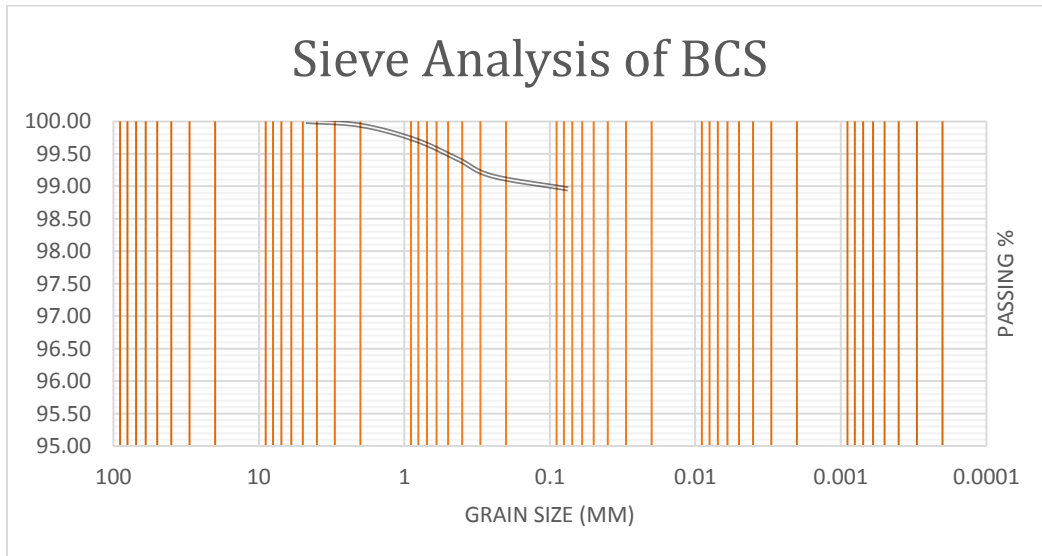
Figure A- 1Particle size distribution curve

Table A 2 Specific gravity of natural soil, lime & IOT

Sample NO	Sample Source	M of B+S+W(M3)	M of B+S(M2)	M of B full of W(M4)	M of B(M1)	M of w(m3-m2)	Mof S(M2-M1)	V of S(M4-M1)-(M3-M2)	GS=(M2-M1) (M4-M1)-(M3-M2)
1	Black Soil	109.4	52.96	97.88	34.78	56.44	18.18	6.66	2.730
		104.65	52.45	93.14	34.22	52.2	18.23	6.72	2.713
									2.721
2	Lime	102.99	51.9	91.61	33.86	51.09	18.04	6.66	2.709
		107.64	51.17	96.26	33.13	56.47	18.04	6.66	2.709
									2.71
3	IOT	110.14	52.87	98.24	34.77	57.27	18.1	6.2	2.919
		104.13	51.93	91.43	34.52	52.2	17.41	4.71	3.696
									3.31

Table A 3: Hydrometer analysis data

Viscosity of water at 25c Temperature	0		Ra	Actual Hydrometer reading		
Specific gravity of soil	2.72		T	Temperature		
Correction for GS	0.99	Symbol	Tc	Temperature Correction		
Weight of dry soil	50		Rc	Corrected Hydrometer reading		
Zero Correction	7		Zc	Zero Correction		
Meniscus Correction	1		L	Effective depth		

Time (min)	Ra	T	Tc=-4.85+0.25T	Rc=Ra-Zc+Tc	%finer=(Rcxa)/Ws	Rcorrected miniscous	L=16.3-0.164Ra	k	D(mm)	Actual % finer wit to total fines in soil
									0.075	98.96%
1	50	27	1.9	44.9	88.9%	51	7.936	0.012947	0.036473	83.00%
2	48	25	1.4	42.4	84.0%	49	8.264	0.012947	0.026318	78.38%
4	47	27	1.9	41.9	83.0%	48	8.428	0.012947	0.018793	77.45%
8	46	27	1.9	40.9	81.0%	47	8.592	0.012947	0.013417	75.60%
15	45	27	1.9	39.9	79.0%	46	8.756	0.012947	0.009892	73.76%
30	44	27	1.9	38.9	77.0%	45	8.92	0.012947	0.00706	71.91%
60	42	27	1.9	36.9	73.1%	43	9.248	0.012947	0.005083	68.21%
120	40	27	1.9	34.9	69.1%	41	9.576	0.012947	0.003657	64.51%
240	38	27	1.9	32.9	65.1%	39	9.904	0.012947	0.00263	60.82%
480	34	26	1.65	28.65	56.7%	35	10.56	0.012947	0.00192	52.96%

PARTICLE SIZE DISTRIBUTION CURVE

% FINER BY WEIGHT (vertical axis)

PARTICLE SIZE IN mm (horizontal axis)

Particle Size Lager Than 2mm = 12%

Fine Sand   (2.00-0.075mm   = 3

Silt (0.075mm -0.002mm)   = 17

Clay (Less than 0.002mm)   = 68
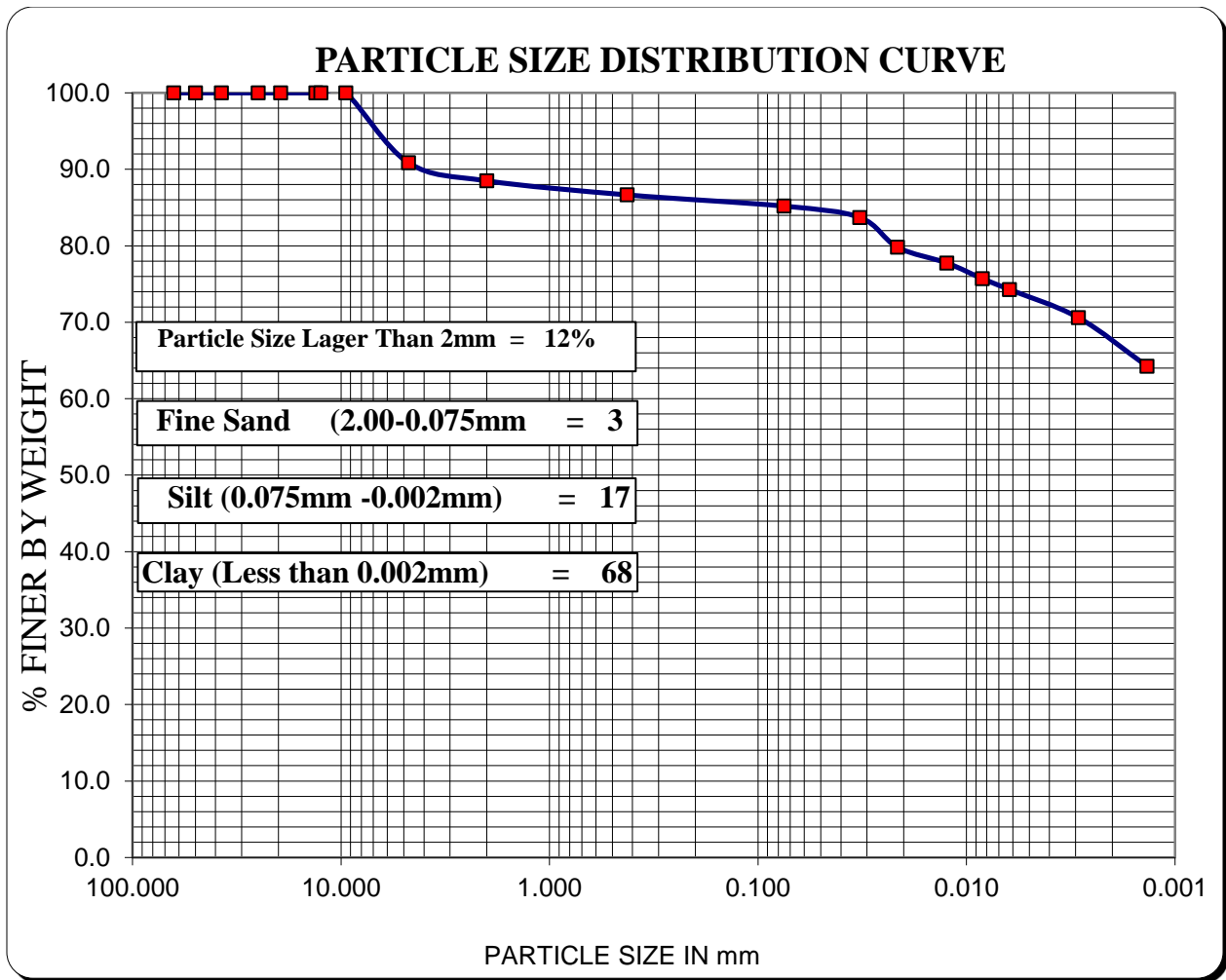
Figure A- 2: Particle size distribution curve with Hydrometer curve

Table A- 4: Free swell of Natural soil, lime & IOT

Sr. No.	Proportion of sample (%)	Initial Reading (L)	Final Reading (F)	Free Swell %(F-L/L)x100
3	BCS	10	20.5	105
5	Lime	10	23	130
2	IOT	10	10	0

Table A -5: Determination if liquid limits & plastic limit of natural soil

	Liquid Limit			Plastic Limit	
No. Blows	35	26	20		
Wt. Of cont. + wet soil (g.)	27.70	33.10	30.22	30.69	25.41
Wt. Of cont. + dry soil (g.)	23.98	27.40	24.85	29.44	24.06
Wt. of water (g.)	3.72	5.70	5.37	1.25	1.35
Wt. container (g.)	19.77	21.11	19.29	26.80	21.17
:	4.21	6.29	5.56	2.64	2.89
Water (%)	88.36	90.62	96.58	47.35	46.71
				AV. PL (%)	47.0
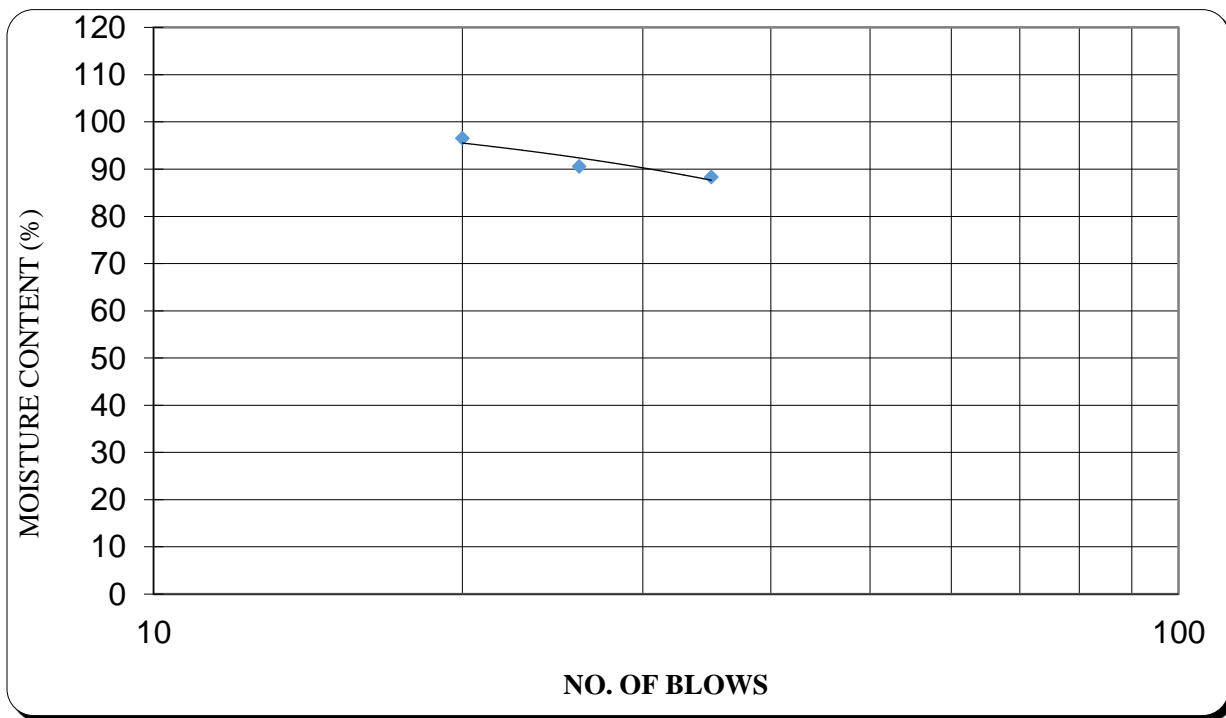
Figure A- 3: Liquid limit chart for natural soil

Liquid Limit	Plastic Limit	Plasticity Index
LL(%)	PL(%)	PI
92	47	45

65

Table A-6: Modified proctor density test for natural soil

Trial	1	2	3	4	5
Wet mold + sample(g)	4620	4760	4830	4950	4900.00
Wet of mold(g)	3220	3220	3220	3220	3220.00
Wet of sample(g)	1400	1540	1610	1730	1680.00
Volume of mold(cm)3	889.6	889.6	889.6	889.6	889.62
Wet density (g/cc)	1.57	1.73	1.81	1.94	1.89
Tare No	Z-1	Z-4	Z-8	Z-3	Z-10
Wet tare + sample(g)	234	270	289	276	290.00
Wet tare + dry sample(g)	215	238	250	235	240.00
Wet of water(g)	19	32	39	41	50.00
Wet of tare(g)	83.4	87.47	88.6	93.2	96.10
Wet of dry sample(g)	131.6	150.53	161.4	141.8	143.90
Moisture content(g/cc)	14.438	21.258	24.164	28.914	34.75
Dry density(g/cc)	1.38	1.43	1.46	1.51	1.40
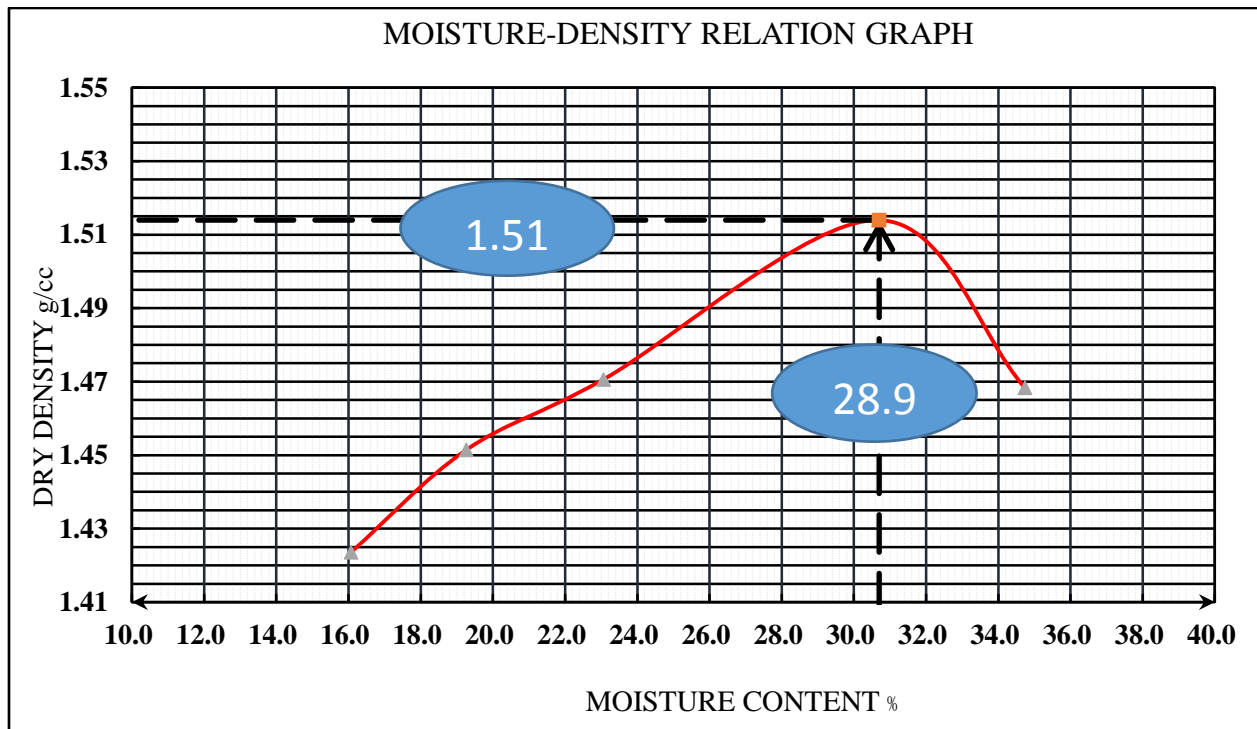
Figure A-4: Moisture density relationship graph of natural soil (BCS)

Table A -7: Socked CBR for natural black cotton soil

Sampling date: 08/01/2021	Intended for:- MSc Research/Stabilization

Test Date : 21/01/21	Material Source: - Housing development Project 18 Road 27
Sample Ref: BCS	Description:- Dark Gray color
Sample Drying: air	Sampled at:- From pit -1 @ 0+530

Pen.(mm.)	Load (KN)	CBR %
	LDR	
0	0	
0.64	1	
1.27	3	
1.91	4.2	
2.54	5	1.710725
5.08	6	1.415625
7.62	7.5	
10.16	7.7	
12.7	8	

Swell data	
Initial reading	4.29
Final Reading	14.42
Height of the spec.	116.4
Swell (%)	8.7
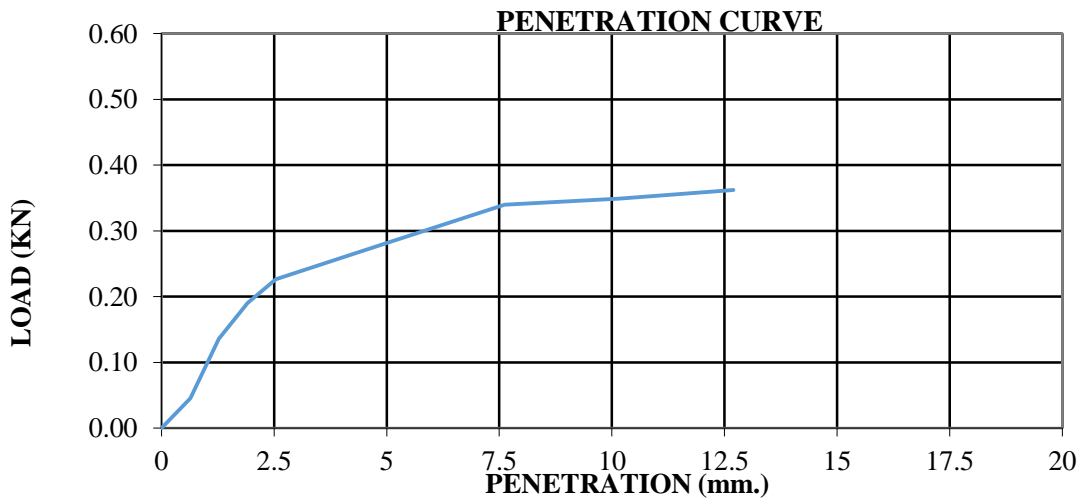
Figure A- 5: Load vs penetration curve of natural soil

Table A-8: Unconfined Compression Strength of Natural soil

Dial Reading	Deformation (mm)	Proving Ring	Load, (KN)	Strain	Corrected Area (m^2)	stress (kN/m^2)
10	0	0.01	0.0667	0.0007	50.27	4.44
20	0.1	0.02	0.1333	0.0013	50.31	9.30
30	0.2	0.03	0.2000	0.0020	50.34	12.50
40	0.3	0.04	0.2667	0.0027	50.37	20.87
50	0.4	0.05	0.3333	0.0033	50.41	26.91
60	0.5	0.06	0.4000	0.0040	50.44	30.75
70	0.6	0.07	0.4667	0.0047	50.48	35.80
80	0.7	0.08	0.5333	0.0053	50.51	44.90
90	0.8	0.09	0.6000	0.0060	50.54	56.50
100	0.9	0.1	0.6667	0.0067	50.58	60.00
120	1	0.12	0.8000	0.0080	50.65	68.10
140	1.2	0.14	0.9333	0.0093	50.71	76.50
160	1.4	0.16	1.0667	0.0107	50.78	85.17
180	1.6	0.18	1.2000	0.0120	50.85	88.22
200	1.8	0.2	1.3333	0.0133	50.92	96.91
240	2	0.24	1.6000	0.0160	51.06	105.58
280	2.4	0.28	1.8667	0.0187	51.20	114.22
320	2.8	0.32	2.1333	0.0213	51.34	122.84
360	3.2	0.36	2.4000	0.0240	51.48	131.26
400	3.6	0.4	2.6667	0.0267	51.62	139.63
440	4	0.44	2.9333	0.0293	51.76	147.96
480	4.1	0.48	3.2813	0.0321	52.00	146.00
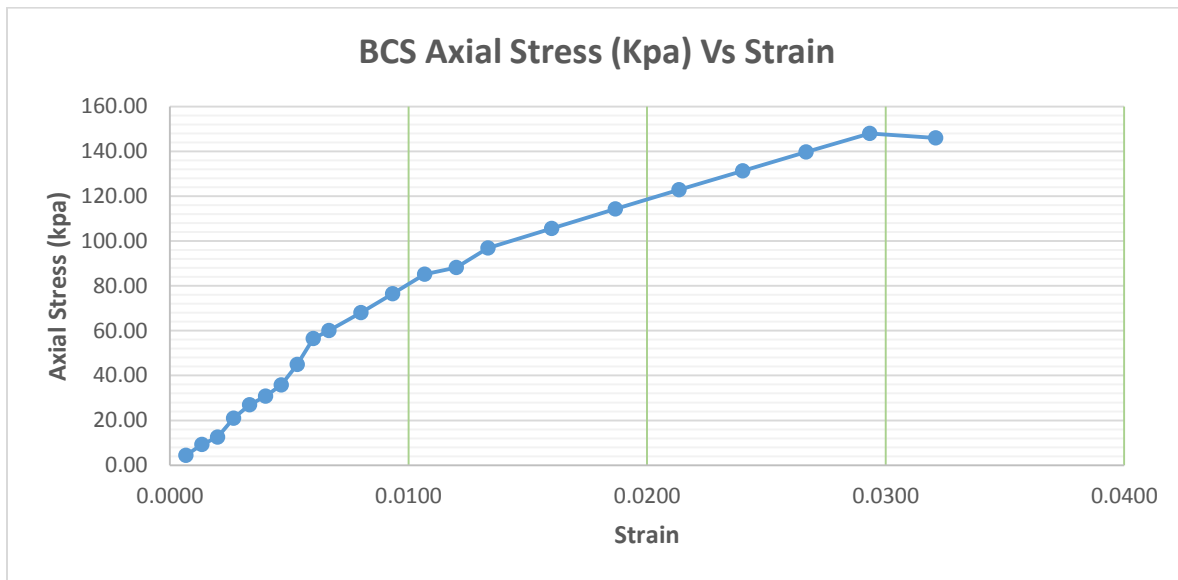
Figure A- 6: Axial stress vs strain graph of natural soil

APPENIX B: Natural soil with IOT test result

Table B- 1: Determination of liquid limit & plastic limit of 98% BCS with 2% IOT

	Liquid Limit			Plastic Limit	
No. Blows	35	23	16		
Wt. Of cont. + wet soil (g.)	37.00	38.98	42.00	19.92	20.21
Wt. Of cont. + dry soil (g.)	31.86	33.34	35.11	18.68	18.98
Wt. of water (g.)	5.14	5.64	6.89	1.24	1.23
Wt. container (g.)	25.45	26.38	26.83	15.42	15.64
:		6.41	6.96	8.28	3.26	3.34
Water (%)	80.19	81.03	83.21	38.04	36.83
				AV. PL (%)	37.4

Figure B- 1: Liquid limit chart for 98% BCS with 2% IOT

Liquid Limit	Plastic Limit	Plasticity Index
LL (%)	PL (%)	PI
81	37	44

Table B- 2: Determination of liquid limit & plastic limit of 98% BCS with 2% IOT

	Liquid Limit			Plastic Limit	
No. Blows	35	23	16		

Wt. Of cont. + wet soil (g.)	37.00	38.98	42.00	19.92	20.21
Wt. Of cont. + dry soil (g.)	31.86	33.34	35.11	18.68	18.98
Wt. of water (g.)	5.14	5.64	6.89	1.24	1.23
Wt. container (g.)	25.45	26.38	26.83	15.42	15.64
:	6.41	6.96	8.28	3.26	3.34
Water (%)	80.19	81.03	83.21	38.04	36.83

AV. PL (%)	37.4

Figure B- 2: Liquid limit chart for 98% BCS with 2% IOT

Liquid Limit	Plastic Limit	Plasticity Index
LL (%)	PL (%)	PI
81	37	44

Table B- 3: Determination of liquid limit & plastic limit of 94% BCS with 6% IOT

	LIQUID LIMIT	Plastic Limit

70

No. Blows	35	24	16			
Wt. of cont. + wet soil (g.)	35.75	37.2	39.10		20.60	20.81
Wt. of cont. + dry soil (g.)	30.90	32	33.70		19.29	19.51
Wt. of water (g.)	4.85	5.2	5.40		1.31	1.30
Wt. container (g.)	24.27	25.13	26.83		15.72	15.89
:	6.63	6.87	6.87		3.57	3.62
Water (%)	73.15	75.69	78.60		36.69	35.91
				AV. PL (%)		36.3
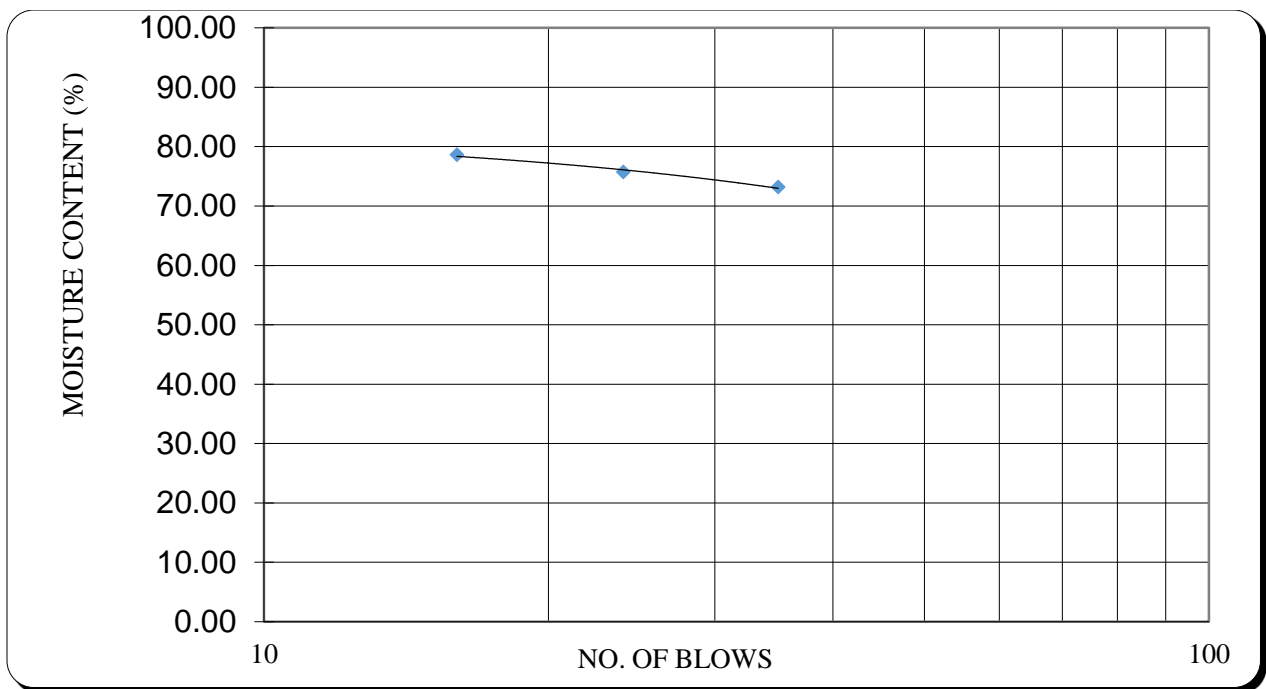
Figure B- 3: Liquid limit chart of 94% BCS with 6% IOT

Liquid Limit	Plastic Limit	Plasticity Index
LL (%)	PL (%)	PI
76	36	40

Table B- 4: Determination of liquid limit & plastic limit of 92% BCS with 8% IOT

	LIQUID LIMIT			Plastic Limit	
No. Blows	35	28	18		
Wt. of cont. + wet soil (g.)	36.00	38.00	41.32	24.38	23.95

Wt. of cont. + dry soil (g.)	31.60	33.25	35.60		23.10	22.58
Wt. of water (g.)	4.40	4.75	5.72		1.28	1.37
Wt. container (g.)	25.24	26.51	27.59		19.20	18.48
:	6.36	6.74	8.01		3.90	4.10
Water (%)	69.18	70.47	71.41		32.82	33.41
				AV. PL (%)		33.1
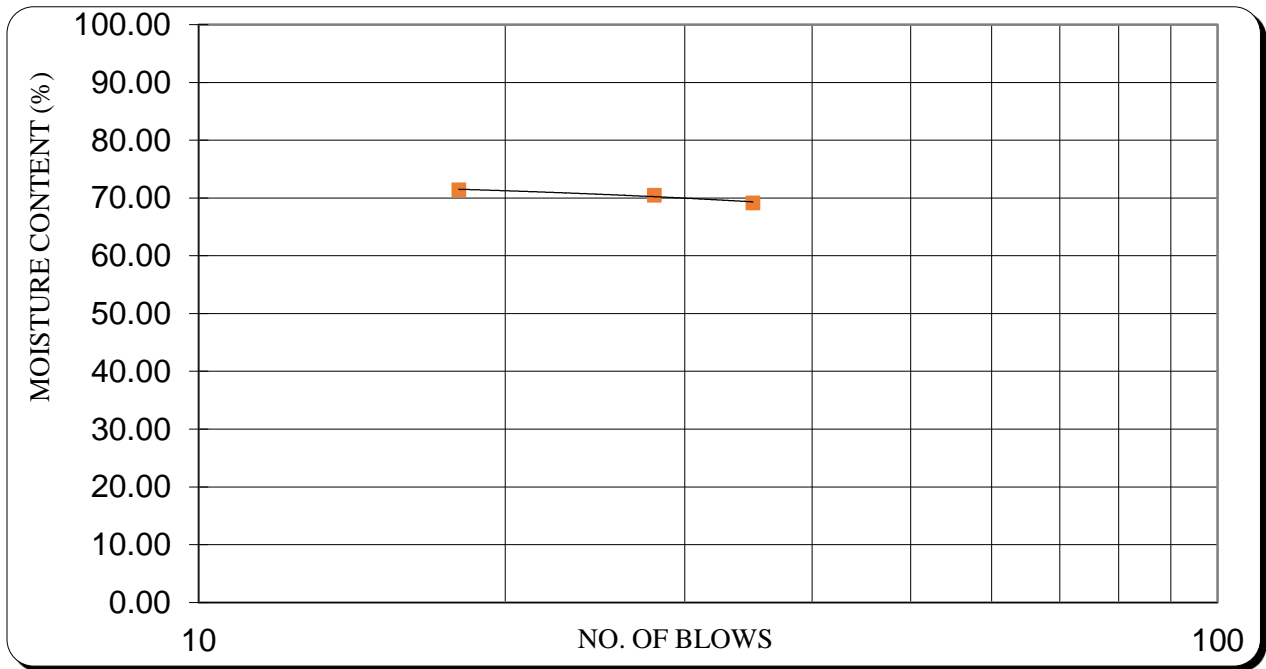
Figure B- 4: Liquid limit chart of 92% BCS with 8% IOT

Liquid Limit	Plastic Limit	Plasticity Index
LL (%)	PL (%)	PI
70	33	37

Figure B- 5: Determination of liquid limit & plastic limit of 90% BCS with 10% IOT

	LIQUID LIMIT			**Plastic Limit**	
No. Blows	35	28	18		
Wt. of cont. + wet soil (g.)	35.85	37.84	41.28	24.24	24.59
Wt. of cont. + dry soil (g.)	31.60	33.27	35.60	22.83	23.10
Wt. of water (g.)	4.25	4.57	5.68	1.41	1.49

Wt. container (g.)	25.24	26.51	27.59		18.40	18.48
:	6.36	6.76	8.01		4.43	4.62
Water (%)	66.82	67.60	70.91		31.83	32.25
				AV. PL (%)		32.0

Figure B- 6: Liquid limit chart of 90% BCS with 10% IOT

Liquid Limit	Plastic Limit	Plasticity Index
LL(%)	PL(%)	PI
68	32	36

Table B- 5: Determination of liquid limit & plastic limit of 88% BCS with 12% IOT

	LIQUID LIMIT			Plastic Limit	
No. Blows	34	27	17		
Wt. of cont. + wet soil (g.)	35.23	37.32	38.33	24.42	24.87
Wt. of cont. + dry soil (g.)	31.45	32.25	33.12	23.08	23.39
Wt. of water (g.)	3.78	5.07	5.21	1.34	1.48

73

Wt. container (g.)	25.24	24.69	25.47		18.80	18.28
:	6.21	7.56	7.65		4.28	5.11
Water (%)	60.87	67.06	68.10		31.31	28.96
				AV. PL (%)		30.1

Figure B- 7 Liquid limit chart of 88% BCS with 12% IOT

Liquid Limit	Plastic Limit	Plasticity Index
LL (%)	PL (%)	PI
65	30	35

Table B- 6: Determination of liquid limit & plastic limit of 86% BCS with 14% IOT

	LIQUID LIMIT			Plastic Limit	
No. Blows	30	22	15		
Wt. of cont. + wet soil (g.)	35.18	36.89	38.12	17.41	18.30
Wt. of cont. + dry soil (g.)	31.45	32.24	33.12	16.80	17.70
Wt. of water (g.)	3.73	4.65	5.00	0.61	0.60

Wt. container (g.)	25.24	24.68	25.48	14.71	15.62
:	6.21	7.56	7.64	2.09	2.08
Water (%)	60.06	61.51	65.45	29.19	28.85
				AV. PL (%)	29.0

Figure B- 8: Liquid limit chart of 86% BCS with 14% IOT

Liquid Limit	Plastic Limit	Plasticity Index
LL(%)	PL(%)	PI
62	29	33

Table B- 7: Determination of liquid limit & plastic limit of 84% BCS with 16% IOT

	LIQUID LIMIT			Plastic Limit	
No. Blows	34	27	17		
Wt. of cont. + wet soil (g.)	36.40	37.98	39.00	17.39	18.29
Wt. of cont. + dry soil (g.)	32.15	32.71	33.69	16.80	17.70
Wt. of water (g.)	4.25	5.27	5.31	0.59	0.59

75

Wt. container (g.)	24.97	24.22	25.20	14.70	15.63
:	7.18	8.49	8.49	2.10	2.07
Water (%)	59.19	62.07	62.54	28.10	28.50
				AV. PL (%)	28.3
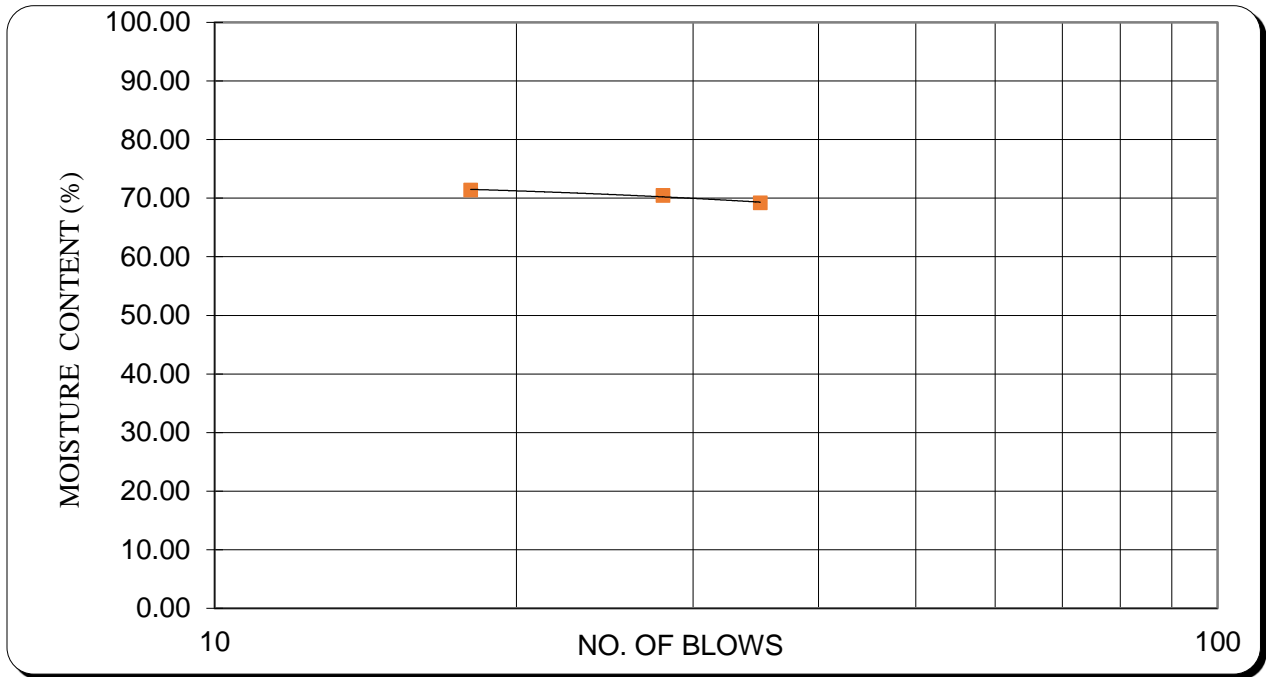
Figure B- 9:Liquid limit chart of 84% BCS with 16% IOT

Liquid Limit	Plastic Limit	Plasticity Index
LL (%)	PL (%)	PI
61	28	33

Table B- 8: Specific gravity of natural soil with IOT

SR NO	Sample NO	Sample Source	M of B+S+W(M3)	M of B+S(M2)	M of B full of W(M4)	M of B(M1)	M of w(m 3-m2)	Mof S(M2-M1)	V of S(M4 -M1)-(M3-M2)	GS=(M2-M1 (M4-M1)-(M3-M2)
1	1	**2%**	103.2	52.3	91.62	33.88	50.9	18.42	6.84	2.69
1.1			103.85	51.9	92.13	33.6	51.95	18.30	6.58	2.78
										2.73

2	2	**4%**	107.24	51.32	95.65	33.14	55.92	18.180	6.59	2.76
2.1			107.14	51.34	95.51	33	55.8	18.34	6.71	2.73
										2.74
3	3	**6%**	106.47	49.5	94.92	30.9	56.97	18.60	7.05	2.64
3.1			102.69	50.1	90.88	31.98	52.59	18.12	6.31	2.87
										2.75
4	4	**8%**	108.03	51.38	96.66	33.15	56.65	18.23	6.86	2.66
4.1			105.12	52.48	93.21	34.23	52.64	18.25	6.34	2.88
										2.76
5	5	**10%**	103.55	51.82	91.83	33.61	51.73	18.21	6.49	2.81
5.1			109.12	51.88	98.28	34.79	57.24	17.09	6.25	2.73
										2.77
6	6	**12%**	103.25	51.9	91.61	33.86	51.35	18.04	6.4	2.82
6.1			107.72	51.17	96.26	33.13	56.55	18.04	6.58	2.74
										2.78
7	7	**14%**	109.82	52.86	98.24	34.77	56.96	18.09	6.51	2.78
7.1			102.99	51.95	91.43	33.96	51.04	17.99	6.43	2.80
										2.79
8	8	**16%**	109.83	52.77	98.24	34.77	57.06	18	6.41	2.81
8.1			102.97	51.97	91.43	33.96	51	18.01	6.47	2.78
										2.80

Table B- 9 Determination of Free swell of black cotton soil with IOT

Sr. No.	Proportion of IOT (%)	Initial Reading (L)	Final Reading (F)	Free Swell %(F-L/L)x100
1	0%	10	20.5	105
2	2%	10	19	90

Sr.No	source	Mold NO	Original Length of specimen (140mm)-Lo	Length of dry specimen(mm)-Ld	Linear Shrinkage %(Lo-Ld/Lo)x100
1	BCS	B-05	140	110	21.43
2	2%	7	140	114	18.57
3	8%	1	140	116	17.14
4	4%	8	140	118	15.71
5	6%	3	140	120	14.29
6	10%	9	140	120	14.29
7	12%	5	140	122	12.86
8	14%	2	140	124	11.43
9	16%	13	140	124	11.43

3	4%	10	18	80
4	6%	10	17.5	75
5	8%	10	17	70
6	10%	10	17	70
7	12%	10	16.5	65
8	14%	10	16	60
9	16%	10	16	60

Table B- 10: Determination of Linear shrinkage limit of black cotton soil with IOT

Table B-12: Summary for Modified proctor density data for BCS % with IOT %

Trial	1	2	3	4	5	%	Maximum
Moisture content(g/cc)	10.25	21.26	24.16	28.91	34.75	0.00	28.91
Dry density(g/cc)	1.31	1.43	1.46	1.51	1.40		1.51
Moisture content(g/cc)	10.38	14.45	18.54	26.14	29.16	0.02	26.14
Dry density(g/cc)	1.31	1.36	1.42	1.52	1.45		1.52
Moisture content(g/cc)	10.42	17.02	21.52	25.50	33.10	0.04	25.50

Dry density(g/cc)	1.33	1.35	1.44	1.53	1.48		1.53
Moisture content(g/cc)	13.14	16.67	21.38	23.68	30.84	0.06	23.68
Dry density(g/cc)	1.35	1.39	1.48	1.54	1.43		1.54
Moisture content(g/cc)	13.31	15.67	19.46	23.24	28.21	0.08	23.24
Dry density(g/cc)	1.41	1.49	1.54	1.55	1.46		1.55
Moisture content(g/cc)	13.24	14.10	18.55	21.55	29.94	0.10	21.55
Dry density(g/cc)	1.35	1.38	1.48	1.58	1.51		1.58
Moisture content(g/cc)	14.76	17.48	19.51	21.37	29.77	0.12	21.37
Dry density(g/cc)	1.33	1.40	1.47	1.61	1.51		1.61
Moisture content(g/cc)	13.38	17.39	19.33	20.92	29.77	0.14	20.92
Dry density(g/cc)	1.37	1.47	1.57	1.62	1.52		1.62
Moisture content(g/cc)	11.87	15.60	18.54	20.60	27.45	0.16	20.60
Dry density(g/cc)	1.39	1.50	1.55	1.62	1.54		1.62
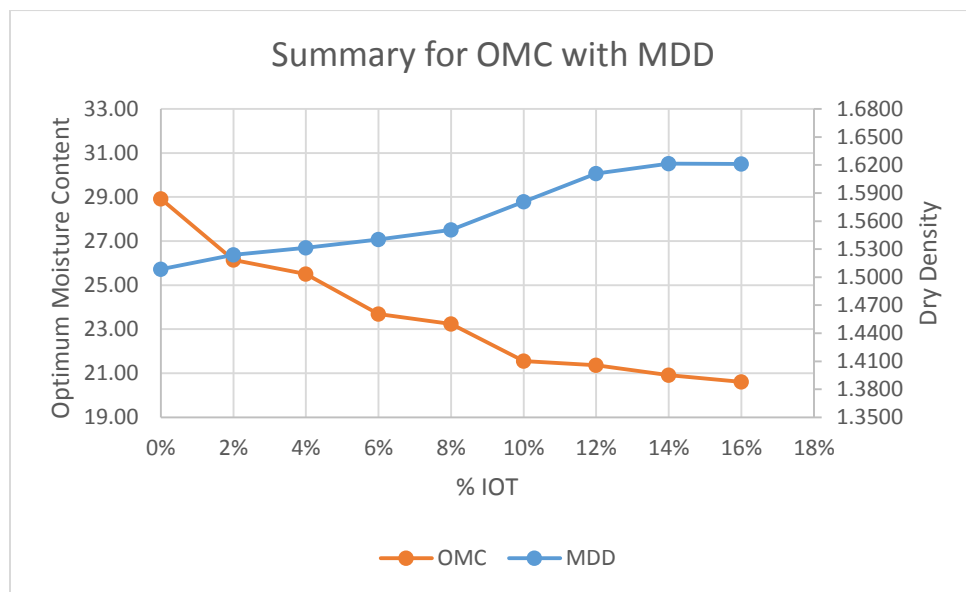
Figure B- 10: Summary for OMC with MDD for BCS% with IOT%

Table B-13: Unconfined Compression Strength data for 98% BCS with 2% IOT

Dial Reading	Deformation (mm)	Proving Ring Reading (P.R.R)	Load, (KN)	Strain	Corrected Area (m^2)	Stress (kN/m^2)
0	0	18	0	0.000	0.005024	0
10	0.1	32	60	0.001	0.005027	11.93
20	0.2	50	140	0.001	0.005031	27.83
30	0.3	55	185	0.002	0.005034	36.75
40	0.4	60	230	0.003	0.005037	45.66
50	0.5	65	260	0.003	0.005041	51.58
60	0.6	70	300	0.004	0.005044	59.47
70	0.7	80	355	0.005	0.005048	70.33
80	0.8	90	405	0.005	0.005051	80.18
90	0.9	100	444	0.006	0.005054	87.85
100	1	110	490	0.007	0.005058	96.88
120	1.2	120	545	0.008	0.005065	107.61
140	1.4	130	590	0.009	0.005071	116.34
160	1.6	140	630	0.011	0.005078	124.06
180	1.8	150	680	0.012	0.005085	133.73
200	2	160	723	0.013	0.005092	141.99
240	2.4	170	790	0.016	0.005106	154.73
280	2.8	180	830	0.019	0.005120	162.12
320	3.2	190	890	0.021	0.005134	173.37
360	3.6	200	925	0.024	0.005148	179.70
400	4	210	940	0.027	0.005162	182.11
440	4.4	220	930	0.029	0.005176	179.68
480	4.8	240	925	0.032	0.005190	178.22
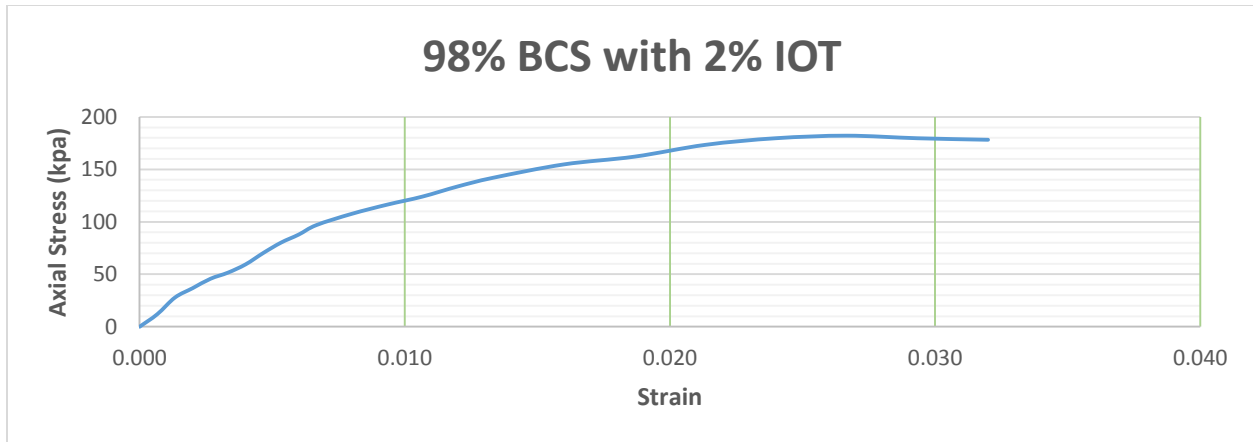
Figure B- 11: Unconfined Compression Strength chart for 98% BCS with 2% IOT

Table B-14: Unconfined Compression Strength data for 96% BCS with 4% IOT

Dial Reading	Deformation (mm)	Proving Ring Reading (P.R.R)	Load, (KN)	Strain	Corrected Area (m²)	Stress (kN/m²)
0	0	18	0	0.000	0.005024	0
10	0.1	32	70	0.001	0.005027	13.92
20	0.2	50	150	0.001	0.005031	29.82
30	0.3	55	190	0.002	0.005034	37.74
40	0.4	60	250	0.003	0.005037	49.63
50	0.5	65	280	0.003	0.005041	55.55
60	0.6	70	320	0.004	0.005044	63.44
70	0.7	80	360	0.005	0.005048	71.32
80	0.8	90	410	0.005	0.005051	81.17
90	0.9	100	465	0.006	0.005054	92.00
100	1	110	520	0.007	0.005058	102.81
120	1.2	120	564	0.008	0.005065	111.36
140	1.4	130	610	0.009	0.005071	120.28
160	1.6	140	655	0.011	0.005078	128.98
180	1.8	150	680	0.012	0.005085	133.73
200	2	160	730	0.013	0.005092	143.37
240	2.4	170	810	0.016	0.005106	158.65
280	2.8	180	870	0.019	0.005120	169.94
320	3.2	190	920	0.021	0.005134	179.21
360	3.6	200	945	0.024	0.005148	183.58
400	4	210	980	0.027	0.005162	189.86
440	4.4	220	965	0.029	0.005176	186.44
480	4.8	240	963	0.032	0.005190	185.55
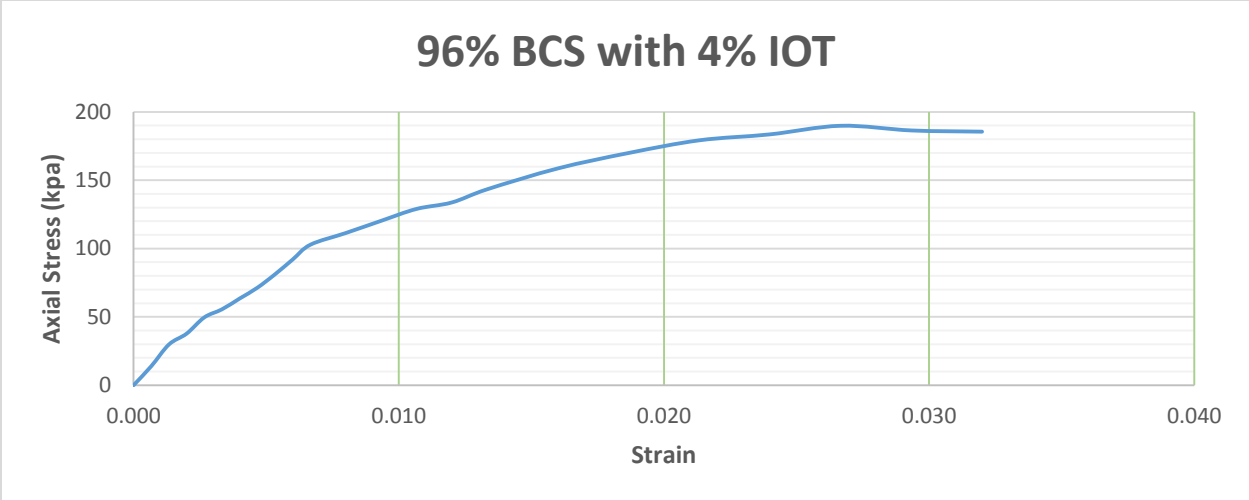
Figure B-12: Unconfined Compression Strength chart for 96% BCS with 4% IOT

Table B-15: Unconfined Compression Strength data for 94% BCS with 6% IOT

Dial Reading	Deformation (mm)	Proving Ring Reading (P.R.R)	Load, (KN)	Strain	Corrected Area (m²)	Stress (kN/m²)
0	0	18	0	0.000	0.005024	0
10	0.1	32	80	0.001	0.005027	15.91
20	0.2	50	160	0.001	0.005031	31.80
30	0.3	55	200	0.002	0.005034	39.73
40	0.4	60	280	0.003	0.005037	55.58
50	0.5	65	325	0.003	0.005041	64.47
60	0.6	70	380	0.004	0.005044	75.33
70	0.7	80	420	0.005	0.005048	83.21
80	0.8	90	477	0.005	0.005051	94.44
90	0.9	100	526	0.006	0.005054	104.07
100	1	110	580	0.007	0.005058	114.68
120	1.2	120	630	0.008	0.005065	124.39
140	1.4	130	660	0.009	0.005071	130.14
160	1.6	140	685	0.011	0.005078	134.89
180	1.8	150	710	0.012	0.005085	139.63
200	2	160	740	0.013	0.005092	145.33
240	2.4	170	830	0.016	0.005106	162.56
280	2.8	180	890	0.019	0.005120	173.84
320	3.2	190	935	0.021	0.005134	182.14
360	3.6	200	1000	0.024	0.005148	194.27
400	4	210	1060	0.027	0.005162	205.36
440	4.4	220	1050	0.029	0.005176	202.87
480	4.8	240	1045	0.032	0.005190	201.35
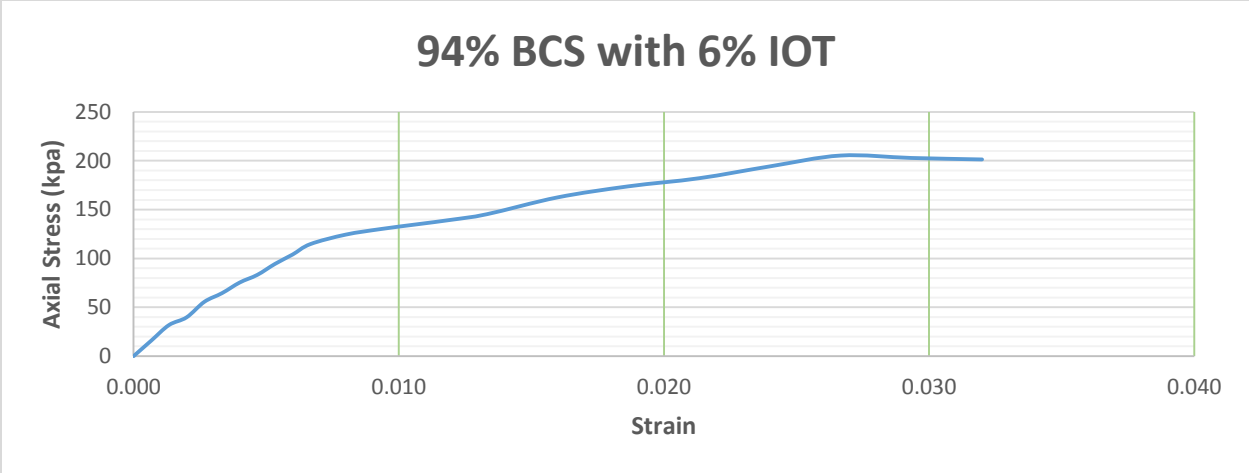
Figure B-13: Unconfined Compression Strength chart for 94% BCS with 6% IOT

Table B-16: Unconfined Compression Strength data for 92% BCS with 8% IOT

Dial Reading	Deformation (mm)	Proving Ring Reading (P.R.R)	Load, (KN)	Strain	Corrected Area (m²)	Stress (kN/m²)
0	0	18	0	0.000	0.005024	0
10	0.1	32	92	0.001	0.005027	18.30
20	0.2	50	175	0.001	0.005031	34.79
30	0.3	55	235	0.002	0.005034	46.68
40	0.4	60	300	0.003	0.005037	59.55
50	0.5	65	368	0.003	0.005041	73.00
60	0.6	70	413	0.004	0.005044	81.88
70	0.7	80	480	0.005	0.005048	95.10
80	0.8	90	525	0.005	0.005051	103.94
90	0.9	100	580	0.006	0.005054	114.75
100	1	110	621	0.007	0.005058	122.78
120	1.2	120	694	0.008	0.005065	137.03
140	1.4	130	730	0.009	0.005071	143.95
160	1.6	140	785	0.011	0.005078	154.58
180	1.8	150	820	0.012	0.005085	161.26
200	2	160	882	0.013	0.005092	173.22
240	2.4	170	931	0.016	0.005106	182.35
280	2.8	180	1000	0.019	0.005120	195.33
320	3.2	190	1078	0.021	0.005134	209.99
360	3.6	200	1136	0.024	0.005148	220.69
400	4	210	1245	0.027	0.005162	241.20
440	4.4	220	1305	0.029	0.005176	252.13
480	4.8	240	1300	0.032	0.005190	250.48
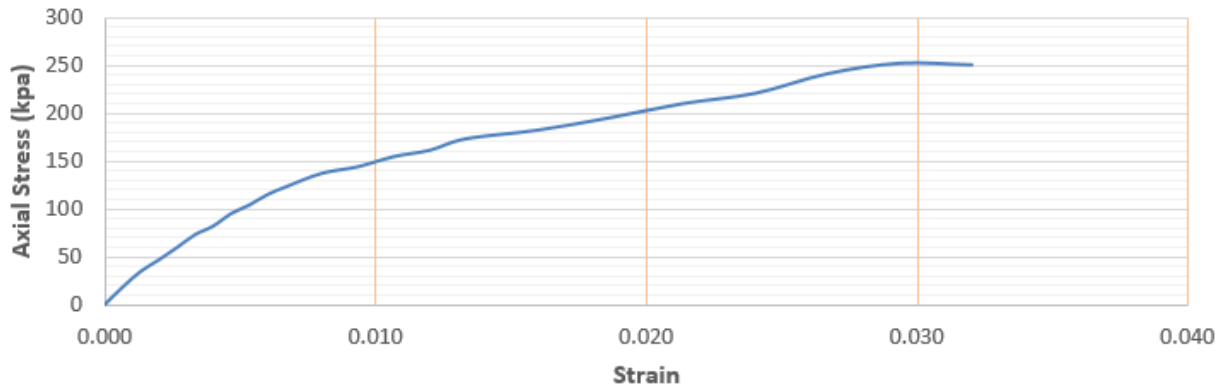
Figure B-14: Unconfined Compression Strength chart for 92% BCS with 8% IOT

Table B-17: Unconfined Compression Strength data for 90% BCS with 10% IOT

Dial Reading	Deformation (mm)	Proving Ring Reading (P.R.R)	Load, (KN)	Strain	Corrected Area (m²)	Stress (kN/m²)
0	0	18	0	0.000	0.005024	0
10	0.1	32	100	0.001	0.005027	19.89
20	0.2	50	210	0.001	0.005031	41.74
30	0.3	55	260	0.002	0.005034	51.65
40	0.4	60	320	0.003	0.005037	63.52
50	0.5	65	360	0.003	0.005041	71.42
60	0.6	70	430	0.004	0.005044	85.25
70	0.7	80	490	0.005	0.005048	97.08
80	0.8	90	530	0.005	0.005051	104.93
90	0.9	100	586	0.006	0.005054	115.94
100	1	110	680	0.007	0.005058	134.45
120	1.2	120	740	0.008	0.005065	146.11
140	1.4	130	777	0.009	0.005071	153.21
160	1.6	140	843	0.011	0.005078	166.00
180	1.8	150	900	0.012	0.005085	176.99
200	2	160	910	0.013	0.005092	178.72
240	2.4	170	960	0.016	0.005106	188.03
280	2.8	180	1035	0.019	0.005120	202.17
320	3.2	190	1090	0.021	0.005134	212.33
360	3.6	200	1120	0.024	0.005148	217.58
400	4	210	1190	0.027	0.005162	230.55
440	4.4	220	1223	0.029	0.005176	236.29
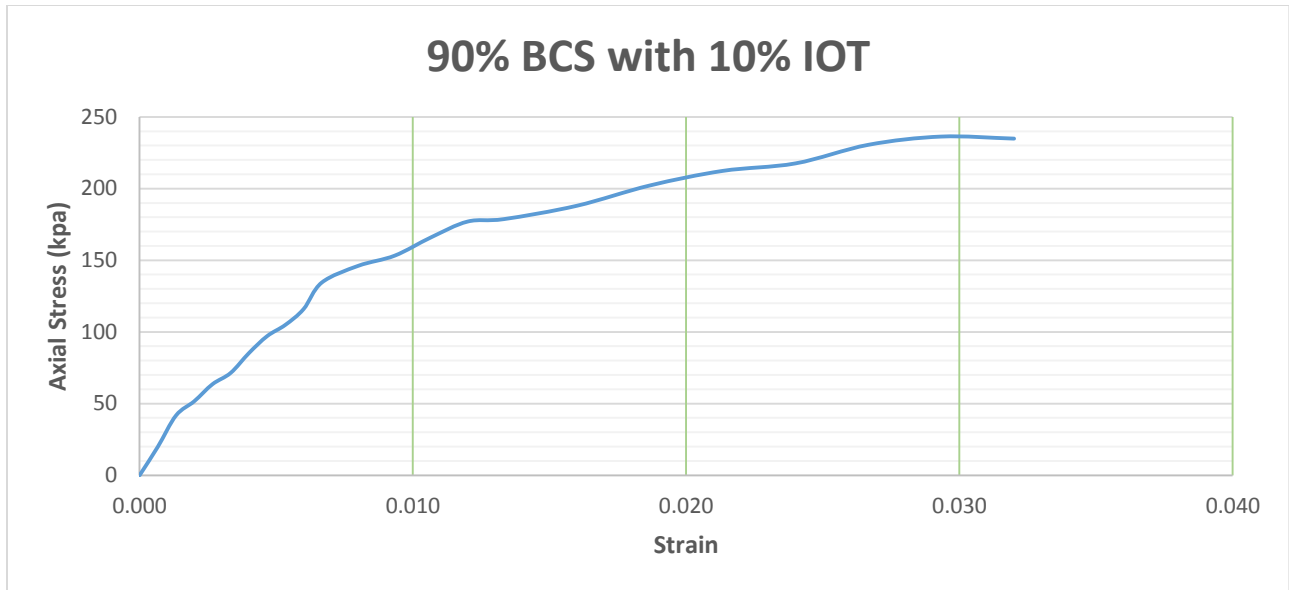
Figure B-15: Unconfined Compression Strength chart for 90% BCS with 10% IOT

Table B-18: Unconfined Compression Strength data for 88% BCS with 12% IOT

Dial Reading	Deformation (mm)	Proving Ring Reading (P.R.R)	Load, (KN)	Strain	Corrected Area (m²)	Stress (kN/m²)
0	0	18	0	0.000	0.005024	0
10	0.1	32	120	0.001	0.005027	23.87
20	0.2	50	205	0.001	0.005031	40.75
30	0.3	55	265	0.002	0.005034	52.64
40	0.4	60	323	0.003	0.005037	64.12
50	0.5	65	388	0.003	0.005041	76.97
60	0.6	70	436	0.004	0.005044	86.44
70	0.7	80	515	0.005	0.005048	102.03
80	0.8	90	586	0.005	0.005051	116.02
90	0.9	100	630	0.006	0.005054	124.65
100	1	110	715	0.007	0.005058	141.37
120	1.2	120	770	0.008	0.005065	152.04
140	1.4	130	830	0.009	0.005071	163.67
160	1.6	140	865	0.011	0.005078	170.34
180	1.8	150	920	0.012	0.005085	180.92
200	2	160	965	0.013	0.005092	189.52
240	2.4	170	1045	0.016	0.005106	204.67
280	2.8	180	1105	0.019	0.005120	215.84
320	3.2	190	1181	0.021	0.005134	230.06
360	3.6	200	1235	0.024	0.005148	239.92
400	4	210	1277	0.027	0.005162	247.40
440	4.4	220	1270	0.029	0.005176	245.37
480	4.8	240	1265	0.032	0.005190	243.73
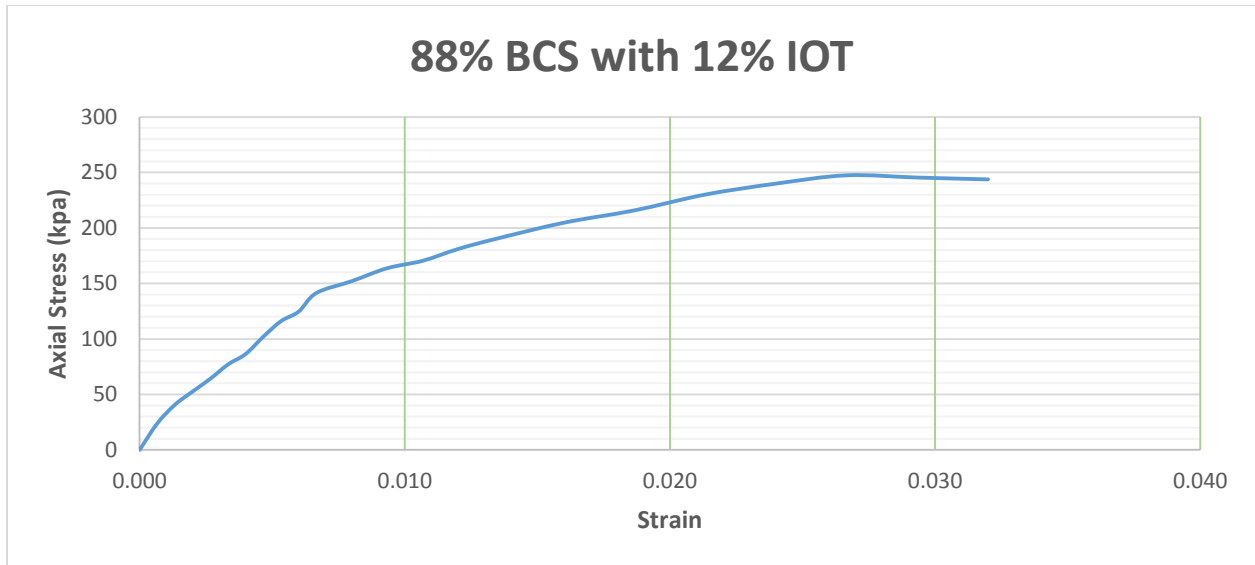
Figure B-16: Unconfined Compression Strength chart for 88% BCS with 12% IOT

Table B-19: Unconfined Compression Strength data for 86% BCS with 14% IOT

Dial Reading	Deformation (mm)	Proving Ring Reading (P.R.R)	Load, (KN)	Strain	Corrected Area (m²)	Stress (kN/m²)
0	0	18	0	0.000	0.005024	0
10	0.1	32	130	0.001	0.005027	25.86
20	0.2	50	220	0.001	0.005031	43.73
30	0.3	55	270	0.002	0.005034	53.63
40	0.4	60	340	0.003	0.005037	67.49
50	0.5	65	415	0.003	0.005041	82.33
60	0.6	70	489	0.004	0.005044	96.94
70	0.7	80	530	0.005	0.005048	105.00
80	0.8	90	596	0.005	0.005051	118.00
90	0.9	100	662	0.006	0.005054	130.98
100	1	110	730	0.007	0.005058	144.33
120	1.2	120	786	0.008	0.005065	155.20
140	1.4	130	835	0.009	0.005071	164.65
160	1.6	140	890	0.011	0.005078	175.26
180	1.8	150	960	0.012	0.005085	188.79
200	2	160	1065	0.013	0.005092	209.16
240	2.4	170	1121	0.016	0.005106	219.56
280	2.8	180	1235	0.019	0.005120	241.23
320	3.2	190	1290	0.021	0.005134	251.29
360	3.6	200	1325	0.024	0.005148	257.40
400	4	210	1387	0.027	0.005162	268.71
440	4.4	220	1423	0.029	0.005176	274.93
480	4.8	240	1420	0.032	0.005190	273.60
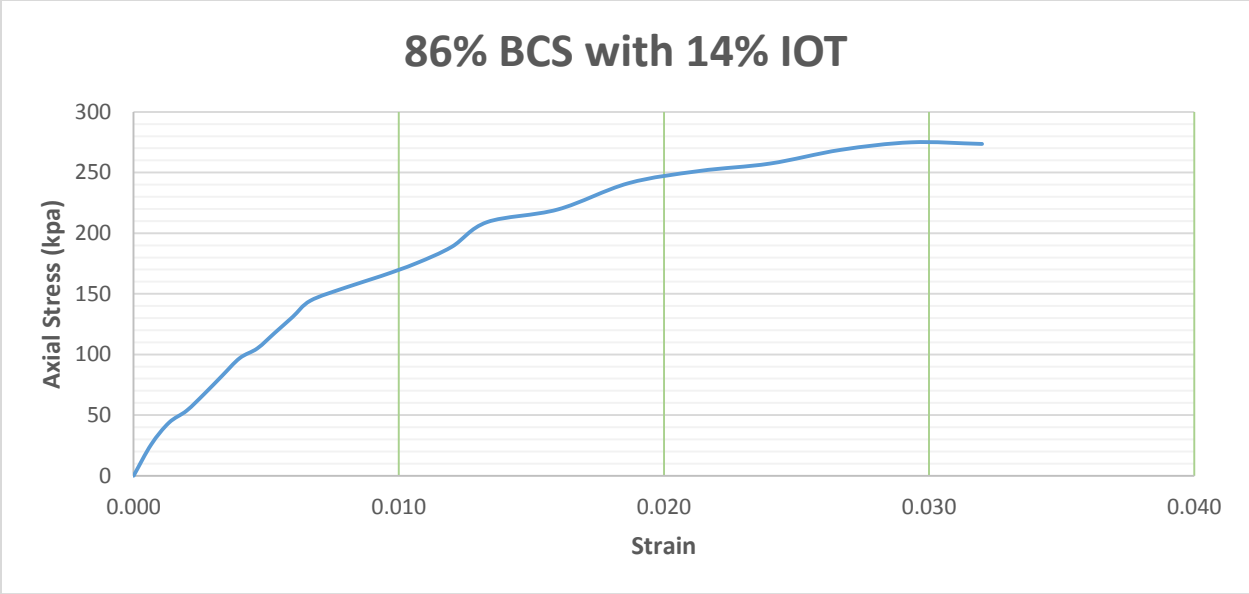
Figure B-17: Unconfined Compression Strength chart for 86% BCS with 14% IOT

Table B-18: Unconfined Compression Strength chart for 84% BCS with 12% IOT

Table C- 1: Specific gravity of natural soil with IOT and lime

SR NO	Sample NO	Sample Source	M of B+S+W(M3)	M of B+S(M2)	M of B full of W(M4)	M of B(M1)	M of w(m3-m2)	Mof S(M2-M1)	V of S(M 4-M1) - (M3 - M2)	GS=(M2-M1 (M4-M1)- (M3-M2)
1	1	BCS + 2% lime + 5% IOT	126.98	51.82	115.3	33.55	75.16	18.27	6.63	2.756
1.1			125.75	51.9	114.15	33.68	73.85	18.22	6.62	2.751
										2.753
2	2	BCS + 2% lime + 10% IOT	107.5	51.5	95.65	33.14	56	18.36	6.51	2.820
2.1			107.3	51.34	95.51	33	55.96	18.34	6.55	2.800
										2.810
3	3	BCS + 2% lime + 15% IOT	104.32	51.86	92	33	52.46	18.86	6.54	2.884
3.1			103.25	50.87	90.88	31.98	52.38	18.89	6.52	2.897
										2.891
4	4	BCS + 2% lime + 20% IOT	103.54	51.7	91.57	33.6	51.84	18.1	6.13	2.953
4.1			103.97	51.4	92.13	33.5	52.57	17.9	6.06	2.954
										2.953

Table C- 2: Determination of liquid limit & plastic limit of 93% BCS with 5% IOT and 2% lime

	Liquid Limit			Plastic Limit	
No. Blows	35	23	16		
Wt. Of cont. + wet soil (g.)	37.00	38.98	42.00	20.00	20.50
Wt. Of cont. + dry soil (g.)	31.92	33.55	35.82	18.82	19.28
Wt. of water (g.)	5.08	5.43	6.18	1.18	1.22
Wt. container (g.)	25.45	26.38	26.83	15.42	15.64
:	6.47	7.17	8.99	3.40	3.64
Water (%)	78.52	75.73	68.74	34.71	33.52
				AV. PL (%)	34.1
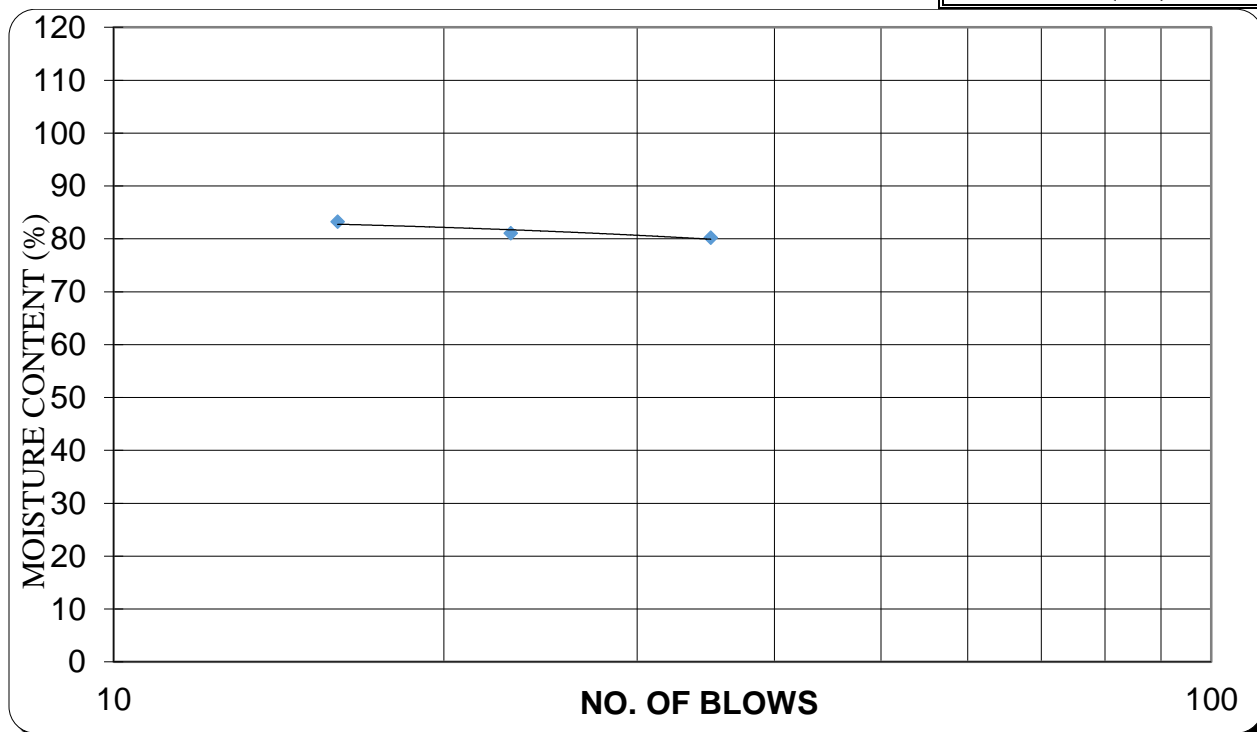
Figure C- 1: Liquid limit chart for 93% BCS with 5%IOT and 2%lime

Liquid Limit	Plastic Limit	Plasticity Index
LL(%)	PL(%)	PI
74	34	40

Table C- 3: Determination of liquid limit & plastic limit of 88% BCS with 10% IOT and 2% lime

	Liquid Limit			Plastic Limit	
No. Blows	33	24	17		
Wt.of cont. + wet soil (g.)	36.00	39.00	42.00	19.52	19.80
Wt.of cont. + dry soil (g.)	32.00	34.30	35.82	18.66	18.81
Wt. of water (g.)	4.00	4.70	6.18	0.86	0.99
Wt. container (g.)	25.50	27.00	26.83	15.87	15.63
:	6.50	7.30	8.99	2.79	3.18
Water (%)	61.54	64.38	68.74	30.82	31.13
				AV. PL (%)	31.0
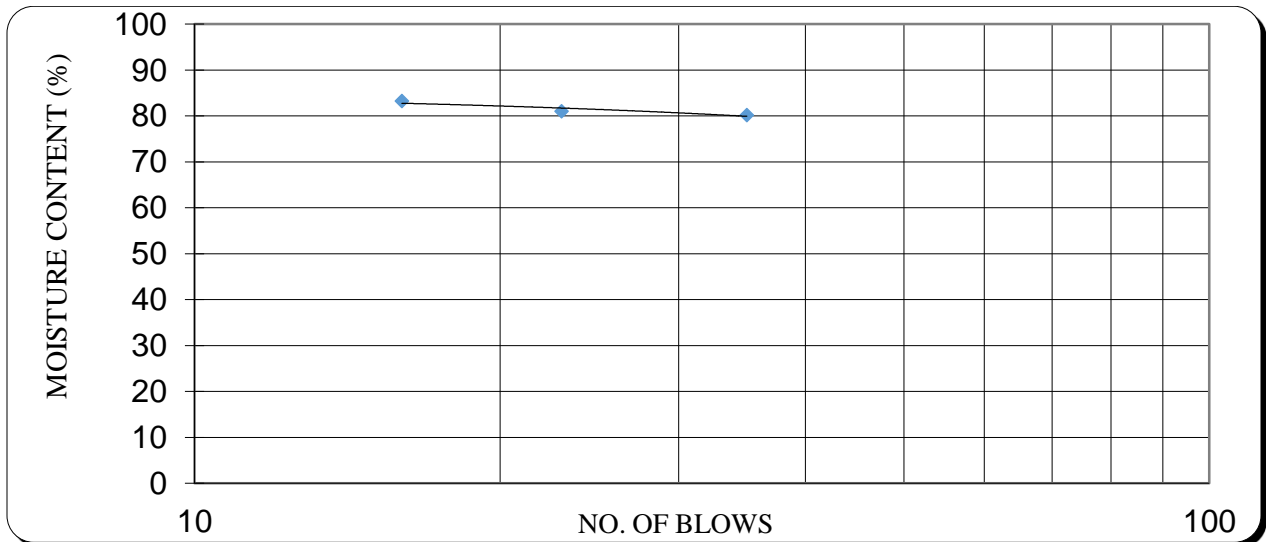
Figure C- 2: Liquid limit chart for 88% BCS with 10%IOT and 2%lime

Liquid Limit	Plastic Limit	Plasticity Index
LL(%)	PL(%)	PI
65	31	34

Table C- 4: Determination of liquid limit & plastic limit of 83% BCS with 15% IOT and 2% lime

	Liquid Limit			Plastic Limit	
No. Blows	35	28	18		
Wt.of cont. + wet soil (g.)	37.00	39.00	41.00	20.26	20.49
Wt.of cont. + dry soil (g.)	32.80	34.29	35.90	19.13	19.34
Wt. of water (g.)	4.20	4.71	5.10	1.13	1.15
Wt. container (g.)	25.00	25.80	26.83	15.10	15.20
:	7.80	8.49	9.07	4.03	4.14
Water (%)	53.85	55.48	56.23	28.04	27.78
				AV. PL (%)	27.9
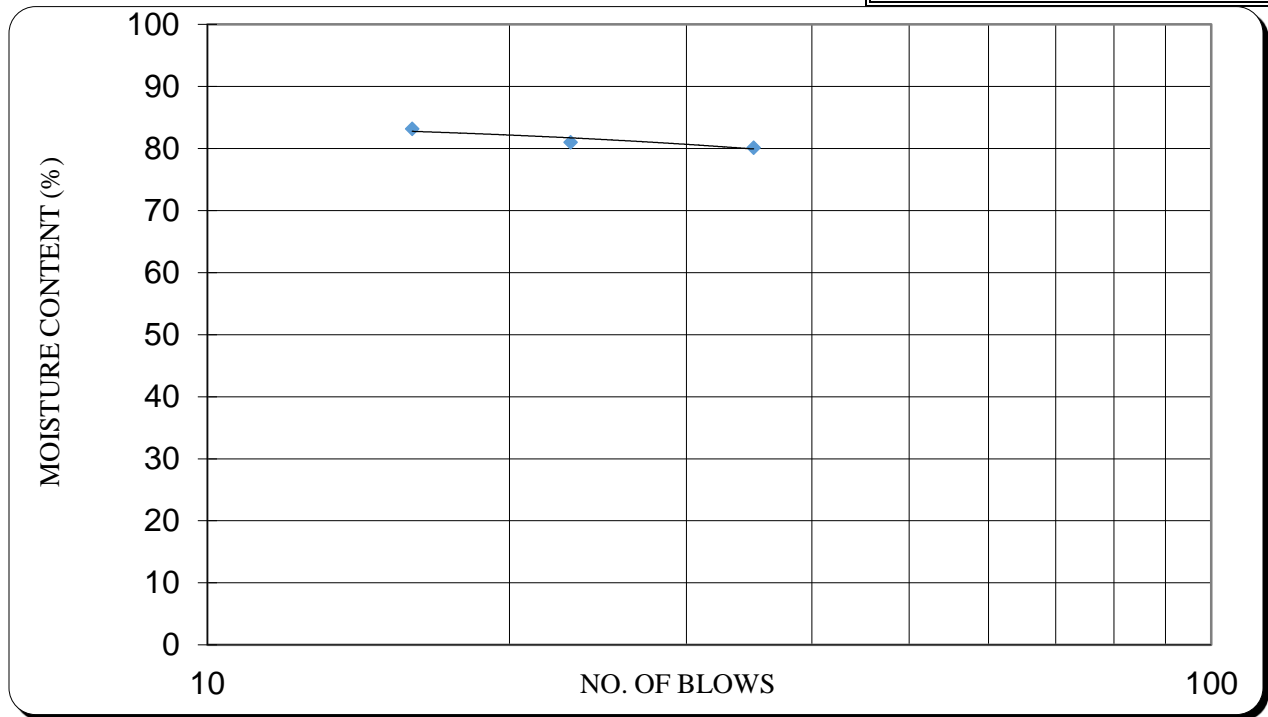
Figure C- 3: Figure C- 2: Liquid limit chart for 83% BCS with 15%IOT and 2%lime

Liquid Limit	Plastic Limit	Plasticity Index
LL(%)	PL(%)	PI
55	28	27

Table C- 5: Determination of liquid limit & plastic limit of 78% BCS with 20% IOT and 2% lime

	Liquid Limit			Plastic Limit	
No. Blows	30	22	15		
Wt.of cont. + wet soil (g.)	36.00	37.00	41.00	19.45	19.88
Wt.of cont. + dry soil (g.)	32.84	33.30	36.10	18.64	19.02
Wt. of water (g.)	3.16	3.70	4.90	0.81	0.86
Wt. container (g.)	26.00	25.80	26.83	15.40	15.64
:	6.84	7.50	9.27	3.24	3.38
Water (%)	46.20	49.33	52.86	25.00	25.44
				AV. PL (%)	25.2
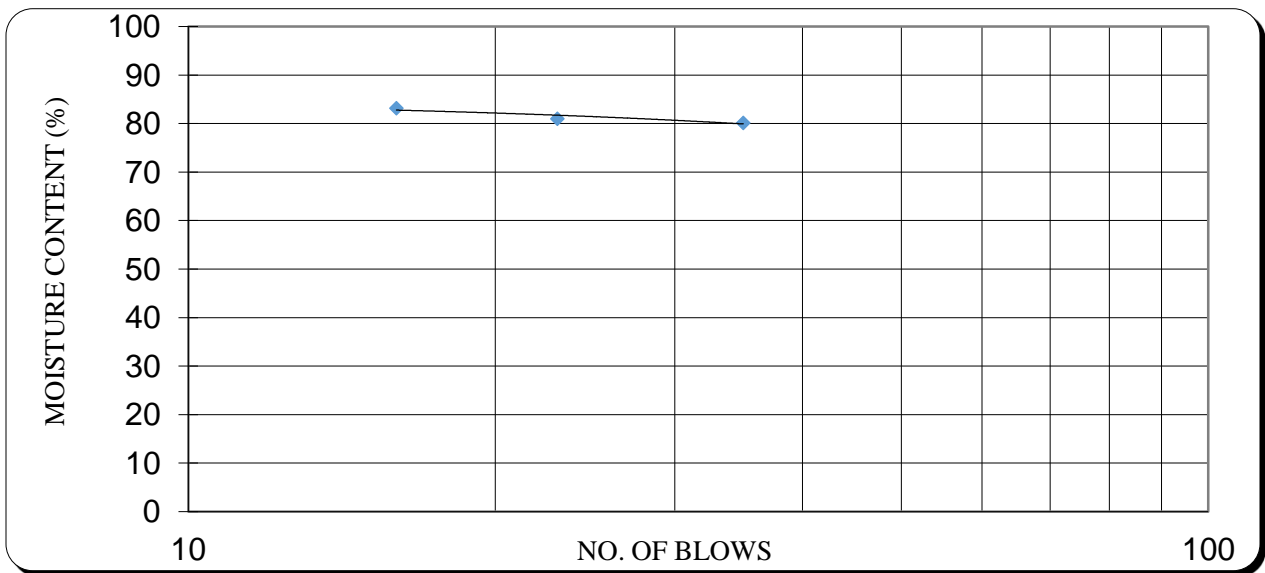
Figure C- 4: Liquid limit chart for 78% BCS with 20%IOT and 2%lime

Liquid Limit	Plastic Limit	Plasticity Index
LL(%)	PL(%)	PI
49	25	24

Table C- 6: Summary Determination of MDD & OMC of BCS % with IOT %

92

Trial	1	2	3	4	5	%	Maximum
Moisture content(g/cc)	14.44	21.26	24.16	28.91	34.75	0%	28.90
Dry density(g/cc)	1.38	1.43	1.46	1.51	1.40		1.51
Moisture content(g/cc)	12.59	17.63	22.22	25.37	33.06	5%	25.37
Dry density(g/cc)	1.42	1.48	1.53	1.54	1.49		1.54
Moisture content(g/cc)	12.59	13.69	17.81	23.88	27.03	10%	23.88
Dry density(g/cc)	1.44	1.46	1.54	1.60	1.47		1.60
Moisture content(g/cc)	12.32	15.04	18.38	20.42	28.57	15%	20.42
Dry density(g/cc)	1.51	1.57	1.62	1.63	1.53		1.63
Moisture content(g/cc)	12.99	15.60	17.86	19.31	26.62	20%	19.31
Dry density(g/cc)	1.53	1.58	1.63	1.66	1.55		1.66
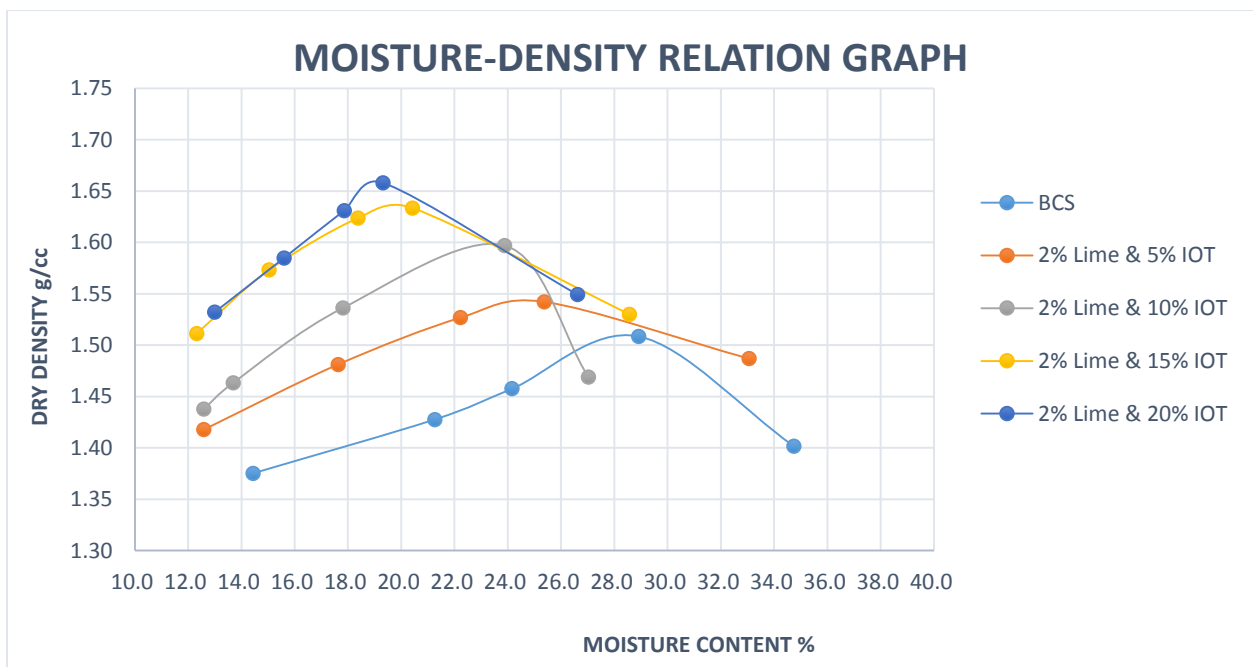
Figure C- 5: Liquid limit chart for 78% BCS with 20%IOT and 2%lime

Table C- 7: Unconfined Compression Strength data for 93% BCS with 5% IOT and 2% lime

Dial Reading			Strain		

	Deformation (mm)	Proving Ring Reading (P.R.R)	Load, (KN)		Corrected Area (m²)	Stress (kN/m²)
0	0	18	0	0.000	0.005024	0
10	0.1	32	100	0.001	0.005027	19.89
20	0.2	50	200	0.001	0.005031	39.76
30	0.3	55	225	0.002	0.005034	44.70
40	0.4	60	264	0.003	0.005037	52.41
50	0.5	65	300	0.003	0.005041	59.51
60	0.6	70	333	0.004	0.005044	66.02
70	0.7	80	389	0.005	0.005048	77.07
80	0.8	90	420	0.005	0.005051	83.15
90	0.9	100	460	0.006	0.005054	91.01
100	1	110	510	0.007	0.005058	100.84
120	1.2	120	560	0.008	0.005065	110.57
140	1.4	130	623	0.009	0.005071	122.85
160	1.6	140	740	0.011	0.005078	145.72
180	1.8	150	790	0.012	0.005085	155.36
200	2	160	830	0.013	0.005092	163.00
240	2.4	170	850	0.016	0.005106	166.48
280	2.8	180	880	0.019	0.005120	171.89
320	3.2	190	910	0.021	0.005134	177.27
360	3.6	200	930	0.024	0.005148	180.67
400	4	210	900	0.027	0.005162	174.36
440	4.4	220	890	0.029	0.005176	171.95
480	4.8	240	880	0.032	0.005190	169.55

BCS with 2% Lime and 5% IOT Axiial Stress (kpa) Vs Strain
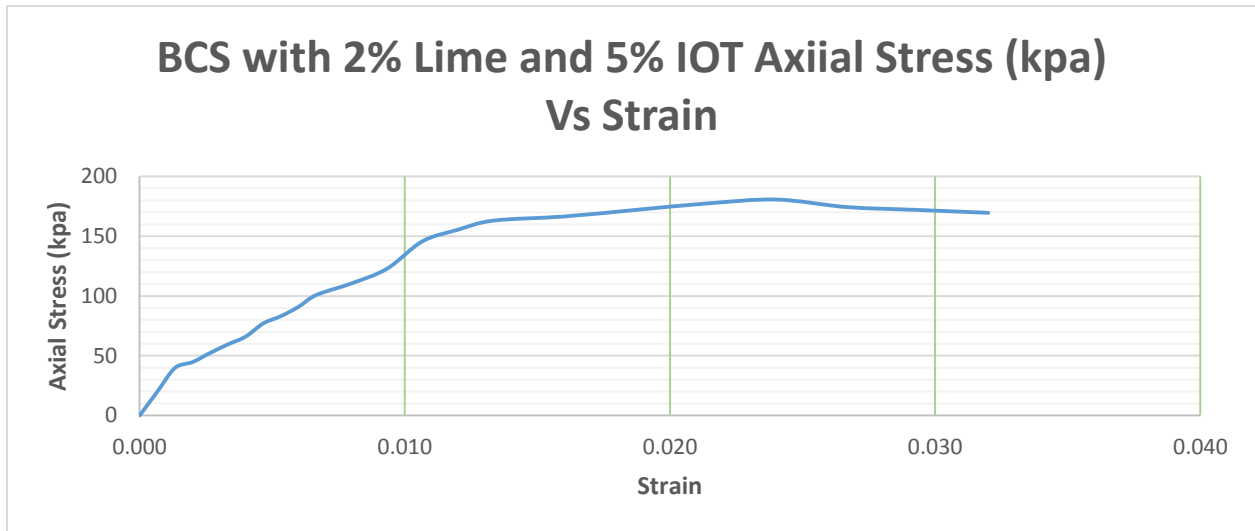
Table C-6: Unconfined Compression Strength data for 93% BCS with 5% IOT and 2% lime

Table C- 8: Unconfined Compression Strength data for 88% BCS with 10% IOT and 2% lime

Dial Reading	Deformation (mm)	Proving Ring Reading (P.R.R)	Load, (KN)	Strain	Corrected Area (m²)	stress (kN/m²)
0	0	18	0	0.000	0.005024	0
10	0.1	32	174	0.001	0.005027	34.61
20	0.2	50	266	0.001	0.005031	52.88
30	0.3	55	311	0.002	0.005034	61.78
40	0.4	60	364	0.003	0.005037	72.26
50	0.5	65	415	0.003	0.005041	82.33
60	0.6	70	476	0.004	0.005044	94.37
70	0.7	80	520	0.005	0.005048	103.02
80	0.8	90	580	0.005	0.005051	114.83
90	0.9	100	644	0.006	0.005054	127.42
100	1	110	700	0.007	0.005058	138.40
120	1.2	120	761	0.008	0.005065	150.26
140	1.4	130	832	0.009	0.005071	164.06
160	1.6	140	895	0.011	0.005078	176.24
180	1.8	150	950	0.012	0.005085	186.82
200	2	160	1036	0.013	0.005092	203.46
240	2.4	170	1112	0.016	0.005106	217.80
280	2.8	180	1176	0.019	0.005120	229.71
320	3.2	190	1240	0.021	0.005134	241.55
360	3.6	200	1285	0.024	0.005148	249.63
400	4	210	1280	0.027	0.005162	247.98
440	4.4	220	1275	0.029	0.005176	246.34
480	4.8	240	1270	0.032	0.005190	244.70
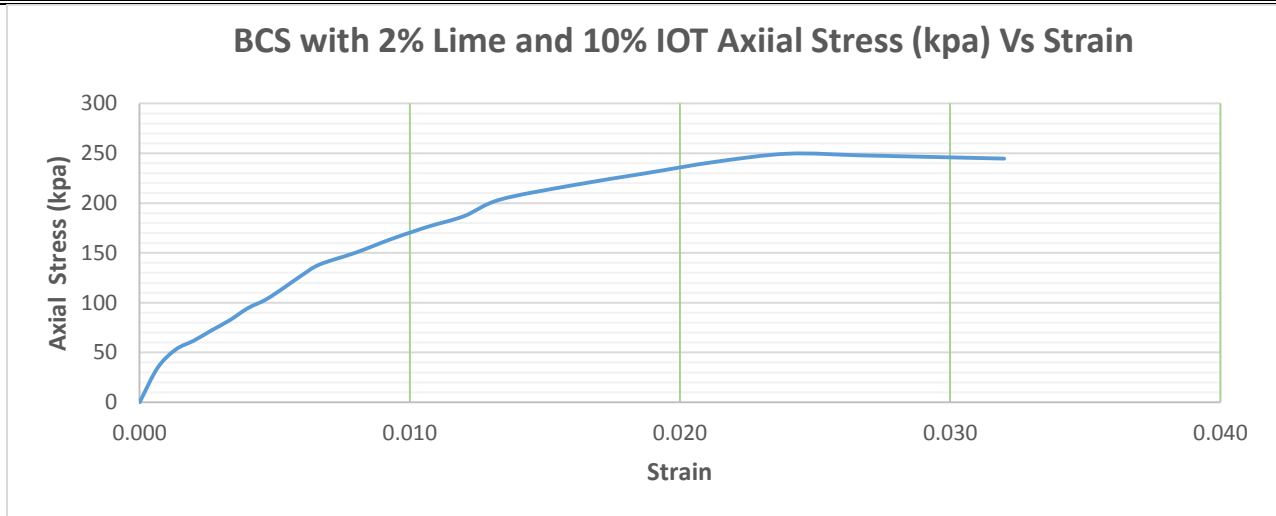
Table C-7: Unconfined Compression Strength data for 88% BCS with 10% IOT and 2% lime

Table C-9: Unconfined Compression Strength data for 83% BCS with 15% IOT and 2% lime

Dial Reading	Deformation (mm)	Proving Ring Reading (P.R.R)	Load, (KN)	Strain	Corrected Area (m²)	stress (kN/m²)
0	0	18	0	0.000	0.005024	0
10	0.1	32	210	0.001	0.005027	41.77
20	0.2	50	280	0.001	0.005031	55.66
30	0.3	55	394	0.002	0.005034	78.27
40	0.4	60	428	0.003	0.005037	84.96
50	0.5	65	490	0.003	0.005041	97.21
60	0.6	70	530	0.004	0.005044	105.07
70	0.7	80	589	0.005	0.005048	116.69
80	0.8	90	668	0.005	0.005051	132.25
90	0.9	100	710	0.006	0.005054	140.47
100	1	110	767	0.007	0.005058	151.65
120	1.2	120	860	0.008	0.005065	169.81
140	1.4	130	1000	0.009	0.005071	197.19
160	1.6	140	1080	0.011	0.005078	212.68
180	1.8	150	1150	0.012	0.005085	226.15
200	2	160	1210	0.013	0.005092	237.63
240	2.4	170	1280	0.016	0.005106	250.70
280	2.8	180	1360	0.019	0.005120	265.65
320	3.2	190	1450	0.021	0.005134	282.46
360	3.6	200	1530	0.024	0.005148	297.23
400	4	210	1580	0.027	0.005162	306.10
440	4.4	220	1560	0.029	0.005176	301.40
480	4.8	240	1540	0.032	0.005190	296.72
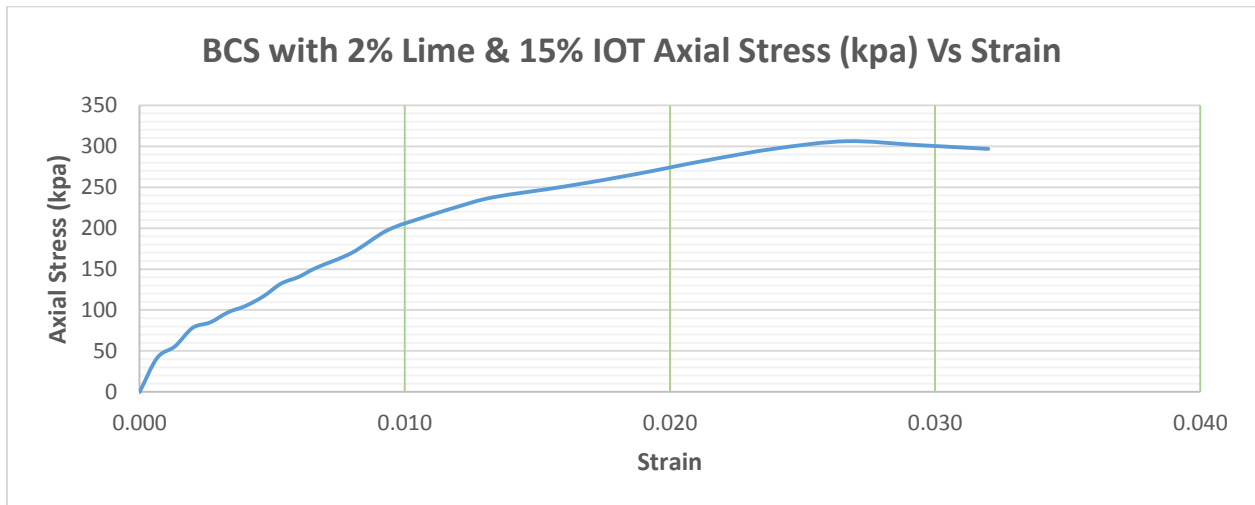
Table C-8: Unconfined Compression Strength data for 83% BCS with 15% IOT and 2% lime

Table C- 10: Unconfined Compression Strength data for 78% BCS with 20%IOT and 2% lime

	Dial Reading	Deformation (mm)	Proving Ring Reading (P.R.R)	Load, (KN)	Strain	Corrected Area (m²)	stress (kN/m²)
0	0	0	18	0	0.000	0.005024	0
210	10	0.1	32	225	0.001	0.005027	44.76
280	20	0.2	50	374	0.001	0.005031	74.34
394	30	0.3	55	425	0.002	0.005034	84.42
428	40	0.4	60	480	0.003	0.005037	95.29
490	50	0.5	65	560	0.003	0.005041	111.09
530	60	0.6	70	612	0.004	0.005044	121.33
589	70	0.7	80	688	0.005	0.005048	136.30
668	80	0.8	90	764	0.005	0.005051	151.26
710	90	0.9	100	850	0.006	0.005054	168.17
767	100	1	110	920	0.007	0.005058	181.90
860	120	1.2	120	1000	0.008	0.005065	197.45
1000	140	1.4	130	1060	0.009	0.005071	209.02
1080	160	1.6	140	1120	0.011	0.005078	220.55
1150	180	1.8	150	1195	0.012	0.005085	235.00
1210	200	2	160	1260	0.013	0.005092	247.45
1280	240	2.4	170	1384	0.016	0.005106	271.07
1360	280	2.8	180	1450	0.019	0.005120	283.23
1450	320	3.2	190	1544	0.021	0.005134	300.77
1530	360	3.6	200	1630	0.024	0.005148	316.66
1580	400	4	210	1688	0.027	0.005162	327.03
1560	440	4.4	220	1685	0.029	0.005176	325.55
1540	480	4.8	240	1683	0.032	0.005190	324.27
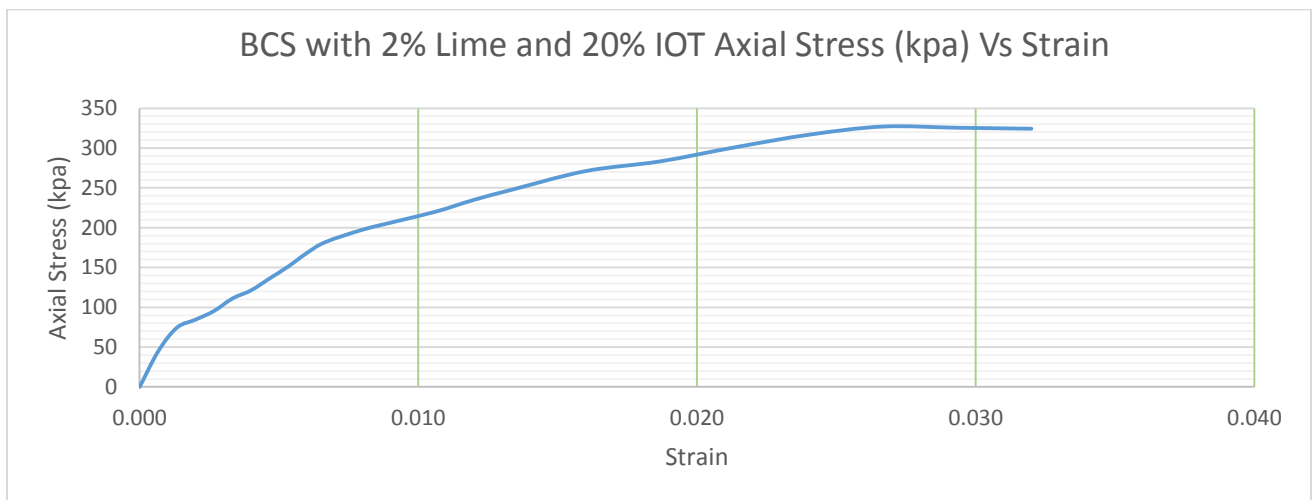
Table C-9: Unconfined Compression Strength data for 78% BCS with 10% IOT and 2% lime

Table C- 11: Modified proctor density test for natural soil

Dry Sieve Analysis data for IOT

Total Dry Weight   = 4500g

Inch/No	Seive Size,mm	Wt Retained	% Retained	% Passing
	75	0	0	100
	63.5	0	0	100
3	50	0	0	100
2 1/2	37.5	0	0	100
2	31	0	0	100
	28	321.6	7.15	92.85
	25	578.9	12.86	79.99
1	19.5	0	0	79.99
3/4	13.2	1336.6	29.7	50.29
1/2	12.5	1082.9	24.06	26.22
3/8	9.5	0	0	26.22
1/4	6.35	849.6	18.88	7.34
	4.75	0	0	7.34
No.4	2.36	294.6	6.55	0.8
No.8	2	0	0	0.8
	1.18	0	0	0.8
No.16	0.85	0	0	0.8
No.30	0.6	13.7	0.3	0.49
	0.425	0	0	0.49
No.50	0.3	0	0	0.49
No.100	0.15	5.4	0.12	`0.37
No.200	0.075	4483.3		
Total (Comu RT)		16.7	0.37	
Pan		4500	100.0	
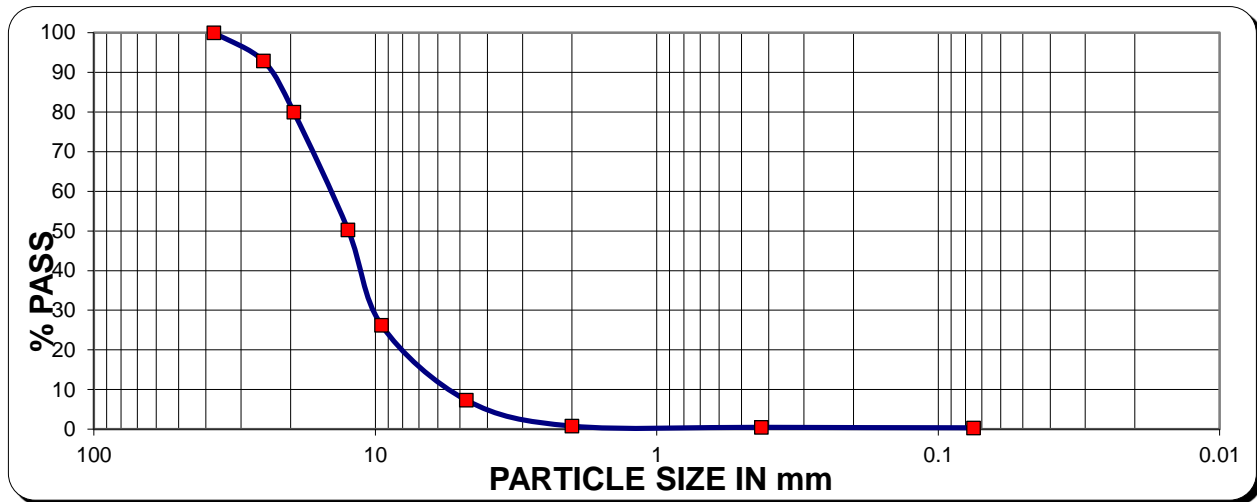
Figure C-10: Particle size distribution curve for IOT

98

Table C- 12: Modified proctor density test for Iron ore tailing

Compaction test result

Trial No.	1	2	3	4	5
Wet soil (kg)	1.04	1.15	1.27	1.418	1.41
Volume of Mold	0.00089	0.00089	0.00089	0.00089	0.00089
Wet density (kg / m3)	1169.0	1292.7	1427.6	1593.9	1584.9

Moisture content determination

Wet soil (kg)	254.905	264.907	275.904	287.903	311.903
Dry soil (kg)	244.905	252.907	261.904	270.903	290.903
Moisture cont. (%)	4.083216	4.744827	5.34547	6.275309	7.218901
Dry Density (kg / m^3)	1123.177	1234.129	1355.137	1499.821	1478.234
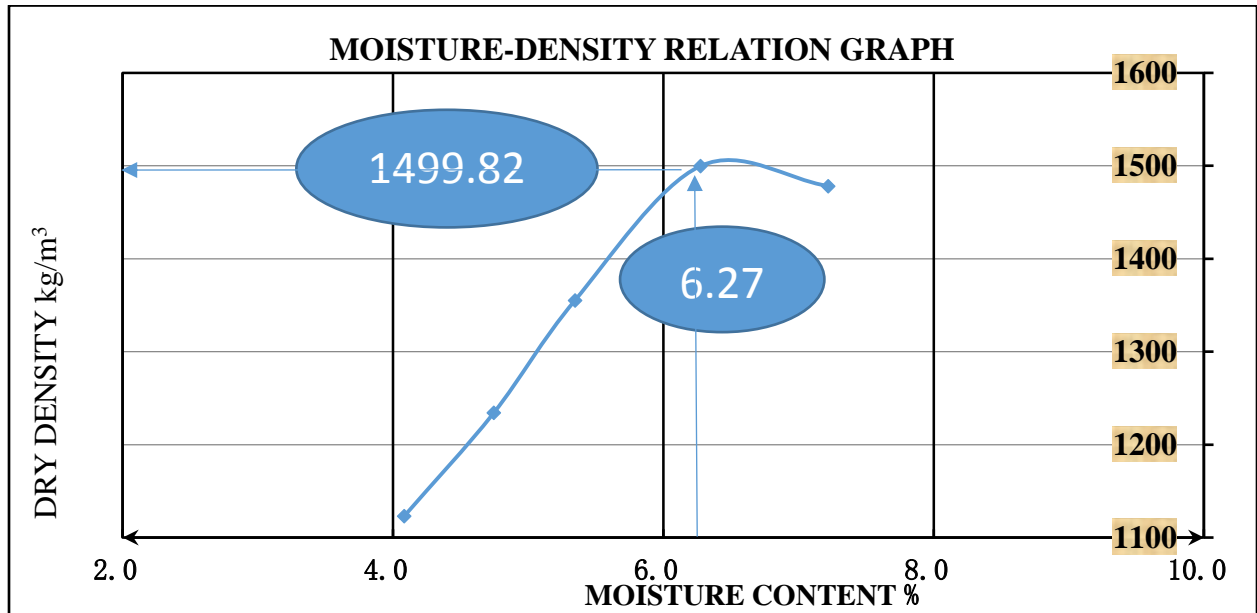
Figure C-11: Moisture density relationship graph of Iron ore tailing